# High speed and angular position sensor for a permanent magnet synchronous motor control

**Auteur :** Hubert, Marine
**Promoteur(s) :** Sacré, Pierre
**Faculté :** Faculté des Sciences appliquées
**Diplôme :** Master : ingénieur civil électricien, à finalité spécialisée en "electronic systems and devices"
**Année académique :** 2020-2021
**URI/URL :** http://hdl.handle.net/2268.2/11466

University of Liège - Faculty of Applied Sciences

---

# High speed and angular position sensor for a permanent magnet synchronous motor control

---

Master thesis in electrical engineering - Electronic systems and devices


*Author:*
HUBERT Marine

*Promoters:*
G. DRION
P. SACRÉ
*Industrial supervisors:*
M. DELANAYE
M. DELVAUX


Academic year 2020-2021

# Acknowledgements

I express my sincere thanks to my industrial supervisor Michel Delvaux for his advice and help throughout my internship and the realization of this thesis.

Then I would like to thank the MITIS team and more particularly Michel Delanaye for my welcome to his company.

Moreover, I would like to thank my academic tutors, Guillaume Drion and Pierre Sacré for their time, encouragement, availability and interest for this thesis.

After, I would like to express my sincere thanks to Fabrice Frebel for its great help throughout the closed-loop control implementation by sharing with me its advice and its knowledge about the control of a PMSM.

I would like to thank Christophe Collette for its availability to be member in my thesis jury.

Finally, I would like to thank my family for their support throughout these five years of study.

# Contents

# List of Figures

# List of Tables

# Chapter 1

# Introduction

This thesis consists in developing a position sensor in order to control a permanent magnet synchronous motor (PMSM). It is the aim of an internship in the MITIS company.

MITIS is an high-tech start-up based at the campus of the University of Liège. The company is developing micro-CHP (Combined Heat and Power) systems and is working on a major project that consists in developing a multi-fuel, liquid and gaseous micro-CHP system. The first idea was to start with biomethanation and over time the business grew and different markets opened up to them. Therefore, in addition to biomethane, projects to use fuels such as hydrogen, gasoline or diesel are in development.

The basic principle of a micro turbine is characterized by two modes. One is the motor mode. Tt consists in using electrical energy in order to produce mechanical energy. The other one is the generator mode which is exactly the opposite, using mechanical energy in order to generate electrical energy. The purpose of the project managed by MITIS is to be able to generate an electrical power in the range of 10kWe with a low emission flameless combustor. This kind of combustion allows a low $NO_x$ and $CO_2$ emissions and so a clean power generation but brings to a real challenge.

In fact, a flameless combustion means that the flame seems invisible and it is possible for a given temperature and pressure in the combustor. Such as temperature and pressure require a large source of energy which is mainly coming from the mechanical energy generated by the motor. So, the methodology is to start with the motor mode to set in motion the compressor, this one allows to increase the temperature and pressure to have the perfect conditions for the combustion. Then, the combustor producing a high-energy fluid allows to the turbine to be in motion with a very high speed. In order to switch in the generator mode and produce electricity, a sufficient rotation speed linked to the range of electrical power is 10kWe corresponds to 110 000 rpm. Once the shaft, driven by the motor, reaches this value, the system can switch in the generator mode. In this project, the objective is fixed to 120 000 rpm in order to have a little margin compared to the sufficient value.
This mode switching is, in reality, characterized by the sign of the torque at the motor. A motor consists in a rotor in motion, and a stator which is static and responsible for either the generation of a rotating speed at the rotor either at a current generation using the rotation speed of the rotor. In other words, the electrical or mechanical energy generation depends, in reality, on the sens of functioning of the system. Indeed, a negative torque corresponds to the case where the rotor wants to follow a reference speed imposed by a rotating magnetic field generated by the stator. So, the rotor consisting of a permanent magnet is rotating by attempting to catch up the rotating magnetic field. In the case of the

generator mode, it is the rotor that imposes a rotation and so a varying magnetic field in the windings of the stator that produces AC current with a frequency proportional to the motor rotation speed.
Note that for this project, the rotor consists of a permanent magnet. This choice compared to windings fed by a DC current for the rotor was done due to these following advantages. First, the motor is smaller and lighter. Then, it allows a low maintenance cost and finally, it is known for its good dynamic performance and wide speed range.

In a such system, it is useful to have a control on the motor speed. Indeed, in order to be able to switch in the generator mode, the motor need first to provide enough of mechanical energy to the shaft and so to the complex compressor- combustor-turbine. In order words, for the start-up of the micro gas turbine, the motor has to achieve a rotation speed of 120 000 rpm and only then it will be possible to switch in a generator mode. Another sub-objective is to achieve a rotation speed of 18 000 rpm in three seconds. This objective concerns the levitation of the foil-bearings. Without going into all the details, foil-bearings are a new technology that replace oil-lubricated rolling-contact bearings. They allow to have a very low maintenance cost as they do not touch the shaft when they are in levitation and they do not need to be lubricated. The price to pay is only an high acceleration at the start-up that initiate an air's high pressure gap between the shaft and foils and so there is no wear which is a good advantage.

As said before, these objectives need a command on the motor. A first idea was to command the system using an open-loop control. Enforcing a speed amounted to impose an amplitude and a frequency to the AC current in the stator using some physical relations, this current generating a rotating magnetic field, it was possible to achieve a reference motor speed. The problem with an open-loop strategy is the lack of feedback. Indeed, one asks to the motor to achieve a speed but it is delivered to itself to accomplish the task. In this case, some issues such as very large current (about 60A) and dropout can occur. A dropout means the situation in which the rotor is no longer able to follow the rotating magnetic field imposed by the stator and so the two magnetic fields loose their synchronous speed and the rotation speed decrease until the complete stop of the motor. Another important issue is the situation where the rotor magnetic field does not hook the magnetic field generating by the stator at the start-up. This is due to the difference between the magnet position (orientation of the rotor magnetic field) and the phase shift in the AC current signal at the stator (orientation of the stator magnetic field). If the difference is too big, the rotor cannot follow at all the rotating magnetic field and the start-up do not occur.
All these issues lead to an idea of implementing a closed-loop control. This one allows to command the motor using feedback information and so the motor is no longer delivered to itself. For the PMSM, there are two kinds of control that could be implemented. A first one, the simplest, controlling only the motor speed and another one controlling the motor speed but also the torque. With this kind of control, the motor follows the reference speed using feedback information on its rotor angular position but also on its currents in the stator. Then, the issues cited before are controlled by a speed control loop for the dropout and the start-up problems and by a torque control loop for the large current.
In order to implement these loops, Hall effect current sensors are used and an angular position sensor being able to follow very high rotation speed need to be developed and that is the challenge and the object of this thesis.

This thesis is structured in different parts. First, in the chapter 2, the concept of micro turbine, PMSM and its controller will be developed. Then, in the chapter 3, a review of state-of-the-art position sensors is presented in order to explain the choice of the Eddy current sensor. After, the hardware design and the software development of the Eddy current sensor are respectively described in the chapter 4 and 5. Finally, closed-loop controls using angular position sensor are developed and supported by simulations on *Simulink*. To conclude, a final part dedicated to the conclusion and possible perspectives is presented in the chapter 7.

# Chapter 2

# Microturbine, PMSM, and its controller

This project is aimed at designing and developing a position and speed sensor in order to implement a control for a permanent magnet synchronous motor. As explained before, in a micro turbine, it is important to be able to control the motor having a feedback on different information. Indeed, some tasks need to be imposed to the motor in order to have a perfect efficiency of the global system and have a feedback allows to accomplish them keeping good conditions of operating. This chapter is dedicated to a good understanding of the system. It starts from the global system, the operating principle of a micro turbine and continues with two sections more precise about the PMSM to finally ends with a kind of control that could be implemented and the purpose of developing an angular position sensor in this project.

## 2.1 Microturbine

In order to understand the global system of the project, let us start with the presentation of a simplified block diagram describing the principle of operating of a micro turbine. This is shown in the Figure 2.1:

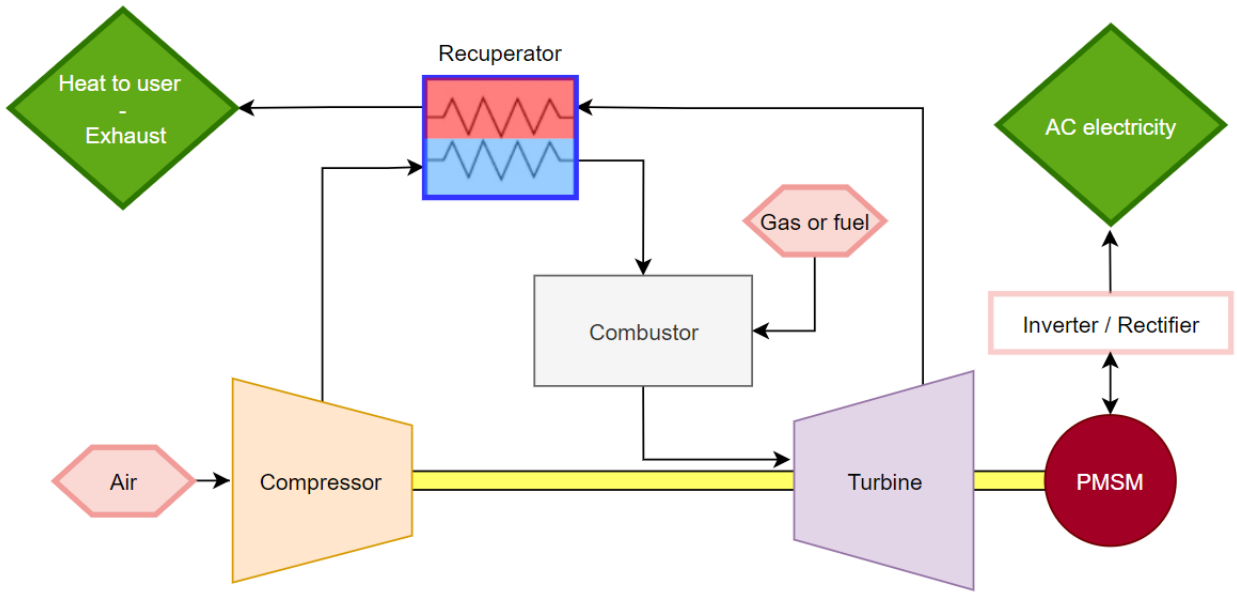


Figure 2.1 – Block diagram micro turbine

Let us start by explaining the motor mode. In this mode, the start point is in the inverter. This component is developed in the section 2.3 but for the moment it is just important to understand that it allows to set the motor in motion using an AC current whose frequency is in direct relation with the rotation speed of the motor. Then, as the motor is moving, the shaft (in yellow) is moving and so the complex compressor-combustor-turbine are in motion.
The compressor use the air as input (1 bar, 40°C) and allows to reject as output higher pressure and temperature air (3 bar, 160°C). The next step for the air is to pass through the recuperator. This part allows to be efficient using the high temperature air at the output of the micro turbine to heat the low temperature air at the output of the compressor. In the recuparator, the very high temperature air give a part of its energy to the fresh air in order to have a balance. The air cools is available for users and the air warmed (3 bar, 670°C)is sent into the combustor. This one, using hot air and gas or fuel for the combustion, will again warm the temperature of the air (3 bar, 950°C). This very hot air enters in the turbine and accelerates it. An illustration of this warming and compressing air is shown in the Figure 2.2.

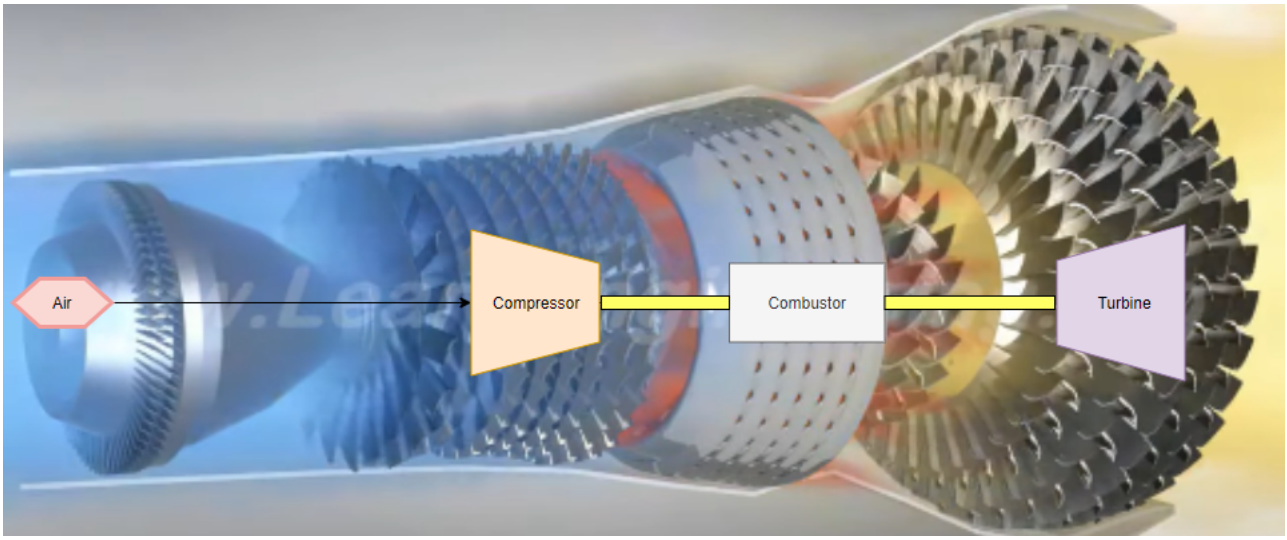


Figure 2.2 – Warming and compressing air [9]

After several seconds, the system has accumulated enough energy to switch in the generator mode. In this mode, the motor can turn no longer thanks to the inverter but thanks to the turbine and the rotation of the motor allows to generate an AC current.
This process is the principle of a micro-CHP (Combined Heat and Power) systems and it is the idea of operating of the global project.

## 2.2 Permanent magnet synchronous motor (PMSM)

A synchronous machine can be used as a generator or a motor. A generator produces a current whose the frequency is equal to the rotation speed of the motor. In the opposite, a motor is fed by an AC current and the rotation speed depends on the current frequency.
The global project consists in developing a micro-turbine using a synchronous machine for the motor and the generator that contribute to the power generation. Although the generator state is the main one of the micro-turbine (almost 99% of the time), the motor state is very important and allows to start-up the micro-turbine thanks to its mechanical energy produced by the rotation of the motor and enables to set in motion the compressor and then the turbine. Moreover, the motor state is used when the machine need to be stopped or cooled. For this specific project, only the motor

state will be considered as the purpose is to control the motor but a similar project of control could be developed for the generator.

A synchronous machine consists of two main parts, the stator and the rotor. The stator is the static part of the motor. It is composed by a cylindrical iron frame with windings located at 120 degrees from each other. With this configuration, a rotating magnetic field can be produced. The rotor is the rotating part of the motor. Composed by either a winding fed by a DC excitation current or a permanent magnet as for this project. In each case, the purpose is to have a magnetic field that wants to follow the rotating magnetic field produces by the stator.

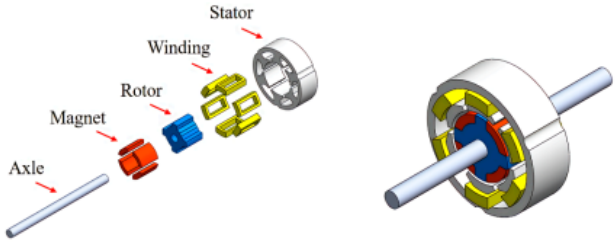


Figure 2.3 – PMSM assembly [4]

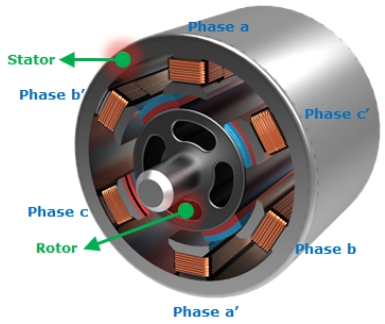


Figure 2.4 – Three-phased magnetic circuit [17]

To understand the working principle of a PMSM let us start by considering the stator windings. Each winding is fed by an alternative current with a phase shift of 120 degrees in each phase. The goal is to produce a total magnetic field rotating at a speed (in rpm) of

$$\dot{\theta} = \frac{120f}{p}$$

with $f$ the frequency of the AC current source and p the number of pairs of poles. So, for instance, with an AC current source of 50Hz and 2 pairs of poles, the rotation speed of the magnetic field generated by the stator is 1500 rpm. An illustration of the generation of the rotating field is shown below :

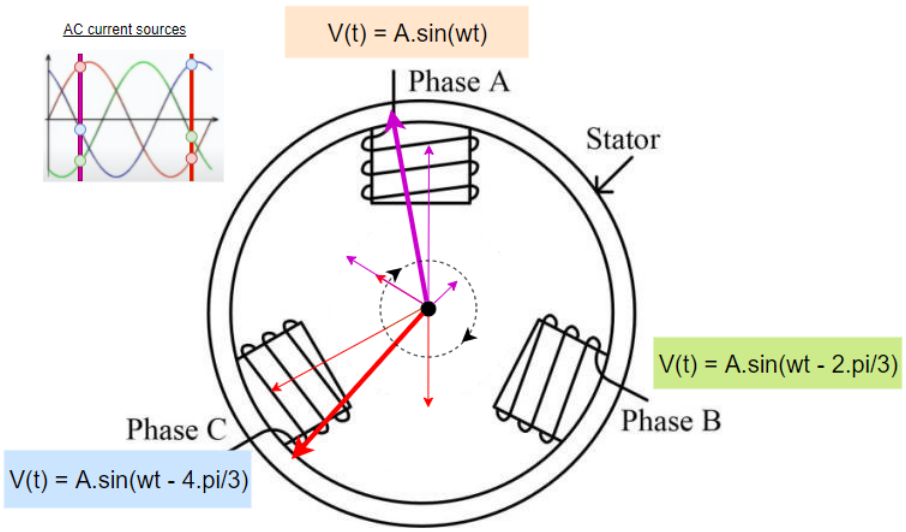


Figure 2.5 – Rotating magnetic field generation

Now, one can understand how the rotating magnetic field is generated. Indeed, at each time, a magnetic field is produced in each winding whose magnitude depends on the amplitude of the AC current which goes through itself and the direction is the same than the winding one. The resulting magnetic field is the addition of the three ones and so, as the AC current is phase-shifted by 120 degrees exactly like the angle separating each winding, the resulting magnetic field will be constant but in rotation at $\dot{\theta}$.

For instance, in the Figure 2.5, only two moments are represented but it could be easy to represent the magnetic field at each time and see that it is rotating. Here, for the moment marked by the purple line, the phase A generates a magnetic field positive and bigger in magnitude than B or C. Then, C has the smallest magnitude and is negative and finally B has a medium magnitude and is negative, the total magnetic field is the sum of the three and it is represented by the large purple arrow. The same reflection is done for the red moment and one can see that, indeed, between the purple and the red moment, the magnetic field has rotated.

The final step to understand the working principle of a permanent magnet synchronous machine is to consider the second part, the rotor. This one is a permanent magnet, placed at the center of the stator. The magnet is, in reality, a magnetic field. In fact, the magnetic field of the rotor and the one of the stator will tend to align each other. In this case, no load torque is applied and the rotor is rotating at $\dot{\theta}$ which is called the synchronous speed.

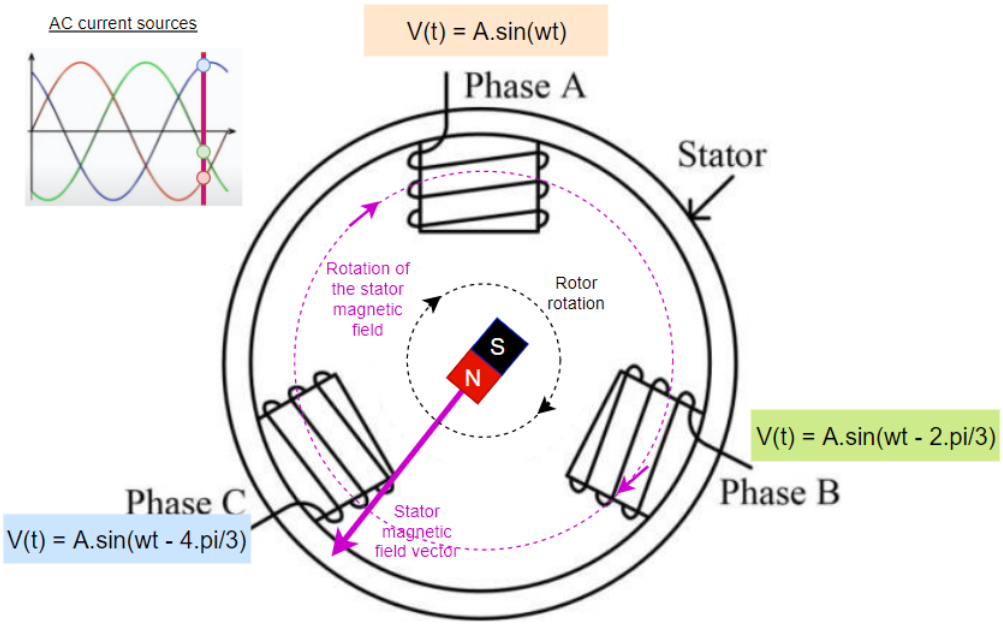


Figure 2.6 – Working principle PMSM

In the case where a mechanical torque is applied, the rotor brakes a number of degrees with respect to the stator rotating magnetic field, continuing to follow it but with a little late in order to develop a torque and counter the mechanical one which is applied to the machine. Note that the maximum phase shift between the two fields is 90 degrees, if it is bigger, the rotor is no longer able to follow the stator magnetic field and the synchronous speed is lost. So, in other word, the maximum torque that can be produced by the rotor is when the angle between the two field vectors is equal to 90 degrees. This maximum angle can be explained by the Potier diagram [7]. First, let us assume

that the electromagnetic power is equal to the electrical power [W] such as :

$$P_{elm} = P_{elec} = 3UI\cos\phi$$

with :

- $I$, the current applied for one phase [A];
- $U$, the voltage applied for one phase [V];
- $\phi$, the phase shift between the $U$ and $I$ .

The relation between the torque C $[\mathrm{N}\cdot\mathrm{m}]$ and the power is the following :

$$C = \frac{P}{\frac{\omega}{p}} = \frac{3p}{\omega}UI\cos\phi$$

- $\omega$, the rotation speed $[\mathrm{rad\,s^{-1}}]$;
- $p$, the number of pairs of poles.

The equivalent circuit of a 3-phase permanent magnet synchronous machine can be represented as following : first, the rotor being in rotation at synchronous speed, the coils of the stator are subjected to the magnetic field of the rotor. So, an electromotive force (EMF), $E_b$, is induced into the armature windings having as effect that the armature reaction voltage lags the current by 90 degrees. Moreover, the self-inductance in each phase has a resistance due to its winding, it is represented by $R_a$. This yields to this first equivalent circuit with the following voltage loop equation :

$$E_b = U_n - jI_aX_s - R_aI_a$$

$X_s$ being the synchronous reactance (armature reaction and self-inductance of one phase of the stator)

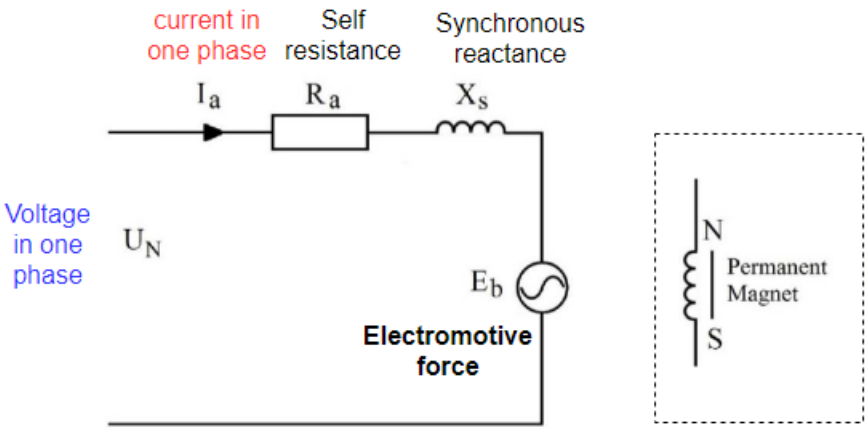


Figure 2.7 – Equivalent circuit one phase of a PMSM

Then, choosing the voltage $U_n$ as the reference, one can represent the synchronous motor phasor diagram, also called Potier diagram. This one consist in representing the voltage loop equation in a phasor form.

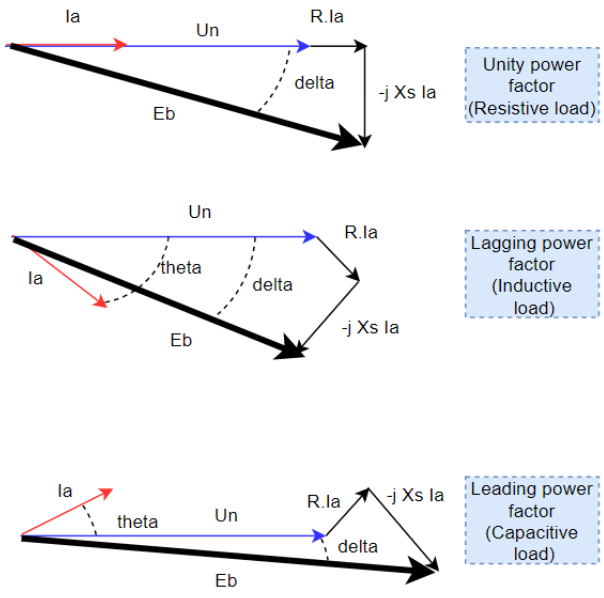


Figure 2.8 – Phasor diagram of a PMSM

The last step is to understand the link between the torque C and the angle (noted delta, $\delta$) separating the phasor $U_n$ and $E_b$. For that, let us show an additional diagram. On this one, a braking torque is applied and $E_b$ is late compared to $U_n$ ($\delta$ is negative). This configuration is the typical one of the motor. Indeed, for the alternator mode, $E_b$ is ahead of $U_n$.
So, as can be seen in the following Figure, assuming that $R_a I_a$ is negligible, the projection of the phasor $-j\ X_s I_a$ on the vertical plane and the one of $E_b$ on the same plane are equal.

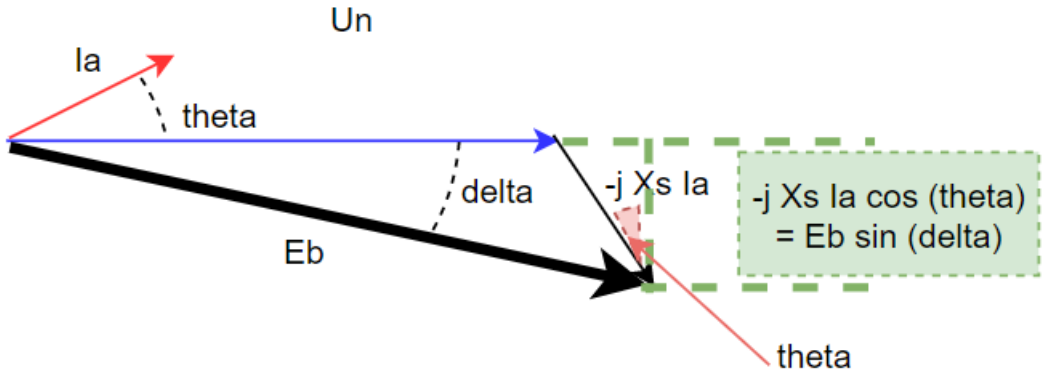


Figure 2.9 – Phasor diagram of a PMSM, projection equivalence

Finally, the expression of the torque can be rewritten such as :

$$C = \frac{3p}{\omega} U I \cos\phi = \frac{3p}{\omega X_s} U E_b \sin\delta$$

with $\delta$ also called the internal angle.

The maximum value of torque occurs when the sine is maximum in absolute value which is an angle of 90 degrees. Note that in motor mode, the torque is always negative, $E_b$ is late with respect to $U_n$. To conclude, have a feedback on the angular position and the motor speed is an advantage considering the previous explanation. Indeed, with a closed-loop control, one can limit the maximum internal angle at 90 degrees in order to have the best acceleration of the motor while maintaining the synchronous speed. Without this control, the internal angle could be bigger than 90 degrees to accelerate faster but, in this case, there is no longer a physical sens. The magnetic field of the rotor will loose the rotating one of the stator and the speed synchronous will be lost.

## 2.3 Sinusoidal driving of a 3-phase PMSM

As explained in the previous section, the rotation speed of a PMSM is called the synchronous speed and is such that :

$$\dot{\theta} = \frac{120f}{p}$$

with $f$ the frequency of the AC current source and $p$ the number of pairs of poles. In other words, the rotation speed of the motor depends directly on the frequency of the AC current source. So, the rotation speed can be chosen by this frequency and it is done by the sinusoidal driving.
First, let us start with a basic schematic of a PMSM circuit controlled by an inverter.

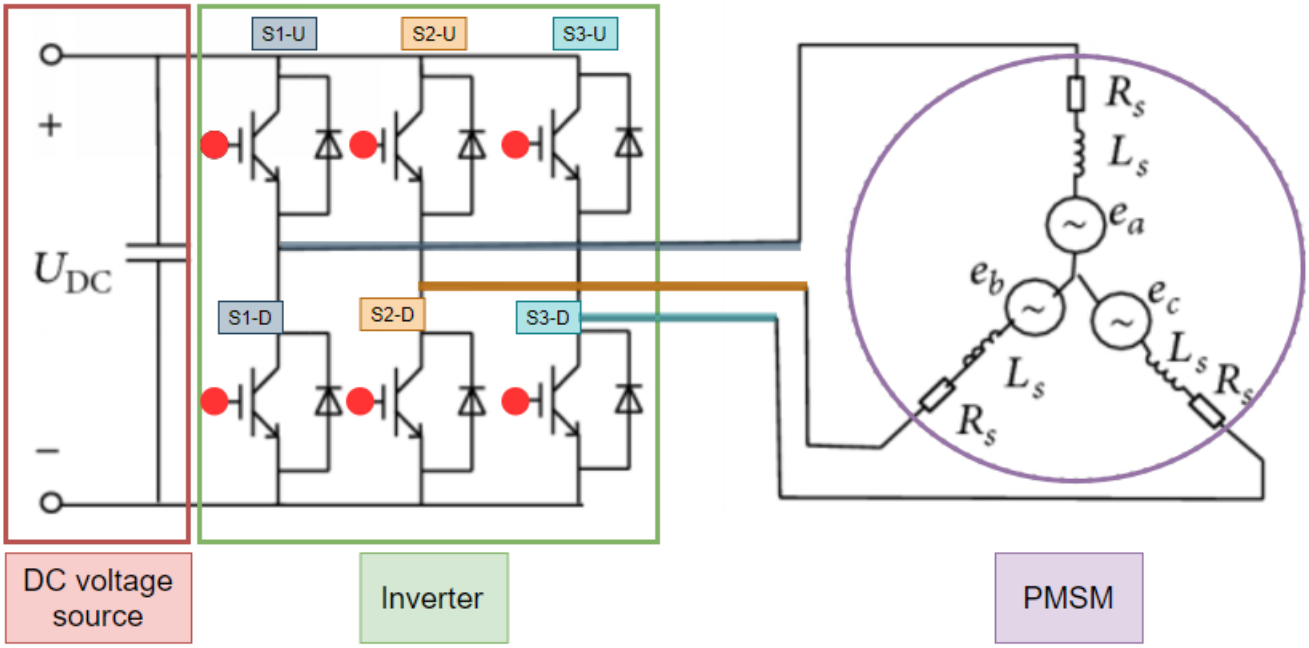


Figure 2.10 – Basic schematic inverter/PMSM circuit

As it can be seen in the Figure 2.10, the PMSM is fed not by directly an AC current source but by a DC source voltage transformed thanks to an inverter. This inverter is composed by 6 switching elements. Here, there are six IGBTs which are great to limit the commutation and conduction losses but accept a frequency of switching lower than the maximum one of the SiC (Sillicon Carbide) for instance. Moreover, MOSFET are adapted for high frequency but not for high voltage system as it is the case in this project. In fact, the nature of the switching element depends on the application and there are some trade-off to make the best choice but this choice is not the subject of this project. In this Figure 2.10, the DC voltage source is connected to three branches (S1-S2-S3) with 2 switching elements (U =

Up, D = Down) on each one. Each branch corresponds to one phase. Let consider only one phase (S1 for instance), the two others being the same principle but with a phase shift of 120 degrees. Each switching element is control by its gate (red point). When the gate is set, the switch is closed and the current can pass through the switch like a short-circuit. The principle is to set S1-U and S1-D alternatively in order to construct a sinusoidal signal. Indeed, as the circuit is symmetric, an artificial neutral is created between the two switches and so, if S1-U is conducting (ON), the output signal is positive and when S1-D is not conducting (OFF), it is negative and the amplitude depends on the period during which the switch is ON. To avoid a short-circuit in parallel with the source, at least one switch has to be OFF and cannot conduct at each time. At the end, choosing the time during which each switch is ON, one can create a sinusoidal output signal as an AC source for the stator of the PMSM.
Now that the idea of alternative output signal is understood, one need to understand how the period of switch ON can be found to have the frequency of the sinusoidal signal that we want. For that, a "carrier" signal is used. This one is a triangular signal with a frequency about 10 times larger than the one of the final signal. This carrier is compared to the desired sine signal in order to obtain the proper PWM (Pulse Width Generation) signal connected to the gate. As a sine signal is symmetric, the supply voltage of one gate (S1-U) is exactly the same for the other gate (S1-D) but inverted. Moreover, the PWM of the two others branches are obtained in the same way with the same "carrier" signal but with a phase shift in the desired sine signal. The PWM generation for one phase is illustrated below :

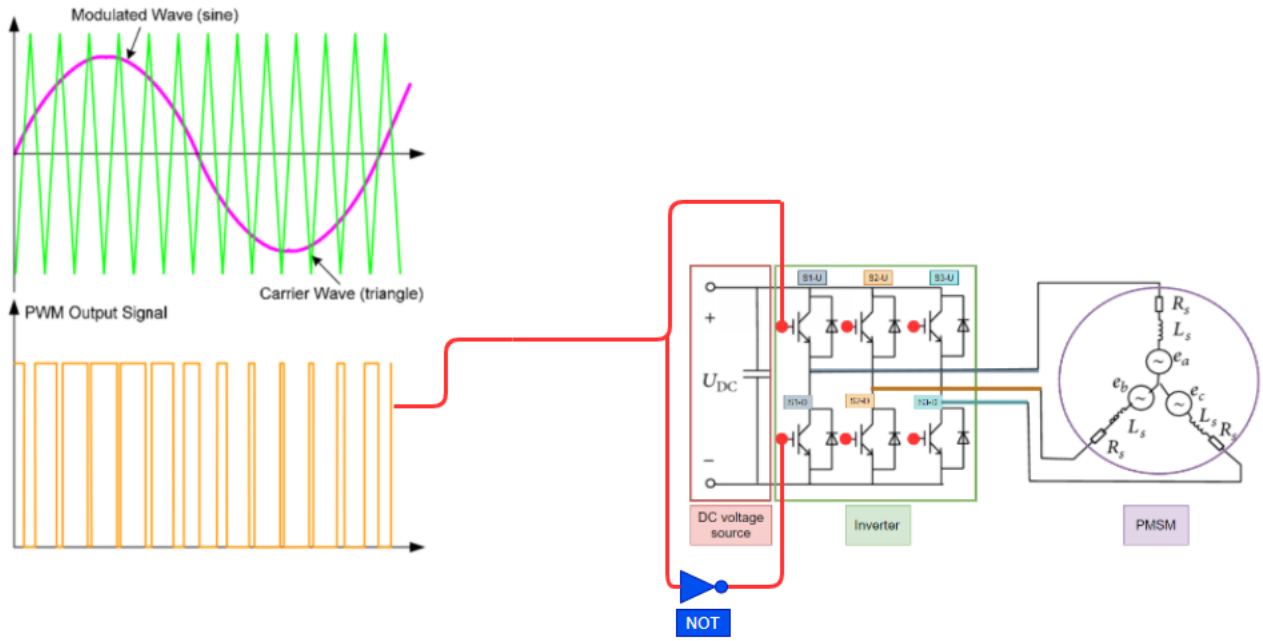


Figure 2.11 – PWM generation in order to construct a sinusoidal signal

As it can be seen in the Figure 2.11, the PWM is generated by comparing a reference sine signal and a triangular signal (the carrier). When the reference is greater than the carrier, the output signal is set (switch ON) and when it is smaller, it stays to zero (switch OFF).
Finally, the frequency of the AC current source, giving the motor speed, can be chosen constructing a PWM which corresponds to the desired signal.

## 2.4 Control idea

To close this introduction, it could be useful to finish with the basic idea of the future control that could be implemented in order to have the best efficiency. A first idea is to control the speed of the motor having a feedback on the actual speed and the actual angular position. A block diagram of the closed-loop speed control that could be implemented later is presented below :

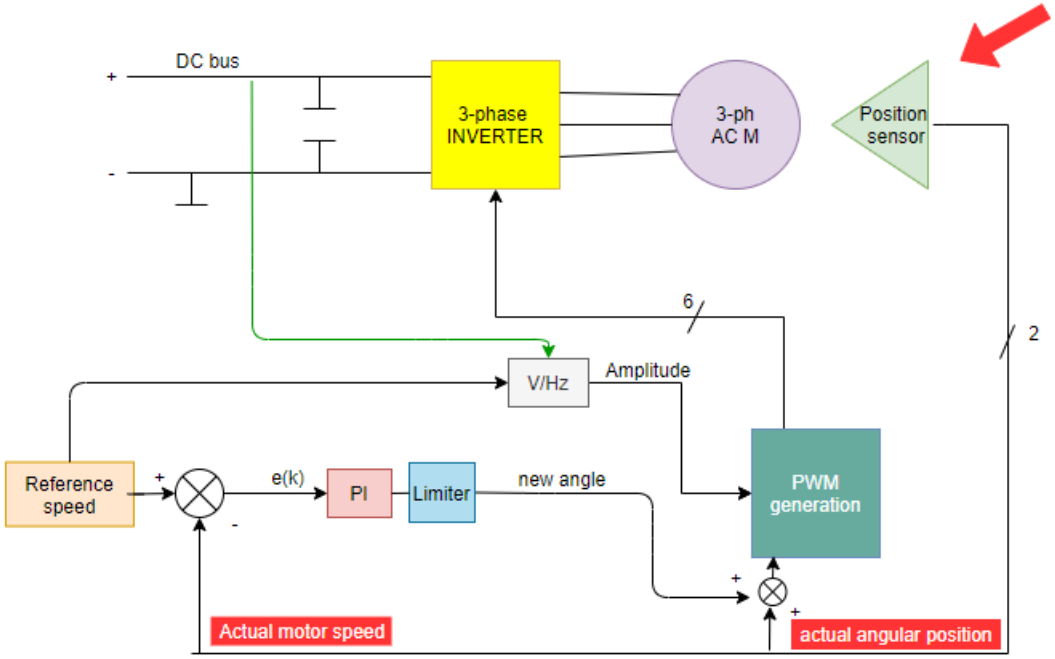


Figure 2.12 – Block diagram : Closed-loop speed control

This block will be explained in detail in the Chapter 6. For the moment, it is just important to understand the role of the position sensor which is the most important part of this project.
In fact, the sensor gives a feedback on the actual angular position and the speed of the motor. With the speed information, a PI is implemented in order to have the appropriate angle needed to adapt the sine signal and so the frequency which give the desired speed. This new angle added to the actual angle (considered as an offset angle) gives the perfect argument for the needed sine which will generate the specific PWM at each step time. Finally, the AC motor speed is controlled, the acceleration can be done progressively and smoothly in order to improve the efficiency. Note that the block V/Hz used to have the appropriate amplitude in function of the frequency will be developed in the Chapter 6. Moreover, in the same chapter, an improvement of this control will be developed. This one corresponds to a torque control mixed to this speed control with a result which is very interesting.

# Chapter 3

# Review of state-of-the-art position sensors

This chapter is dedicated to compare different kind of angular position sensor. The goal of this chapter is to choose the most appropriate sensor in order to be able to acquire data considering the constraints of the project. The most important constraint is the high rotation speed. Indeed, in the global project, the final goal being to have a combustion at very high temperature, the rotation speed of the compressor has to be very high and so the rotation speed of the motor is about 120 000 rpm. This very high speed induces required characteristics for an adapted sensor :

- Contactless sensor to avoid weak
- Resistant to harsh environment
- Balanced geometry that does not disturb the balance of the global system. Indeed, at high speed, a very low unbalance in weight could be very important at high speed due to inertia.
- High sensitivity and accuracy

The comparison is done between four kinds of sensor presented in the following sections:

- 3.1 Eddy current sensor (Inductive sensor)
- 3.2 Hall effect sensor (Galvanomagnetic sensor)
- 3.3 Capacitive sensor
- 3.4 Optical sensor

The information presented in this Chapter comes from the course of *"Sensors, microsensors and instrumentation"* given by Mr Philippe Vanderbemden at the University of Liège [26].

## 3.1 Eddy current sensor

### 3.1.1 Physical theory of operation

When a magnetic field is varying with respect to the time, Eddy currents are induced in any conducting plate in the vicisity of the coil in order to oppose the variation and it is done thanks to the generation of an induced magnetic field $B_2$. The basic idea linked to this physical phenomenon is to use a primary and secondary coils. The primary one is fed by an excitation sinusoidal current an generates a variable magnetic field. The secondary coils subject to this same

varying magnetic field develop an induced emf that can be measured. The effect of the occurrence of Eddy current is a decrease in the magnetic field embraced by the primary coil and so the output voltage measured at the extremity of a secondary coil will change if the conducting plate is present or not. Attaching a piece of conducting plate on a rotating target, the output voltage measured will change with the rotation of the target and one can know easily the angular position of the target.
The particularity of this sensor is to return an absolute angle as output. Moreover, the sensor does not need to be close to a magnet, it just needs coils made of few turns and a metallic plate in motion. Then, it is robust, contactless and very sensitive and accurate. Finally, the high impedance of the excitation coil ($X = j\omega L$ with $\omega = 2\pi f$ and $f$ about 1 to 5 $\mathrm{MHz}$) brings to a small input current and so low power consumption. The bad point is about the complexe design and minimum dimension required for the diameter and the thickness of the plate so it cannot be miniaturized.

## 3.2 Hall effect sensor

### 3.2.1 Physical theory of operation

The Hall effect is due to two transverse forces applied to carriers :

- Lorentz force : $\vec{F} = (q\vec{v}) \times \vec{B}$
- Electrostatic forces caused by transverse charge : $\vec{F} = q\vec{E_H}$

Matching the two forces, one have the following relation :

$$\vec{E_H} = -\vec{v} \times \vec{B} = \left(\frac{1}{n \cdot e}\right) \vec{B} \times \vec{J}$$

with the second equality coming from the Ohm's law :

$$\vec{v} = \mu \vec{E}$$

$$\vec{J} = n \cdot e \cdot \mu \cdot \vec{E} = \sigma \vec{E}$$

with :

- $J$, the current density $[\mathrm{A\,m^{-2}}]$;
- $n$, the density of charge carriers $[\mathrm{m^{-3}}]$;
- $e$, the charge $[\mathrm{C}]$;
- $v$, the velocity $[\mathrm{m\,s^{-1}}]$;
- $\mu$, the mobility $[\mathrm{m^2\,V^{-1}\,s^{-1}}]$;
- $\sigma$, the conductivity $[\Omega^{-1}\,\mathrm{m^{-1}}]$.

These laws describe the fact that when a current is subject to a magnetic field, the carriers are forced to move in the direction gives by $\vec{E_H}$ and using the right-hand-rule (RHR). Be careful to the sens of the vectors when using the RHR, indeed, if it is electron that is considered, the charge is negative and so the sens of $\vec{B}$ is reversed.

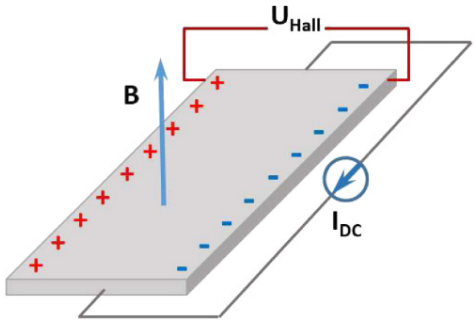


Figure 3.1 – Hall probe design [11]

The basic principle is the following : a Hall probe is used (this one can be seen in the Figure 3.1 in grey) and fed by a DC current. When the probe is subject to a magnetic field, a voltage ($U_{Hall}$) becomes different from zero whose the sign and the amplitude depend respectively on the sens and the direction of $\vec{B}$. If $\vec{B}$ is vertically upward, the negative charges will be forced to move to the right side (left side for positive charge) and the measured voltage $U_{Hall}$ will be the maximum voltage. If $\vec{B}$ is identical but downward, it is the opposite and $U_{Hall}$ will be the minimum voltage. Finally $U_{Hall}$ is equal to zero when $\vec{B}$ is parallel to the probe. Intermediate values occur with an inclined $\vec{B}$. An angular position and speed sensor based on this effect can be easily developed. Indeed, an encoder as shown in the following Figure is based on this principle. It consists in a probe subject to a permanent magnet. It can be designed by different way in function of the application but the one that will be illustrated here is the one used for a PMSM speed measurement.

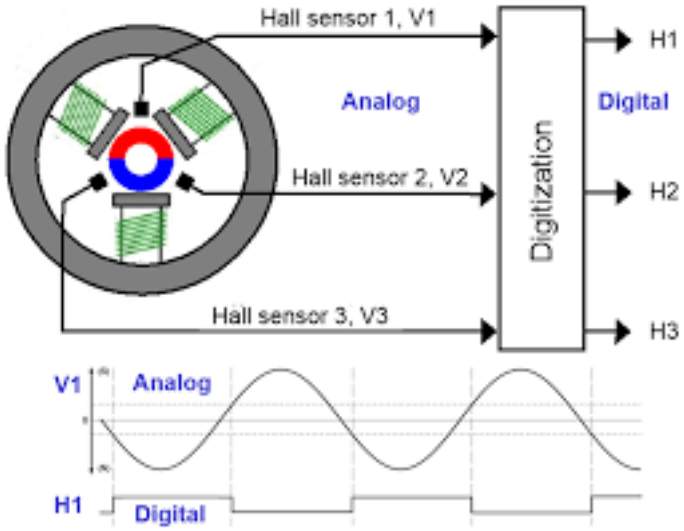


Figure 3.2 – Hall effect - output signal [28]

Using the fact that V is varying with the magnetic field and so the position of the permanent magnet, it is easy to know the position and the rotation speed of the rotor.
The particularity of this sensor is to be very robust, contactless, resistant to harsh environment and very accurate. The disadvantages are that it requires a proximity with the magnet for its operation, and it is sensitive to external magnetic field. Moreover, its lifetime with high temperature is low which leads to a frequent maintenance. Finally, there are three sensors that try to determine the angular position but there is inevitably a loss of information.

## 3.3 Capacitive sensor

### 3.3.1 Physical theory of operation

The basic principle of a capacitive sensor is to create a variation in the value of its capacitance. Indeed, the capacitance [F] is expressed such as :

$$C = \frac{\epsilon_0 \epsilon_r S}{d}$$

with

- $\epsilon_0$, vacuum permittivity equal to $8.854 \times 10^{-12}$ $[\mathrm{F\,m^{-1}}]$;
- $\epsilon_r$, relative permittivity of the dielectric material between the 2 plates;
- S, the active area $[\mathrm{m}^2]$;
- d, the distance between the two plates $[\mathrm{m}]$.

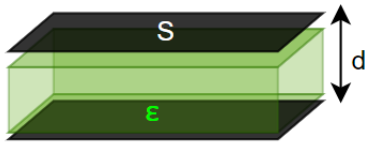


Figure 3.3 – Capacitor specifications

Creating a variation in S, d or $\epsilon$, the capacitance value (C) changes and one can detect it by measuring the impedance. The most popular angular position capacitive sensor is a sensor based on the active area S. Using the fact that when the surface shared by the two parallel plates is changing (variation of S), C changes. The principle is to fix a semicircle as the first plate and attach an other one as the second plate to the target in rotation. As the second plate is moving, the surface S is changing with time and it is proportional to the output voltage. So, measuring the impedance of the capacitor, one can know S and so the angular position of the moving part.

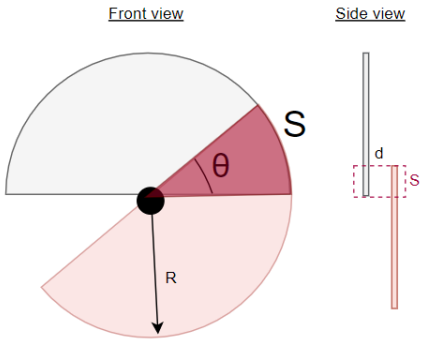


Figure 3.4 – Angular position capacitive sensor

The capacitive sensor is contactless. Its particularity is its design simplicity, its robustness and its weak temperature dependence. Indeed, at high frequency (about 1 MHz), the relative permittivity does not change drastically with the temperature. The other parameters do not depend on the temperature. The disavantages are about the capacitance measurement that require a LCR meter, and its is really less accurate than an inductive sensor.

## 3.4 Optical sensor

### 3.4.1 Physical theory of operation

The most popular optical sensor to measure an angular position is an encoder which consists in a transmitter and a receiver. The transmitter sending a beam of light at each time, the receiver is waiting for it. When the receiver detects the beam of light, the output is set to 1. In the opposite case, the output stay to zero. Using an opaque circle plate moving with the rotating target and designing with a lot of holes it is easy to know the angular position by counting the number of step, each step corresponding to a predetermined angle. An illustration of this sensor is shown below :

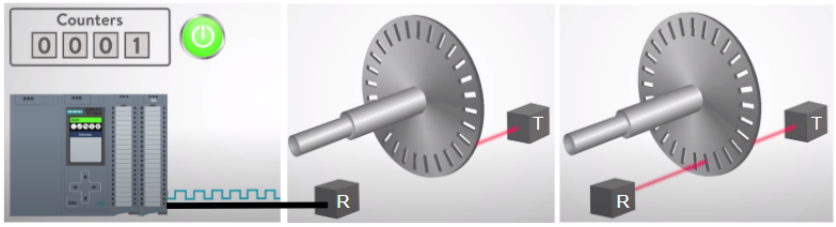


Figure 3.5 – Angular position optical sensor [16]

This sensor is contactless. Its particularity is to be based on light. The light having a wavelength of 500$\mathrm{nm}$, this sensor can detect very small object and can be miniaturized. Moreover, its frequency being in the range of 400$\mathrm{THz}$, it is completely insensitive to parasitic signals. The bad point is due to its sensitivity to any other source of light and obstructing object.

## 3.5 Sensors comparison

In order to visualize which are the advantages and disadvantages of each sensor, a comparison is done for several characteristics in the Table 3.1 below :

| | Eddy current sensor | Hall effect sensor | Capacitive sensor | Optical sensor |
|---|---|---|---|---|
| Absolute angle output | yes | no | yes | no |
| Sensitivity | very high | high | medium | high |
| Accuracy | very high | high | low | low |
| Resistant to harsh environment | high | high | medium | medium |
| Contactless | yes | yes | yes | yes |
| Temperature dependence | high | high | low | low |
| Affected by external light | no | no | no | yes |
| Cost | low | medium | high | high |
| Robustness | high | high | high | medium |
| Can be miniaturized | no | no | no | yes |
| Design complexity | high | high | low | low |
| Accepted range of rotation speed | large | large | large | low |

Table 3.1 – Comparison between the four different position sensors

## 3.6 Conclusion

Following the analysis of this chapter, the sensor chosen for this project is an inductive sensor based on Eddy current. Indeed, the rotation speed of the motor being about 120 000 rpm, the high accuracy and sensitivity is very interesting. Moreover, as in the control the actual angle is needed at each time, a sensor having as output an absolute value is perfect for the application. Finally, this kind of sensor is robust, resistant to harsh environment such as vibration at very high speed, it can be adapted to the particular shape of the system and the most important, it is contactless and so with a theoretical infinite life size. The particular sensor that is chosen for the project is an IPS2200 from Renesas company [18]. This one can reach a rotation speed up to 250 000 rpm and is really appropriate for the motor application. It is a new technology that has just become recently available, precisely in 2020, the design is a challenge but it promises very good result. An illustration of the Eddy current sensor can be seen in the Figure 4.1.5.

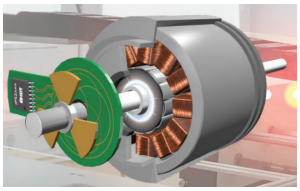

Figure 3.6 – Eddy current sensor (green) - IPS2200 from Renesas [20]

With the intention to be effective, different steps are followed in this project.
Once the choice of the more appropriate sensor is made, the practical part can start. First, a development kit provided by Renesas [19] is used to understand to physical principle of the sensor. This kit is composed of one Eddy current sensor and one board that allows a communication between the sensor and the computer. Then, a new Eddy current sensor is designed and adapted to the dimensions of the project. Still using the board of the kit, the new sensor can be tested and a communication with the computer is possible. The final step consists in developing the software on a micro-controller with the purpose of completely forget the board provided by Renesas but use directly our proper communication with the computer. This is the subject of the two next Chapter, with the hardware design in the Chapter 4 and the software development in the chapter 5. An illustration of these different steps is shown in the Figure 3.7.

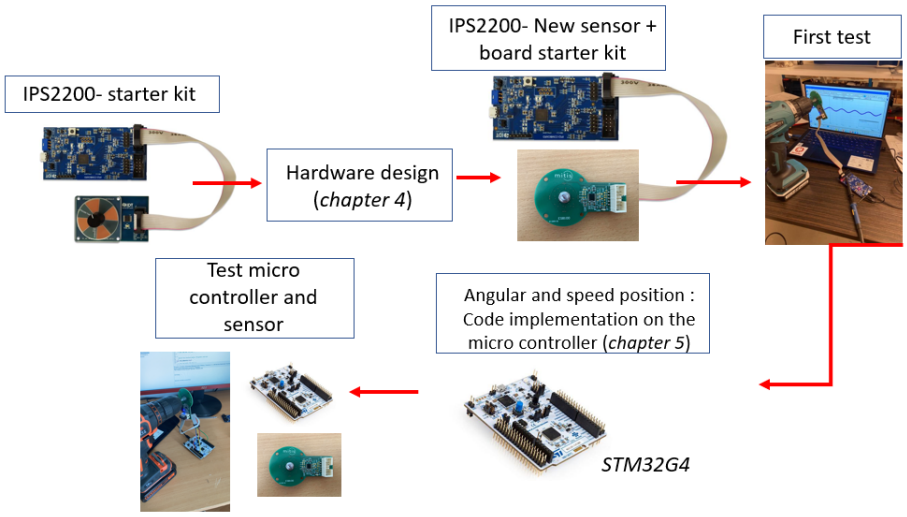


Figure 3.7 – Planning of the Eddy current sensor development

# Chapter 4

# Hardware design of an Eddy current sensor

This chapter is dedicated to the angular position sensor chosen for the project. As explained in the previous chapter, a sensor based on Eddy current is the most appropriate to reach a very high rotation speed (120 000 rpm). The development of the sensor is based on the documentation, application notes, evaluation kit and application provided by Renesas [18]. The sensor is the IPS2200 whose the datasheet is referred by [21].
In this part, I started by having a good understanding of the sensor by using all the documents provided by Renesas. The purpose of this part is to determine exactly how the sensor can be designed with respect to mechanical constraints. As these mechanical constraints were very strict and that the electrical specifications depend directly on the dimensions of the sensor, the challenge was to choose appropriate electrical components, and design the PCB to have a sensor perfectly that operates with a good accuracy and adapted to the motor of the project.
In this chapter, theoretical notions are first presented. The following sections concern the working principle of the sensor, the different steps that I performed in order to choose the right electrical components and right dimensions and finally, explanation of how I designed and thereby produced the sensor.

## 4.1 Theoretical notions used for the sensor

The inductive sensor is based on different electrical principles such as LC oscillator, RC filter, magnetic field of current loop, wireless power transfer and finally the Eddy current. This section describes these different principles and help to understand the working principle of the sensor explained in the next section.

### 4.1.1 LC circuit

LC circuit, also called tank circuit or oscillatory circuit is used to produce electrical oscillation at any frequency as it depends on the capacitor and inductor value.
The LC circuit working principle is based on different steps. First, the capacitor is charged by an external DC source. The switch between the inductor and the capacitor is opened :

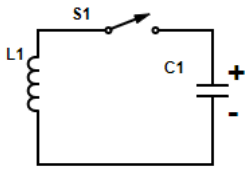


Figure 4.1 – Capacitor charging by DC source

Then, as shown in the following figure, the capacitor is charged with a positive and a negative plate creating electrostatic energy and so there is a voltage across itself. When the switch is turn-off, the capacitor can discharge its energy in the inductor and a current flow appears as indicated below :

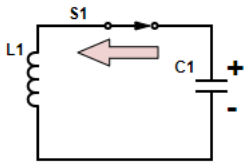


Figure 4.2 – Capacitor discharging

The current flow progressively achieve its maximum value in the inductor and a magnetic field inside and around the coils is produced. The electrostatic energy of the capacitor is converted in electromagnetic energy. When the capacitor is completely discharge, the magnetic field start to collapse and try to stop its variation creating a counter emf as defined by the Lenz's law such as :

$$e = -\frac{d\Phi}{dt}$$

with $\Phi$, the magnetic field flux. So a current flow appears between the inductor and the capacitor which is charging in the opposite polarity than the previous step.

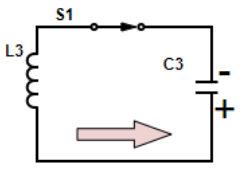


Figure 4.3 – Capacitor recharging in the opposite direction

Then, the circuit acts exactly like before but the current flow is now in the opposite sens.
Finally, we can observe a voltage signal oscillating at the resonance frequency. This one appears when the reactance of the inductor is equal to the one of the capacitance. So we can know the frequency using the small development below

$$X_L = 2\pi f L$$

$$X_C = \frac{1}{(2\pi f C)}.$$

Using these two relations, we have :

$$X_L = X_C$$

$$2\pi f L = \frac{1}{(2\pi f C)}$$

$$f^2 = \frac{1}{4\pi^2 LC}$$

$$f = \frac{1}{(2\pi\sqrt{LC})}.$$

And so the oscillator frequency depends only on the value of C and L.

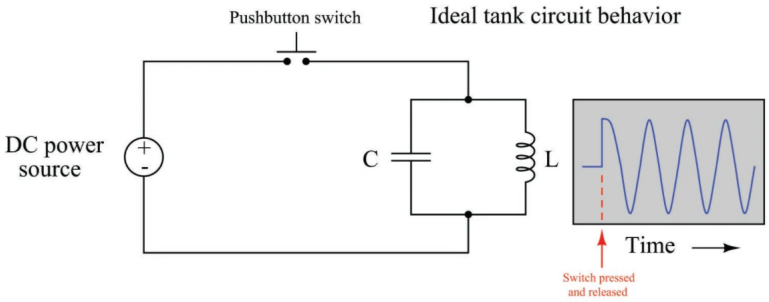


Figure 4.4 – LC oscillator output signal [2]

Note that due to dielectric and resistive losses in the capacitor and inductor respectively, a small part of energy is lost at each cycle so for a continuous oscillation with a constant magnitude voltage, a supply amount of energy is needed after a proper interval of cycle.

### 4.1.2 RC filter

The simple RC circuit is a first-order passive low-pass filter. It is used to reject undesired high frequencies of an analog signal and keep the low frequencies. It can be useful when the noise need to be rejected in order to keep only the useful part of the electrical signal.
A low-pass filter is characterized by its cut-off frequency expressed by $f_C = \frac{1}{2\pi RC}$.After this frequency, the gain of the signal goes down and so the parasitic frequencies are removed from the final signal. This principle is illustrated below :

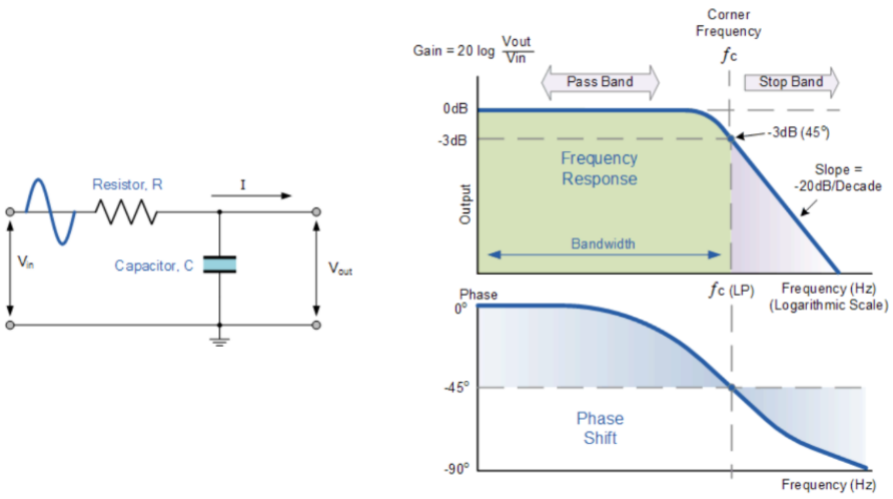


Figure 4.5 – RC circuit - Gain w.r.t frequency [25]

### 4.1.3 Magnetic field of current loop

A circular current carrying-wire produces a magnetic field with a bigger concentration in the center of the loop than the concentration outside. The direction of the magnetic field can be simply determined using the right hand rule, with the thumb showing the direction. Then the magnitude $[\mathrm{T}]$ is expressed as below:

$$B = \frac{\mu_0 I}{2R}$$

with:

- $\mu_0$, the vacuum permeability equals to $4\pi \times 10^{-7}$ $[\mathrm{H\,m^{-1}}]$;
- $I$, the carrying-current of the loop $[\mathrm{A}]$;
- $R$, the radius of the loop $[\mathrm{m}]$.

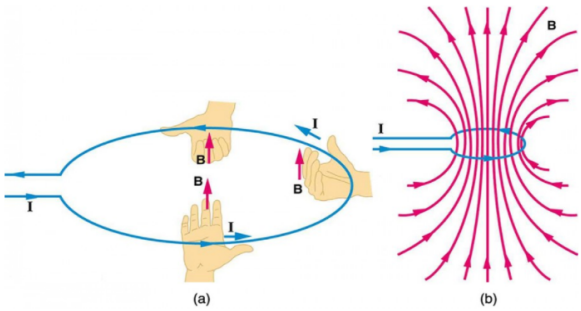


Figure 4.6 – (a) Right-hand-rule (b) Magnetic field in a current loop [10]

### 4.1.4 Wireless power transfer

A wireless power transfer consists in transmitting energy using electric or electromagnetic field. For instance, a capacitive coupling is an energy transfer by means of an electric field and an inductive coupling, the conjugate of the

capacitive one, is a transfer by means of an electromagnetic field.
In this section, although the capacitive coupling be equally interesting, one will be focused only on the inductive coupling which will be very useful to understand the section 4.2.
For an inductive coupling, there is a transfer of power between two coils. One coil is the transmitter and the second one is the receiver. The both form a transformer. The working principle is the following : an AC current is carrying the transmitter which creates, by Ampere's law, an oscillating magnetic field in and around the transmitter coil. Then, by Faraday's law of induction, this oscillating magnetic field passing through the second coil will induces an alternative electromotive force in the receiver. Finally, this EMF creates an AC current in the receiving coil with a frequency proportional to the transmission efficiency. This wireless power transfer is illustrated below :

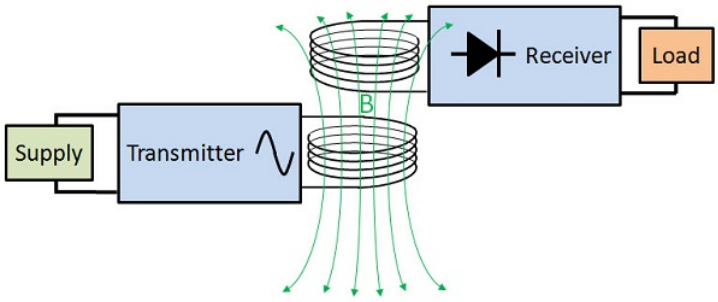


Figure 4.7 – Wireless power transfer : Inductive coupling [27]

### 4.1.5 Eddy current

The Eddy current phenomenon is the most important physical principle on which the position sensor is based. Also called Foucault's currents, Eddy currents are electrical current loops induced within conductors. Indeed, by the Faraday's law, when a magnetic field is changing in a conductors, an EMF is induced and creates an AC current. In other words, when a conductor like a metallic plate is subject to an oscillating magnetic field, current loops appear in the plate and they are called Eddy current. Note that the oscillation of the magnetic field can also be due to a relative motion between a constant magnetic field and the conductor.
In fact, loops are created in order to neutralize the change in magnetic field which is happening in the conductor. This principle is the Lenz's law :

$$EMF = -\frac{N d\phi_B}{dt}$$

with :

- N, number of turns (1 in the case of a metallic plate : 1 simple loop);
- $\phi_B$, magnetic field flux.

When here is AC current circulating in a conductor, the skin effect has to be taking into account. This one describes the phenomenon where the current density is largest near the surface of the conductor and decreases exponentially when it moves away from the surface goes inside the conductor. It said that the current was moving only in a "skin" whose the formulae is expressed below to simulate the fact that inside the conductor, the current density is almost null regarding the density near the surface. So the skin thickness $[\mathrm{m}]$ is calculated as following (note that this formulae can be used assuming that the frequency is away from strong atomic or molecular resonances):

$$\delta = \sqrt{\frac{2\rho}{\omega\mu}}$$

with:

- $\rho$, the resistivity of the conductor $[\Omega\,\mathrm{m}]$;
- $\omega$, the angular frequency of current ($\omega = 2\pi f$, with f the frequency $[\mathrm{Hz}]$);
- $\mu$, the permeability of the conductor $[\mathrm{H\,m^{-1}}]$.

## 4.2 Working principle

As explained in the previous section, the position sensor developed in this chapter is based on the Eddy current principle. To understand why, let's start with the basic idea of body design of the sensor and continue with the electrical design that will be explained more precisely how the position can be acquired as the output data of this sensor.

### 4.2.1 Body design

The sensor is composed by a first part containing three coils that form a transformer. One coil, the transmitter one, is subject to an AC current produces by an LC oscillator. Indeed, the DC current source of the micro-controller need to be transform in an oscillating voltage source in order to produce a magnetic field in the transmitting coil. The second and third coil, acting as a receiver individually, will be subject to an oscillating magnetic field and so an AC current will be created in the coils.
With the presence of a metallic plate in relative movement with the coils, Eddy current are induce in the plate to oppose the variation of the magnetic field and so the voltages measured across the two receiver coils are related to a sine and cosine values which give a precise angular position.
The body design is illustrated below, the first Figure shows different configuration to use the sensor and the second one shows the design of the metallic plate with respect to the number of poles of the motor :


Figure 4.8 – Up : Design with respect to the shaft configuration. Down : Target design with respect to the number of pole pair [20]

For the particular application of the project, the end-of-shaft configuration will be designed for the part containing the transformer and for the target, the 1-pole pair configuration is used as the motor is characterized by only one pair of poles. The choice of the semicircle for 1-pole pair will be clearly explained in the section 4.2.2.

Finally, the basic sensor design is the one illustrated below :

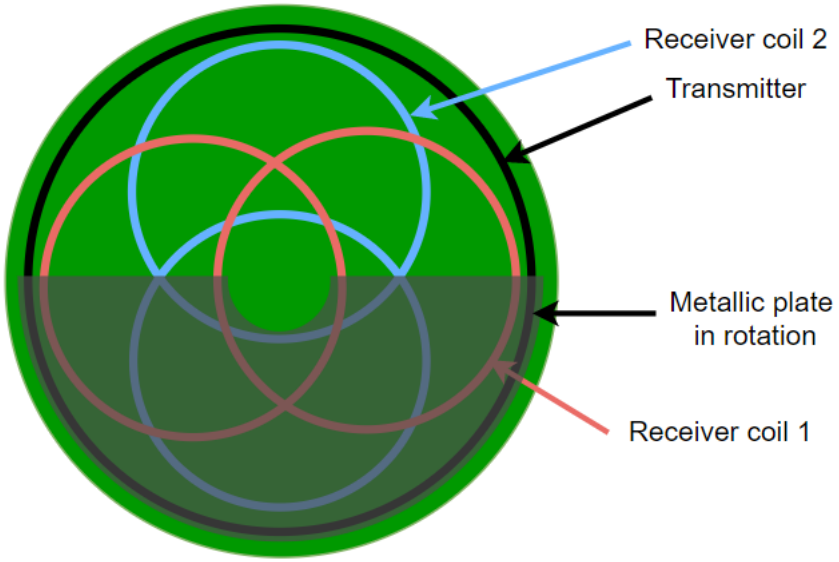


Figure 4.9 – Basic sensor design

### 4.2.2 Electrical design

To understand more precisely how is working the sensor and how the sine and cosine signals are obtained, it is necessary to understand exactly the precise design of the coils and how is varying the output voltage of each receiver coil according to the target position.

First, let's start with the coils design. As explained earlier, a transmitter fed by an alternative current produces a magnetic field changing with respect to the time. A receiver coil, subject to this magnetic field react to counter this change in its winding by inducing an electromotive force resulting in a voltage across the coil of the receiver. To understand how an angular position can be obtained using this sensor, at first, one will not consider the conductive plate (the target). The sensor has a transmitter which surrounds two receiver coils. In this way, the two receiver coils being designed exactly in the same way (radius of the coil, number of turns, wire section) embraced exactly the same variation of the magnetic field and so they have exactly the same induced voltage. So, without an external disturbing element, the two receivers have as output the same value.

The output voltage value of each receiver can be easily determined by using an illustration of the precise design of the coils :

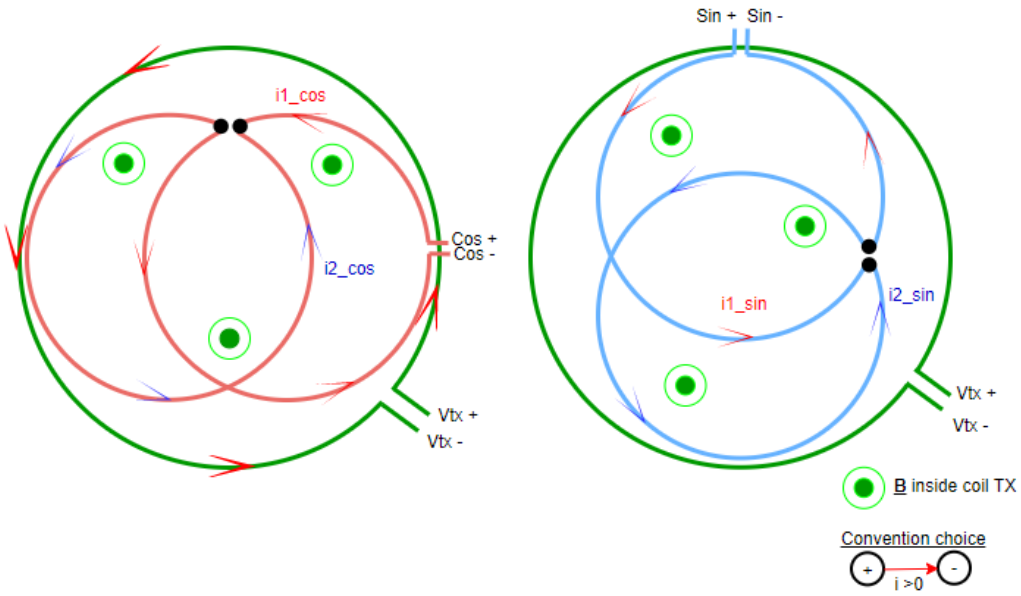


Figure 4.10 – Coil design

In the Figure 4.10, one can see the transmitter (in green) and the two receivers, one in red corresponding to the cosine signal and one in blue corresponding to the sine one. Note that in reality they are superposed but for simplicity and good understanding, the design is separated in two parts. First, let be focused on the left part. The transmitter, fed by an AC current, creates a magnetic field coming towards us. As explained previously, when a loop is subject to a variation of a magnetic field, an emf is induced and the loop is fed by a current flowing with respect to the right hand rule described in the Figure 4.6. So, as the magnetic field is towards us, the induced current is flowing in the anti-clockwise in the two red loops. The fact is that, as the cosine loop is composed by these two loops forming by two folds at different place in the coil (black points), the current in the left sub-loop is equal but opposed to the one in the right sub-loop. The result is a null current and so an output voltage measured equals to zero as the currents induced in the sub-loops are balanced. In other words, we have:

$$i_{1cos} = -i_{2cos}$$

$$\Delta V_{cos} = 0V.$$

The same reflection can be done for the sine loop to conclude with :

$$i_{1sin} = -i_{2sin}$$

$$\Delta V_{sin} = 0V.$$

Then, one consider the presence of a conductive plate. As explained in the section 4.1.5 about Eddy current, when a conductive plate is subject to a varying magnetic field, an EMF is appearing too, creating loops of current (Eddy current) in order to counter the variation. In this application, this phenomenon has as effect to decrease the magnetic field embraced by the receiver coils placed under the metallic plate and so the output voltage of the receiver is decreasing. Some illustrations to have a better understanding are presented in the Figure 4.11:

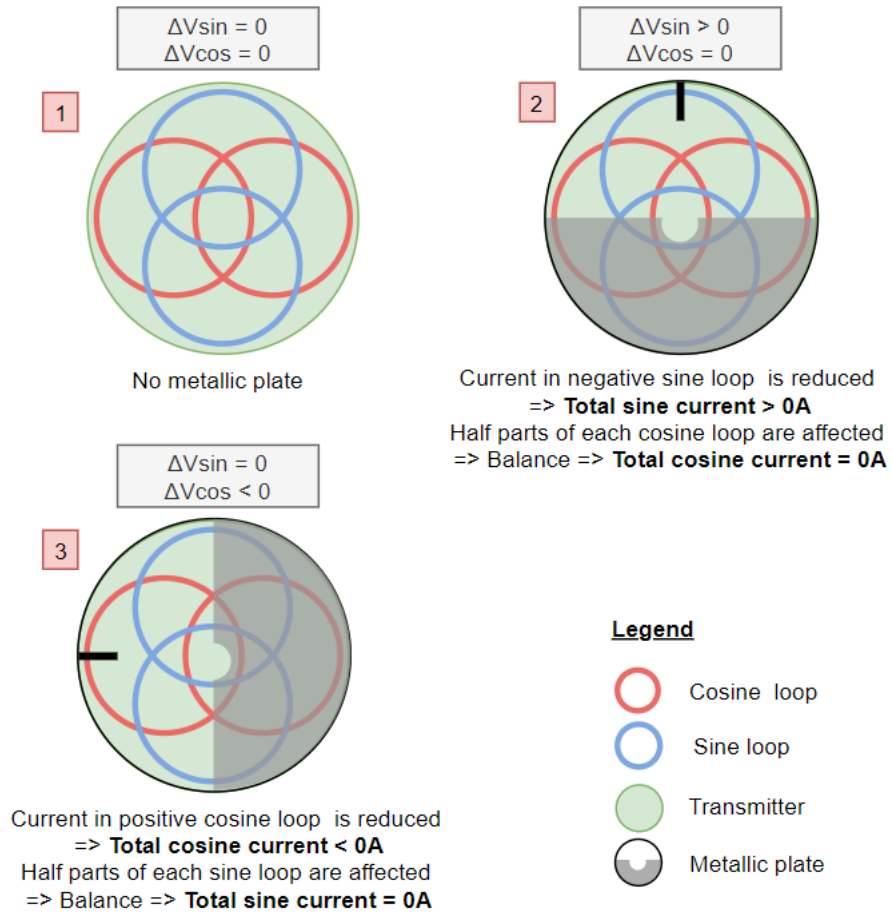


Figure 4.11 – Output signal w.r.t the plate position

As can be seen in the Figure 4.11, an angular position can be found by measuring the output voltage of the sine and cosine loop. Indeed, the position of the black line attaches to the target is given by :

$$\theta = \arctan \frac{\Delta V_{sin}}{\Delta V_{cos}}.$$

Note that to avoid a division by zero, when $\Delta V$ is equal to zero at the denominator, $\Delta V$ is set to $e^{-20}$ in order to don't have an error as output angle. Moreover, the output voltage has to be scaled to 1 when it is maximum and -1 when it is minimum. For instance, for the configuration 2 in the Figure 4.11, there is a $\Delta V_{sin} > 0$ and maximum in this case and a $\Delta V_{cos} = 0$ set to $e^{-20}$, so the output angle is

$$\theta = \arctan \frac{1}{e^{-20}} = 89.999 \approx 90.$$

In the same way, one can obtain an absolute angle between 0° and 360° at each time by measuring the output signal of the sine and cosine loops.

Finally, some words about the design of the target. As the motor, in this particular project, has one pair of poles, one complete turn corresponds to one period of current in the stator. In order to match with this property, the target is designed as a semi-circle moving above four sub-loops. Indeed, with this configuration, one period of the sine (or cosine) output signal corresponds to one turn. In the case of two pole pairs, the target is designed as a two-bladed plate moving above eight sub-loops and therefore one turn corresponds to two periods of the output signal.

## 4.3 Practical development

This section is dedicated to the practical design of the sensor. As explained previously, the design is based on the information provided by Renesas. All the design has been done on Altium using a student license. Altium is a program dedicated to schematic and PCB (Printed Circuit Board) design. In electronic, when a new electronic card has to be developed, the first step is to realized the schematic of the project. Then, linking each electrical component to its own footprint, the PCB can be designed. These steps are done on Altium and the approach adopted for the project is explained step-by-step in the following subsections.

### 4.3.1 Schematic design

For this project the schematic designed is based on a schematic provided by Renesas. Indeed, a lot of tools are available and the challenge is to use these tools to create the sensor perfectly adapted to a particular project. In the evaluation kit of the IPS2200 [19], one can find an application module document providing a basic schematic to start the project. Adapting it and adding some parts useful for the project, the following schematic has been designed. An illustration of it with different important parts that will be presented below is presented :

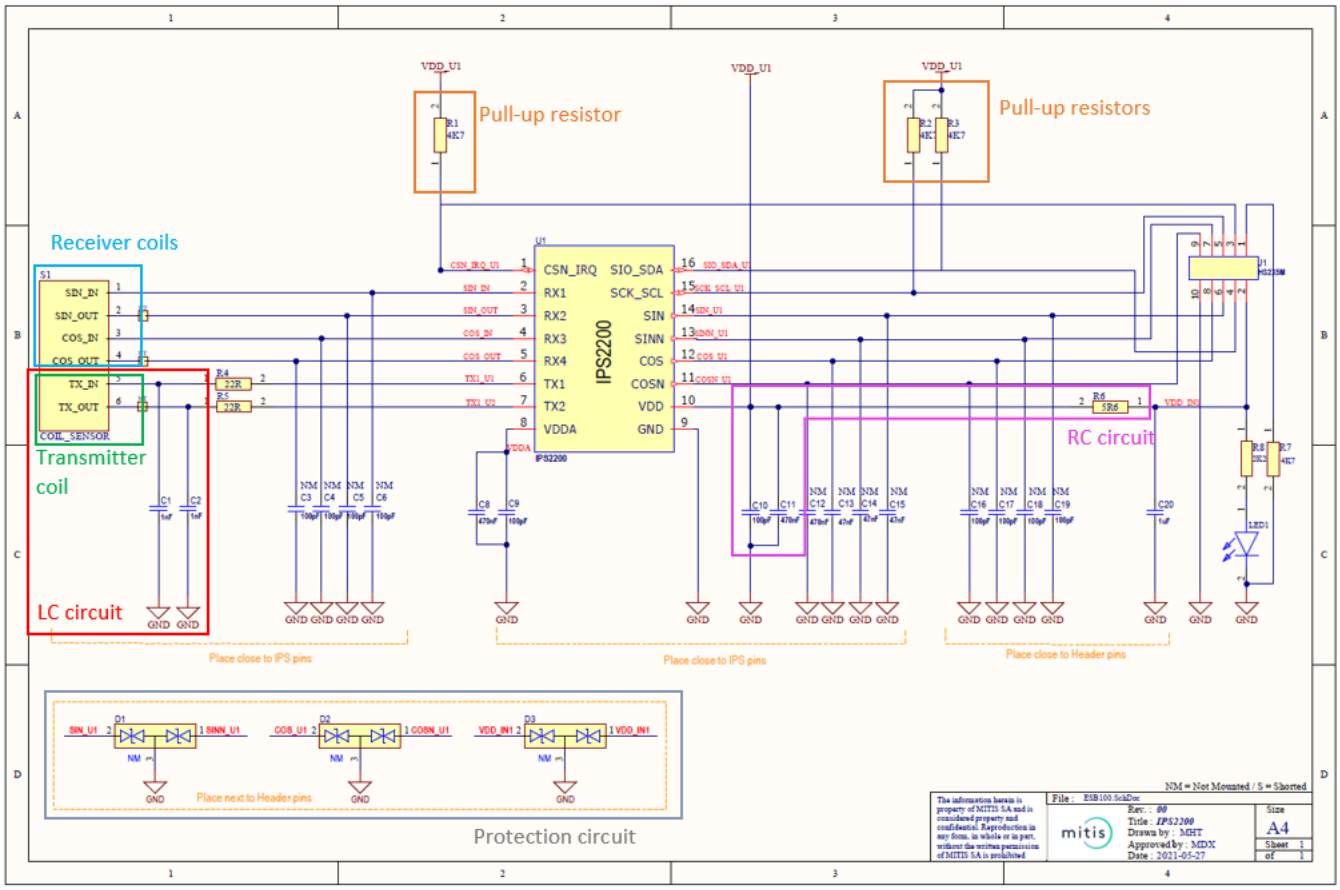


Figure 4.12 – IPS2200 schematic

Note that the Figure 4.12 can be found in its clear and original format in the Appendix A. This Figure is used just to have a support in order to explain the different part of the circuit. First, the central part is the IC directly provided by Renesas whose register can be read and modified by using the $I^2C$. This is a means of communication

implemented in software and whose the protocol will be explained in the Chapter 5 (subsection 5.1.1). For this protocol of communication, pull-up resistors are used. They allow to avoid a conflict between the direction of sending data. Indeed, as it is a bi-directional half-duplex bus communication on only one wire, data can not be sent and received in the same time, the pull-up resistor is there to permitted or not a transfer of data in a particular direction. In other words, it is a communication in open-drain and these resistors are important to avoid a collision between a set information and a received one.
Also, an RC circuit is used in other to remove the parasitic signals from the power supply.
Then, on the left, the transmitter and receiver coils are presented. It is evident that, in the case of the schematic part, the loops are, in fact, represented by a simple short circuit. But, in order to work efficiently, a component has been created in order to link it directly to one footprint. In this way, the complex coils design can be designed in the footprint designer of altium which is more easier than draw directly the copper tracks in the PCB designer. More information about this will be done in the next section.
After, the LC oscillator is a very important part of the schematic. As explained previously, this one allows to have an AC current source whose the frequency depends on the inductance and capacitance value L and C. Indeed, in a LC circuit, the output signal frequency is :

$$f = \frac{1}{(2\pi\sqrt{LC})}$$

So, here, we have :

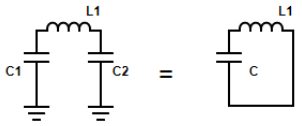


Figure 4.13 – LC circuit

with :

$$C = \frac{C_1 C_2}{C_1 + C_2}$$

Then, an inductance can be expressed by:

$$L = \frac{\mu_0 \mu_r N^2 A}{l}$$

with :

- $\mu_0$, the vacuum permeability equal to $4\pi \times 10^{-7}[\mathrm{H\,m^{-1}}]$;
- $\mu_r$, the relative permeability of the material present in the loops;
- N, the number of turns of the coil;
- A, the section of the coil $[\mathrm{m}^2]$;
- l, the length of the coil $[\mathrm{m}]$.

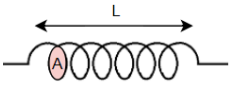


Figure 4.14 – Inductor definition

At this step, it is important to use another tool provided by Renesas. This one is the "Inductive Coil Design Tool" which can be found in the Renesas website [18]. This software allows to test the mechanical constraints of the project, verify if it is possible to design the IPS2200 sensor with these particular constraints and finally, generate the footprint of the coils.
First, the mechanical constraints dedicated to the PCB design will be presented in the next section. At this step, only the constraint relative to the coil design is needed and this one corresponds to a target with a radius equal to maximum 11.25mm to respect the following mechanical design :


Figure 4.15 – Mechanical design of the target

As the target required this maximum size the transmitter and receivers are designed to be covered by the target. So, using the following description provided by the tool :

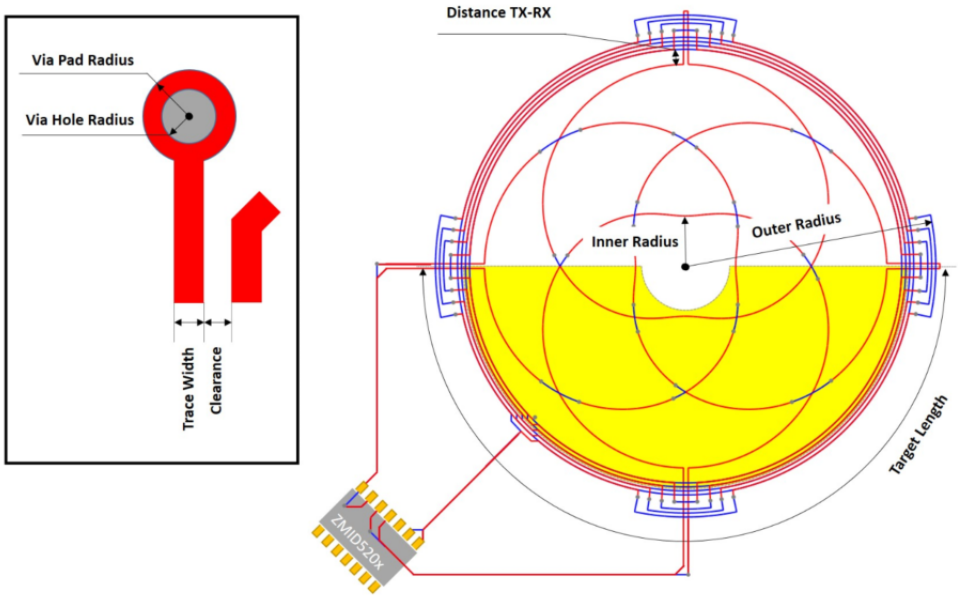


Figure 4.16 – Help diagram

one can choose the following parameters in order to have a valid design :

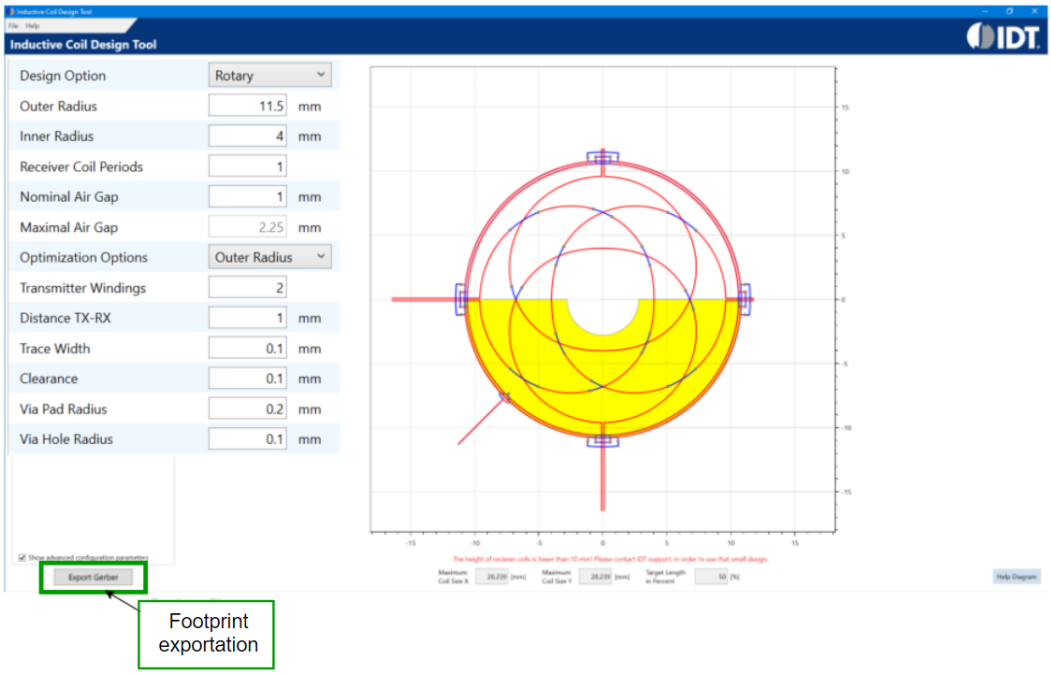


Figure 4.17 – Inductive coil design with parameters adapted to the project

Note that, the outer radius value is not 11.25mm as the target but 11.50mm. Indeed, as it can be seen in the Figure4.16, the outer radius is defined to be until the total extremity of the transmitter (blue part) and the target (yellow part) does not need to cover it. So, 11.50 mm is totally acceptable. Moreover, a trace width equal to 0.1mm is needed. The problem is the fact that the cost is increasing when the trace width is decreasing. But, this outer radius combined to a bigger width is not available by the design tool. So there is no choice to accept this consequence in order to be able to design the sensor. In fact, the cost for the manufacturing depends on the class of the project. The class represents the complexity, for the manufacturer, to produce the project. When the class is high the price is high and vice versa. As the class depends on the hole size and the trace width, when the trace is decreasing, the class change and the cost is higher.

Now that the design parameters are fixed, the best way to be precise and know the exact dimension of the coil is to export the footprint file simply by using the application. Then, the footprint is imported in Altium, and we have an access to the real design of the coil which is the following :

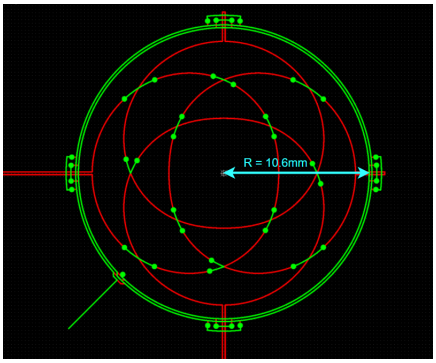


Figure 4.18 – Measurement of the real radius of the coil

As it can be seen in the Figure 4.18, the design of the coil extracted from the application is composed of two layers (the red and the green one). Adding the number of turns for the two layers, there is a total of four turns. Then, the radius is measuring in order to be able to calculate the section of the coil. After, the relative permeability of the epoxy (material used for manufacturing the PCB) is 1. Finally, as we know that the thickness of the PCB will be equal to 1.55 $\mathrm{mm}$, the value of the inductance can be calculated :

$$L = \frac{\mu_0 \mu_r N^2 A}{l} = \frac{4\pi \times 10^{-7} \times 1 \times 4^2 \times (\pi(10.6 \times 10^{-3})^2)}{1.55 \times 10^{-3}} = 4.579\ [\mu\mathrm{H}].$$

Knowing L, one can calculate the capacitance in order to have a excitation frequency between 1.7 and 5.8 $\mathrm{MHz}$ as recommended in the datasheet of the sensor [21].

$$f_{LC} = \frac{1}{2\pi\sqrt{LC}}$$

$$C = \frac{1}{(2\pi f_{LC})^2 L}$$

So, $0.16\,\mathrm{nF} < C < 1.91\,\mathrm{nF}$ which correspond to $0.32\,\mathrm{nF} < C_1 = C_2 = 2C < 3.82\,\mathrm{nF}$ and in order to use a standard value, one choose $C_1 = C_2 = 1\ \mathrm{nF}$. The excitation frequency is the following :

$$f_{LC} = \frac{1}{2\pi\sqrt{4.578 \times 10^{-6} \times \frac{1}{2} \times 10^{-9}}} = 3.326\ \mathrm{MHz}$$

Finally, in the Figure 4.12, other parts are present such as capacitors to act as a voltage reservoir and stabilized the signals, one LED to verify if the voltage source is operational and a circuit of protection for the electronic circuit allowing to avoid static electricity by deflecting the signal to the ground if it is too high or too low. Note that some capacitors and the circuit of protection has not been mounted, these components were suggested by the application notes of Renesas but there are not mandatory. So, in a first time it has been decided to do not mounted them and the tests have confirmed that they are not essential for a good operating of the sensor.

With this value of frequency, one can now verify if the skin effect can have an impact on the sensor operating. This one, as explained previously, is characterized by the skin thickness $\delta = \sqrt{\frac{2\rho}{\omega\mu}}$. Using the Table 4.1, and $\omega = 2\pi f = 20.90 \times 10^6\ \mathrm{rad\,s^{-1}}$, one can find $\delta = 36\ \mathrm{mm}$ which is largely grater than the layer of copper used in this project ($35\,\mu\mathrm{m}$). So, as the skin thickness is at least three times the thickness of the copper plate, the skin effect does not need to be taken into account.

| | |
|---|---|
| Resistivity | $0.0171\ \Omega$ |
| Permeability | $1.25 \times 10^{-6}\ \mathrm{H\,m^{-1}}$ |

Table 4.1 – Copper properties

### 4.3.2 PCB design

Once the schematic is done, the next step is to design the PCB. By linking each schematic element to its footprint, Altium is able to switch to a PCB design while keeping the link between the different components described in the schematic. This is illustrated below with a resistor and a capacitor linked as an example :

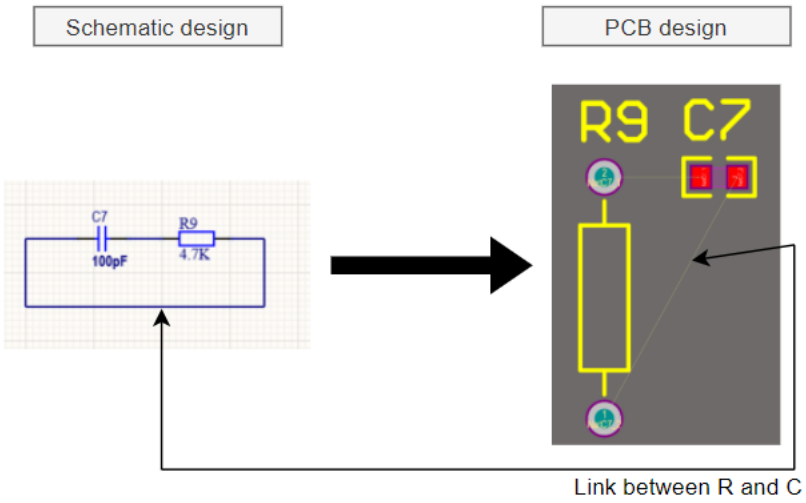


Figure 4.19 – Switching from schematic design to PCB design : Example with a simple scheme

As it can be seen in the Figure 4.19, each element has its own footprint and the link between them are kept. So, the final step is to realize the routing in order the really link the component using some track of copper.

In the same way, the schematic A is imported in the PCB design. Before to dispose the components, one need to defined the size and the shape of the PCB. For that, mechanical constraints have to be taken into account and it is the subject of the following sub-section.

**Mechanical constraints**

For the project, two PCB's will be developed. The first one is the sensor itself with the IC, the coil design and all the components present on the schematic. The second one is the metallic plate (the target).
Indeed, as explained previously, the target is a semi-circle. Moreover, the most important constraint of the project is to reach a very high speed such as 120 000 rpm. At this rotation speed, an unbalance could create consequent disruption in the system. To avoid it, the target is designed on a PCB which has a perfect circle shape and whose the base material is the FR-4 (Flame Resistant 4).
FR-4 is an epoxy resin used for the fabrication of PCB. This material is known for its good stability, insulating property, very good flammability rating and moisture resistance.
So, as the base material of a PCB is an insulating, the metallic plate can be designed using a thin layer of copper (35µm) for the semi-circle deposited onto the circle composed of FR-4. Using this configuration for the target, the semi-circle induced an unbalance which can be negligible compared to other unbalance of the global project which will be corrected during the final balancing of the machine.
Then, the PCB containing the electronic of the sensor has to be designed. This is done in cooperation with the mechanical team of the company. The first step is to use a ".DXF" file which is the mechanical design of the project. This file can be directly imported in Altium in order to have the board shape of the PCB with the correct dimension. This method is illustrated below :

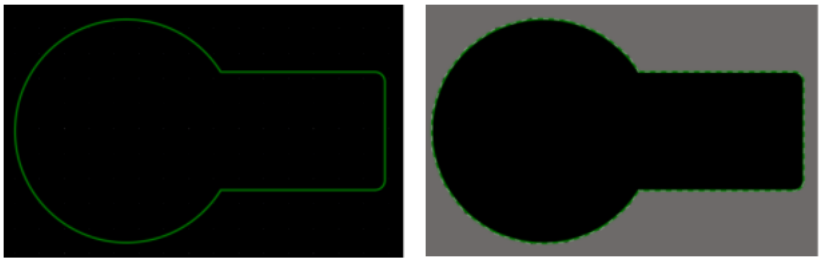

Figure 4.20 – Left : Board shape of the PCB obtained from the DXF file. Right : Final shape of the PCB

### Manufacturing constraints

For this project, the company chosen for the manufacturing of the PCB is Eurocircuits [6]. Provided the gerber files of the PCB design, this company manufactures the PCB as far as the design rules imposed by them are observed. As all the electronic need to be placed in the rectangle part on the right of the PCB (Figure 4.20) which is a length of 29.5 $\mathrm{mm}$ and a width of 23.6 $\mathrm{mm}$, these rules represent a challenge for the design. The most restrictive of them are explained below, they come directly from [5] :

- Overlapping Drilled Holes:
  "The minimum drill hole to drill hole distance is 0.25 $\mathrm{mm}$ (10mil), this is measured edge to edge of the drill TOOLSIZE with Plated Through Holes (PTH) TOOLSIZE = ENDSIZE + 0.100 $\mathrm{mm}$ (4mil) and Non-Plated Through Holes (NPTH) TOOLSIZE = ENDSIZE"

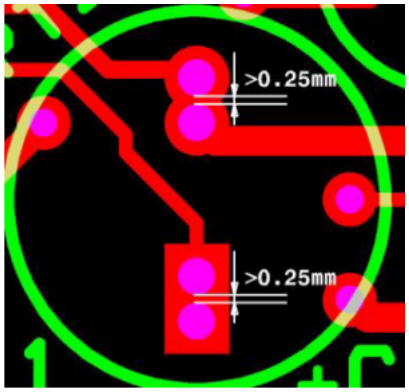


Figure 4.21 – Illustration of Overlapping Drilled Holes (from Eurocircuits PCB design guidelines) [5]

- Copper to Board Edge Clearance:
  "The minimal clearance between edge of board and pattern is 0.25 mm on the outer layers."
- Poolable Options To ensure the best price your board needs to be poolable. Poolable values :
  - "(TT) Track to Track isolation gap is 0.100 $\mathrm{mm}$ (4mil)";
  - "(TP) Track to Pad isolation gap is 0.100 $\mathrm{mm}$ (4mil)";
  - "(TW) Track Width is 0.100 $\mathrm{mm}$ (4mil)";

  - "Via Holes under the device – the smallest finished Via Hole Size is 0.10 mm (4mil). Min. Outer Layer Pad size is 0.400 mm (16mil) for a 0.10 mm (4mil) finished hole size. (Min. Outer Layer Pad size is the finished hole size + the plating (0,10 mm) + 2 x OAR (Outer Annular Ring))."

- Specifications for Legend Print:

  - "Minimum Legend Line Width: 0.10 mm (4mil)";
  - "Minimum Text height for good readability: 1.00 mm (39.5mil)."

Note that 1 mil = 0,0254 mm.

In order to save space on the board, the PCB is designed using two layers. Indeed, two tracks conducting different signals cannot intersect, with two layers, intersection can be bypassed by using via which acts as a tunnel between the two layers. Moreover, to avoid to have a lot of tracks conducting the ground signal, two ground planes are used. In this way, components connected to the ground are almost directly connected, they just need to be connected to a via linked to the both ground planes.

Then, in order to respect the poolable option and more particularly the track to track isolation gap (0.1 mm) a change in the footprint generated by the application "Inductive Coil Design Tool" of Renesas [19] has to be done. In fact, with the original footprint, the track forming the loops is designed by a succession of copper point as can be seen below :

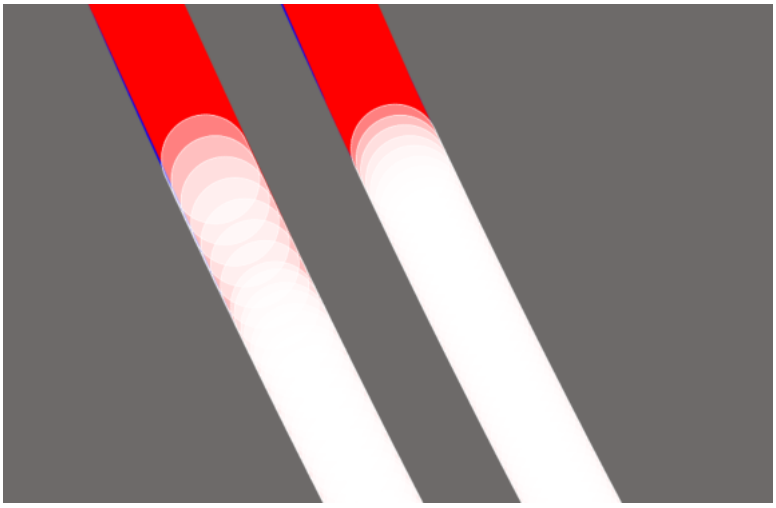

Figure 4.22 – Zoom on the track of the loop : succession of copper points

At first, it is not a problem but when the request for the manufacturing is done to Eurocircuits, a denial report explaining that the clearance between two tracks (0.1 mm) is not respected is received while the parameter of 0.1 mm of clearance has been entered in the application (see Figure 4.17). As it can be seen below, the minimum isolation is 0.1 mm (or 0.09 mm but but this is again a more expensive cost that can be avoided).

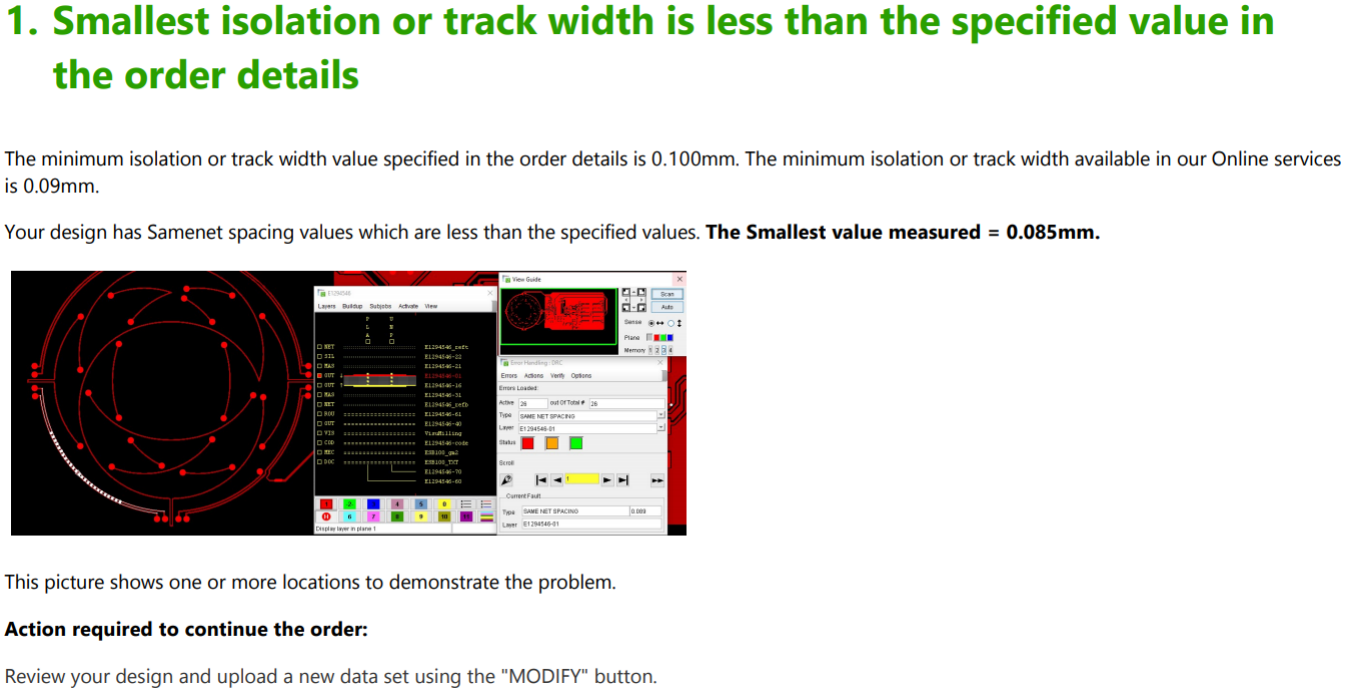

# 1. Smallest isolation or track width is less than the specified value in the order details

The minimum isolation or track width value specified in the order details is 0.100mm. The minimum isolation or track width available in our Online services is 0.09mm.

Your design has Samenet spacing values which are less than the specified values. **The Smallest value measured = 0.085mm.**

This picture shows one or more locations to demonstrate the problem.

**Action required to continue the order:**

Review your design and upload a new data set using the "MODIFY" button.

Figure 4.23 – Extract of the report from Eurocircuit

The solution to avoid it is to delete all the tracks forming the transmitter loops and replace them by a perfect circles of copper. In this way, choosing the exact radius of each circle, the isolation gap between the tracks can be easily respected.

### Final design

Once the constraints are taken into account, the routing step can be done. For the routing, three different width of track are used :

- W = 0.1 $\mathrm{mm}$ for the coil design, this is extremely small for a signal but, as a recall, there was not any other choice of width in view of the dimension of the coil (radius of 11.5 $\mathrm{mm}$).
- W = 0.2 $\mathrm{mm}$ for the tracks linking the different components of the electronic circuit. A trade-off need to be done between a too small track (deterioration of the signal) and too large ones (lost of place on the board). Note that in order to change the dimension in the middle of a track, a solution such as using Net-Tie is needed. It will be developed in the next paragraph.
- W = 0.35 $\mathrm{mm}$ for the tracks conducting the power signals such as VDD and VDDA. For these ones, the wider they are the better it is but due to the board size, this value has been chosen.

The, a Net-Tie is a "virtual component" used in order to link to wire that have different net. In other words, they correspond to different signals. The idea is to create a virtual component that is able to link the signals simply being composed by 2 connected pads. In reality, they form a short-circuit with a transfer of net. The net tie is useful in this project as the coil receives an input signal and return an output one while in reality, a coil is just a short circuit. The schematic component and its footprint are illustrated in the Figure 4.24

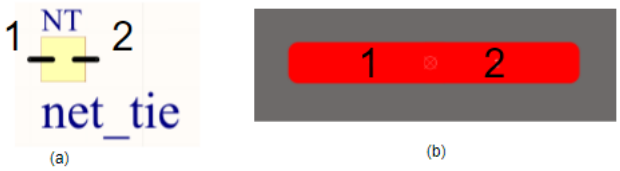


Figure 4.24 – Net-Tie (a) schematic illustration (b) footprint of the component (short-circuit between two pads)

A final comment about the PCB design is the creation of a component containing the full coil design. In this way, the coil design is seen as an unique component with six connections (two for the transmitter, two for the cosine and two for the sine signal). The advantage is that one can easily choose the orientation of the coils and so place the connections in the more efficient way. This is illustrated below :

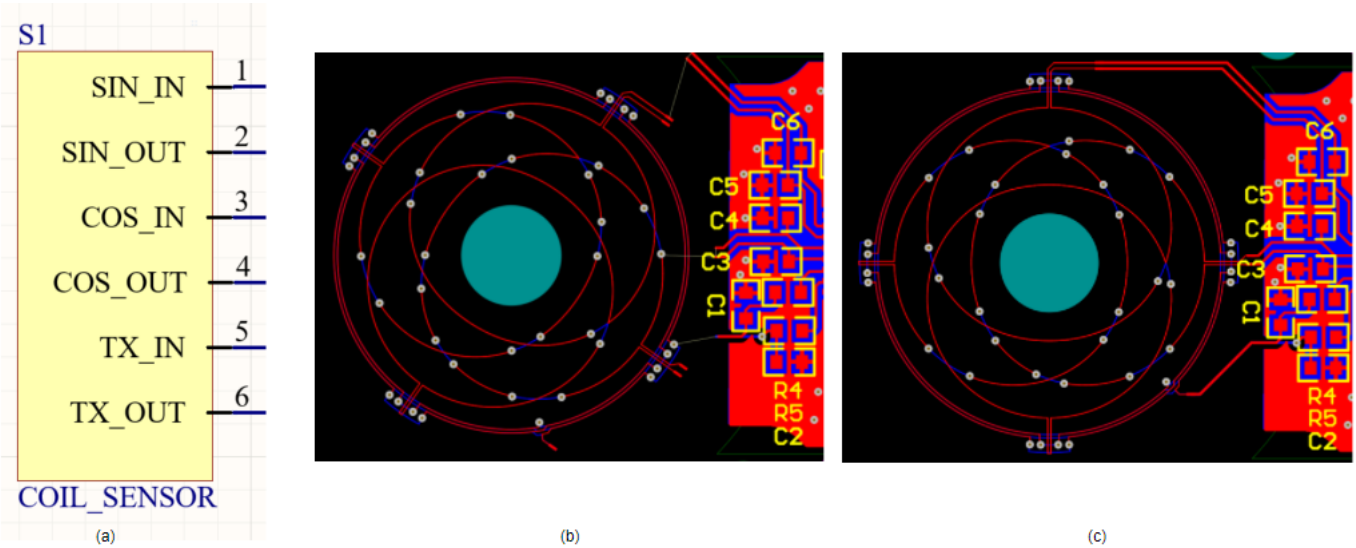


Figure 4.25 – Coil design as one component (a) Schematic component (b) orientation = 145 degrees (c) orientation = 180 degrees

So, in function of the shape of the board or the location of the other components, it is important to have a design which can be adapted to different configurations.

Finally, the design is illustrated for the top layer and the bottom one of the PCB, as well as the 3D view. The second illustration concerns the second PCB acting as the target. For this one, only the top layer is used to have the semi-circle of copper.

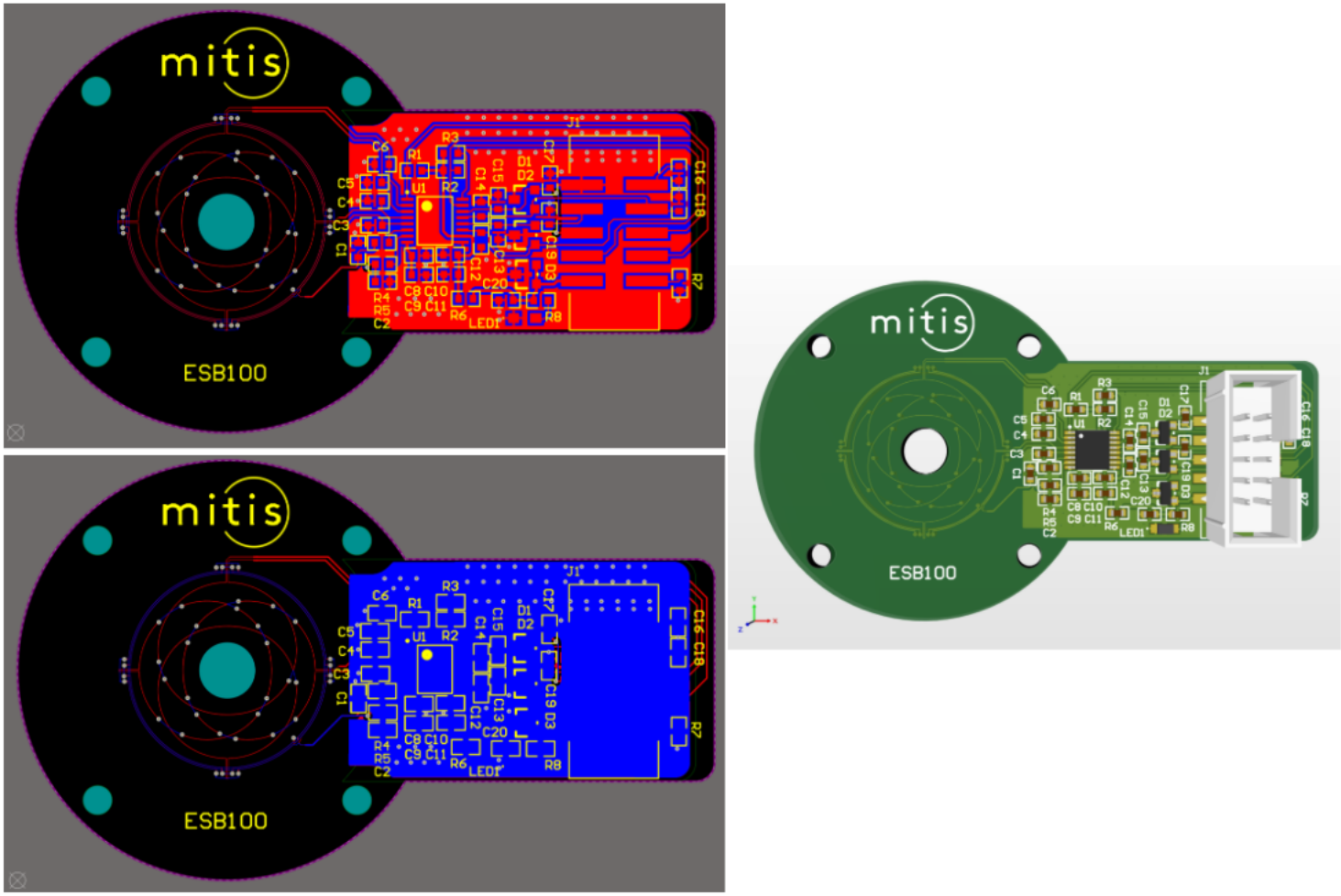


Figure 4.26 – PCB design. Top left corner : Top layer, bottom left corner : Bottom layer, right : 3D view

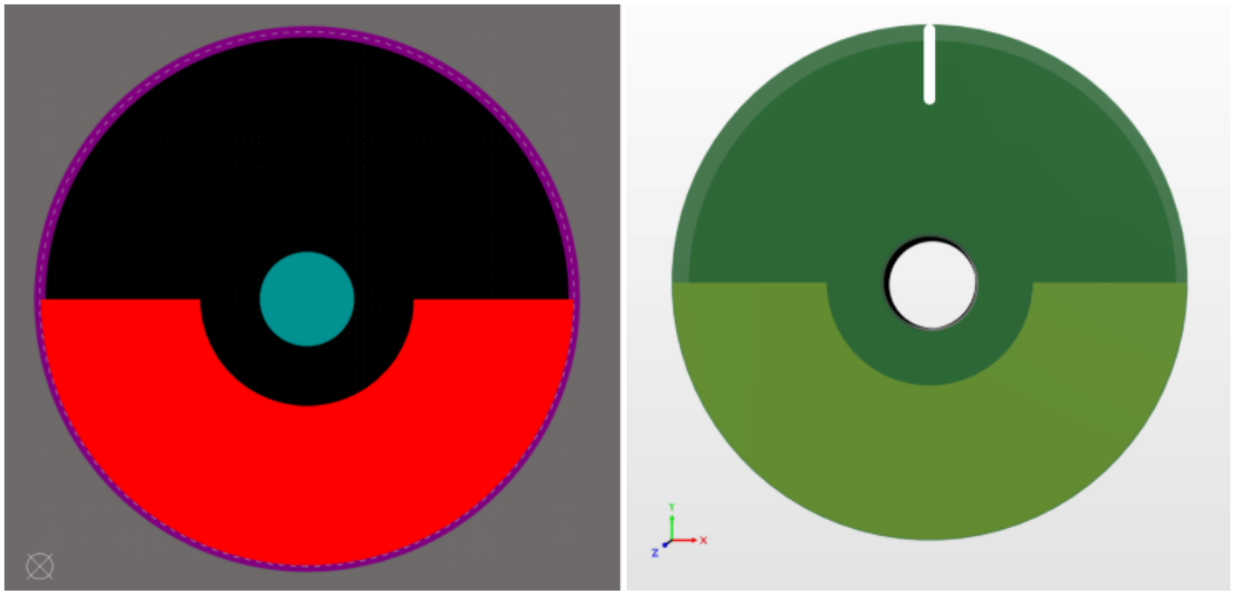

Figure 4.27 – Target design. Left : Top layer of the PCB, right : 3D view

## 4.4 Assembly and first test

Once the PCB's are received from the manufacturing company (Eurocircuits [6]), it is time to assemble the card and start the first test. An illustration of the assembly is shown below. Note that all the components are not mounted. Indeed, the place for each one was planned but for the first test only the main components are welded. Later, if the signal need to be improved, it will be possible to add some other components.

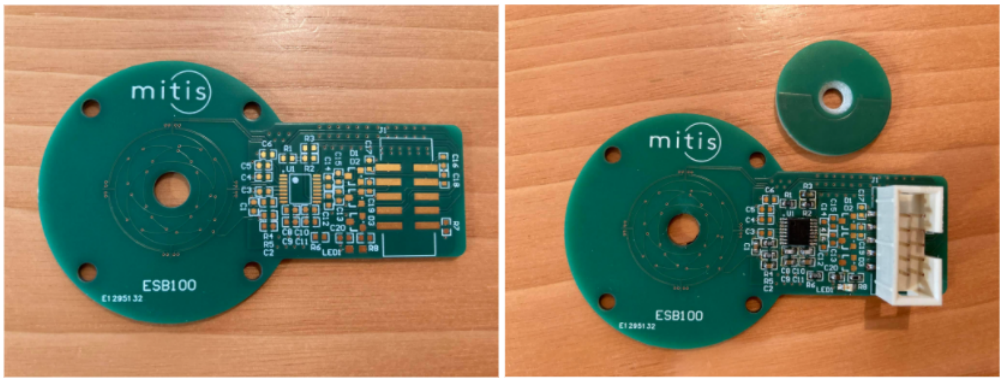


Figure 4.28 – (a) PCB's received from the manufacturing company (b) Assembled card

As the software is not yet implemented, in order to test the hardware, an application provided by Renesas is used. This one is, at first, used to discover the sensor by using a product of demonstration. The information about the starter kit can be found on the website of Renesas and more particularly in the document "Starter kit user manual" [19].

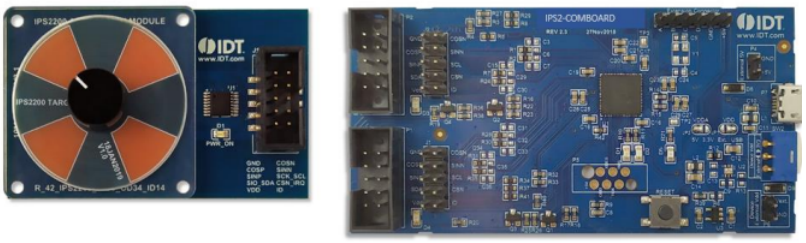


Figure 4.29 – . Left : IPS2-COMBOARD - Right: IPS2200MROT4x90001 Application Module [19]

As it can be seen in in the Figure 4.30, in the starter kit, there are the sensor (this one is a configuration with two poles pair but it is useful to understand how it is working) and the electronic card. This one allows to set some parameters and use the interface provided by Renesas which is the following :

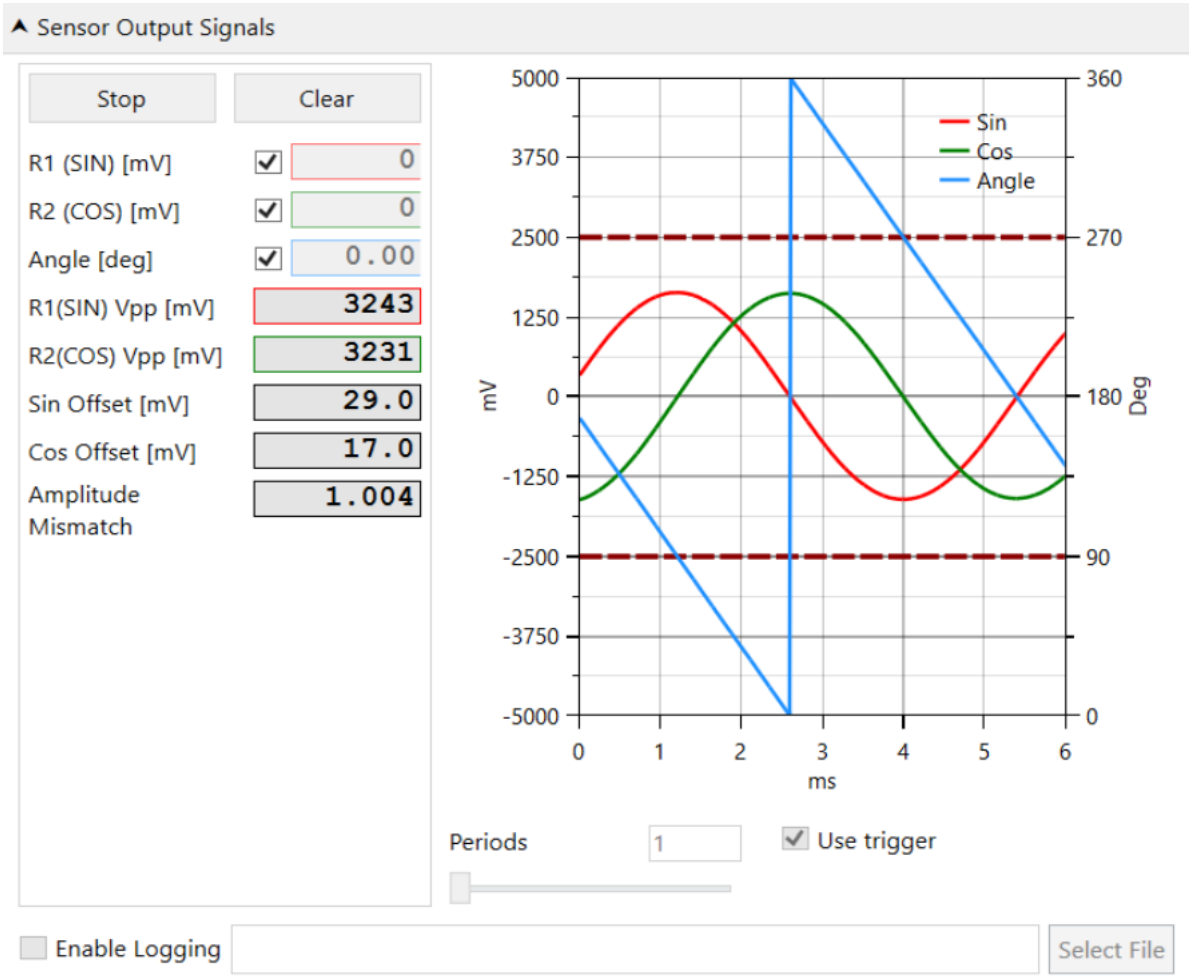


Figure 4.30 – Interface IPS2200 application - Starter kit

First, the specifications about the chip IPS2200 are presented in the Table 4.2. In this Table, the pin number corresponds to the one presented in the Figure 4.31. These following informations are coming from the datasheet of the IPS2200 [21].

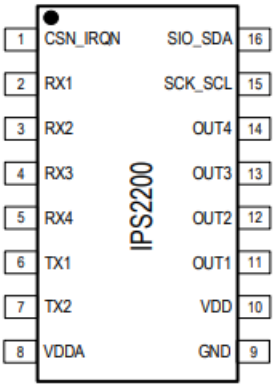


Figure 4.31 – Pin assignments of the IPS2200

Regarding this pin assignments, the pin description is detailed.

| Pin number | Name | Type of signal | I/O specification | Description |
|---|---|---|---|---|
| 1 | CSN_IRQN | Digital | Input/Output | Chip select input for the SPI interface. In this case, a pull-up resistor is needed. This pin is also used to implement a push/pull interrupt output for SPI and I2C communication. |
| 2 | RX1 | Analog | Input | These two pins are connected at the extremity of the receiver coil 1 (sine) |
| 3 | RX2 | Analog | Input | |
| 4 | RX3 | Analog | Input | These two pins are connected at the extremity of the receiver coil 2 (cosine) |
| 5 | RX4 | Analog | Input | |
| 6 | TX1 | Analog | Input/Output | These two pins are connected at the extremity of the transmitter coil. |
| 7 | TX2 | Analog | Input/Output | |
| 8 | VDDA | Supply | - | Internal analog voltage supply |
| 9 | GND | Supply | - | Common ground connection |
| 10 | VDD | Supply | - | External supply voltage. It can be set to 5V or 3.3V |
| 11 | OUT1 | Analog / Digital | Output | Buffered analog or digital output |
| 12 | OUT2 | Analog / Digital | Output | |
| 13 | OUT3 | Analog / Digital | Output | |
| 14 | OUT4 | Analog / Digital | Output | |
| 15 | SCK_SCL | Digital | Input | Clock input for digital programming and diagnostic interfaces. For I2C communication, the clock input is SCL and for the SPI communication it is SCK. |
| 16 | SIO_SDA | Digital | Input/output | Bi-directional data I/O line used for digital programming. For the I2C communication, SDA is the open drain data line and for the SPI, SIO is the bi-directionnal push-pull data line. |

Table 4.2 – IPS2200 pin descriptions [21]

With respect to this Table 4.2, different choices have to be done. First the protocol $I^2C$ is used and so the pin 15 and 16 corresponds respectively to SCL and SDA. Then, The external supply voltage (pin 10) is set to 3.3 V to be compatible with the power supply provided by the future micro controller (see chapter 5). Finally, the pins 11 to 14 the output used for measuring the angle. These can be digital or analog. In order to conserve as more as possible the information and have the most accurate angle output, the analog type of signal is chosen. Moreover, in the analog mode, there are either the differential mode, either the single-ended mode. Again, in order to have the best accuracy, the analog differential mode is chosen. Indeed, with two differential signals, external perturbations are limited and the output of the sensor is cleaner.

Once the principle of working is understood thanks to the interface provided by Renesas and the chip IPS2200 is well analyzed, the next step is to connect the new sensor to the electronic card from Renesas and see if the output angle is the one expected. Furthermore, some parameters as the gain or the offset can be adapted in order to have the most appropriated signals for the following step of the project which is the software implementation. To conclude, the basic test using the application has confirmed the proper functioning of the new sensor. Moreover, an additional test was been done. By using again the electronic card from Renesas, one can measure the output signals of the sensor, connecting the specific pins to an oscilloscope. The cosine and sine signals were been tested. Note that a gain higher than the one used by default (90 instead of 8) was been set in order to have a better amplitude. A first test consists in measure the sine and cosine signal output and understand the link between these values and the angular position of the sensor. Then, the second test consists in, using a screwdriver attach to the moving part of the sensor, measuring the frequency of the cosine output signal. As the sensor is designed to have as output one period for one turn, the frequency can be compared to the maximum rotational speed of the screwdriver and conclude about the efficient performing of the sensor.
The different tests were been conclusive, the hardware was been validated and one can, now, switch to the next important step of the project, the software implementation.
Some illustrations of the final product of the sensor and of the experiment are shown below. Note that a screw is used in order to perform some tests but in the future it will not be used. The target will be on the rotating shaft of the motor and the PCB containing the electronic part will be fixed just in front the extremity of the shaft, separated by a small gap ($\approx$ 5mm).

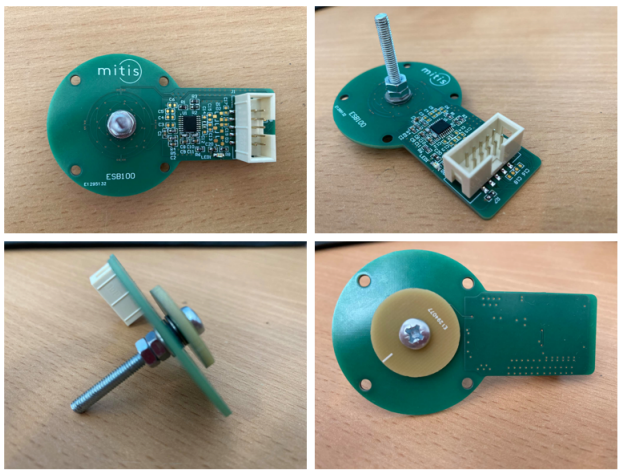


Figure 4.32 – Final product of the IPS2200

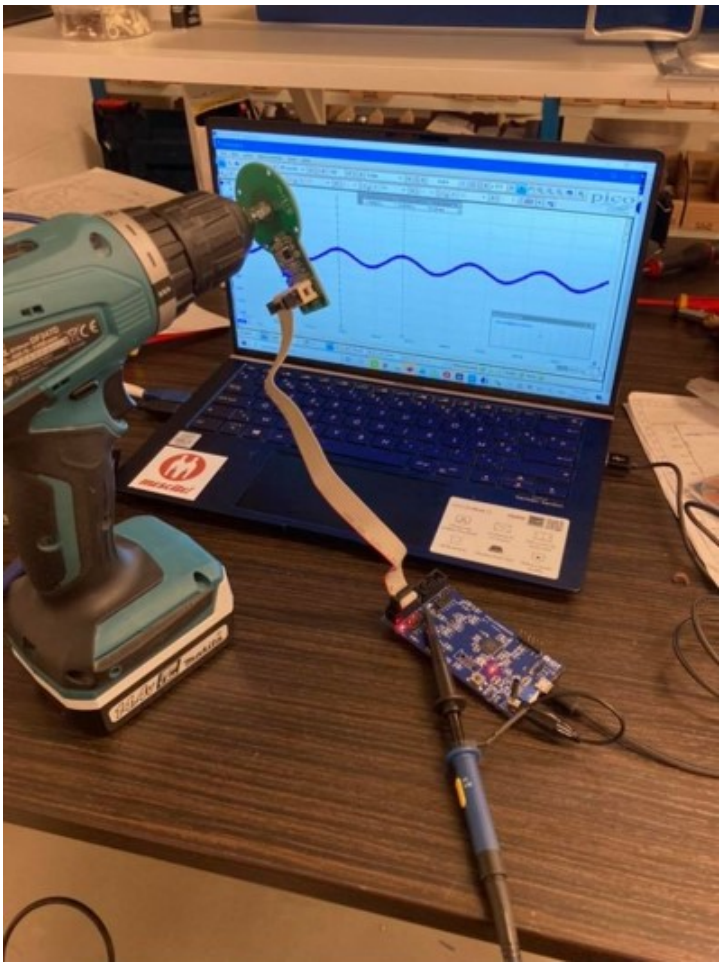

Figure 4.33 – Test of rotational speed measurement with a screwdriver (max rotational speed : 1400 rpm)

# Chapter 5

# Software development of an Eddy current sensor

This chapter is dedicated to the software development. It consists in developing the way to establish a communication between the sensor and the micro-controller but also between the user and the sensor. This will be developed in the first part of the chapter. Moreover, the purpose of the sensor is to be able to implement a closed-loop control with the feedback on the angular position and the rotational speed. The challenge is the acquisition of data at high rotational speed. Indeed, if the time needed by the micro-controller to calculate a speed is too long, the output rotational speed could be wrong. A development to improve the rapidity of calculation is given in the second part of this chapter.
The micro controller used for this project is an STM32G4 from the ST company [24] and more particularly the *NUCLEO-G474RE* [23]. It is a development board specifically adapted to the motor control. Indeed, its performance can reach 170 MHz with a flash memory equal to 512 Kbytes and it is equipped with a FPU (floating-point unit) used for operation on floating point numbers. Moreover, some functions such as ADC and DAC converter, Cordic, comparators, timers,... are already implemented in hardware and it can improve considerably the execution time of operations.

## 5.1 Communication implementation

The first communication between the user and the sensor is done by using tools provided by ST which is the *Cube IDE*. This one is an integrated development environment used to assign the pins of the microcontroller to their proper signals, implement the C code source and programming the board. With this application, it is possible to see the live expression of the variable which is very useful for debugging and tests. Then different communications need to be implemented and it is the subject of the three next subsections.

### 5.1.1 I2C bus communication

The $I^2C$ bus communication is implemented in order to be able to set some parameters on the sensor. Indeed, at this time, the sensor can be set up only with the help of the application provided by Renesas and by the intermediary of the application module (see Figure 4.29). The purpose of this communication is to no longer depend on the application module but set up the sensor directly from the nucleo board.
Each parameter is set in a specific register. By using the $I^2C$ protocol, it is possible to read the value contained in the register but also to overwrite in in order to set a new value. Let start with the development of the protocol. Following

information come from the course of Embedded System given by B.Boigelot at the University of Liège [3].

### I2C protocol

Basically, the bus is composed by a pair of two lines : SDA (Serial Data) and SCL (Serial Clock). The first one contains the data that one can read or write and the other one is the clock signal. When the lines are unused, the value is always high. When a device is connected to the bus, it is able to either read the value of SDA and SCL or force the lines down in order to write a low value.
Each line is connected to the voltage source by the intermediary of a pull-up resistor. This one is used to control transitions from high and low states and is necessary when the communication is half-duplex on a bi-directional bus. In this configuration, the lines are naturally high. Then, a transistor is placed between the ground and each lines in order to force the low value when it is necessary.

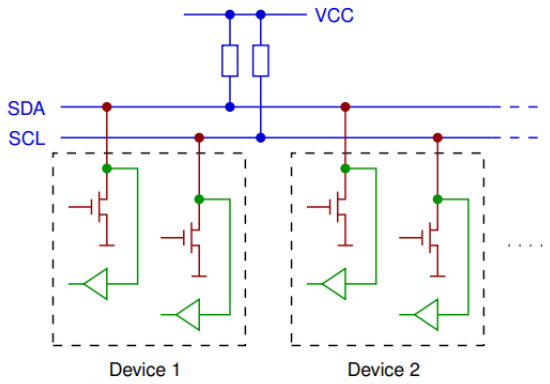


Figure 5.1 – $I^2C$ bus[3]

In the $I^2C$ protocol, there is a master and a slave. The device that take over the line becomes the master and the one with which it wants to communicate is the slave. During a transaction, the master is responsible for the generation of the clock signal and also alert the start (S) and the end (P) of a transaction. These alerts are reflected in the two possible transitions of SDA when SCL is high. In other words, the beginning of a transaction can only happen when SCL is high and SDA goes from high to low state. In opposite, the end of the transaction is happening when SCL is high and SDA goes from low to high value. These are illustrated below :


Figure 5.2 – $I^2C$ transaction [3]

During a transaction, data are sent either by the slave or the master. A data is transferred by 8-bit groups (with the most significant bit, MSB, sent in first) and each group is closed by an acknowledgment which corresponds to a low value on SDA forced by the receiver. A transaction is immediately stopped by the master if a group of 8 bits is not acknowledged. Finally, each bit of data coincides with the value of SDA in the course of a low to high transition of

SCL.
At an initiation of a transaction, the master has to refer which device is chosen to communicate with it. This set is the addressing. In fact, each device corresponds to an address. When a transaction is beginning, the first group of 8 bits is always sent by the master. Indeed, in this group, the first seven bits represent the address of the slave and the 8th allows to specify the direction of the future data transfer. This bit is zero if the master will send a data (write operation) and one if it wants to receive data from the slave (read operation). For sure, the 8-bits group has to be acknowledged by the slave in order to continue the transfer regardless of the asked operation.
A general data transfer is illustrated below :

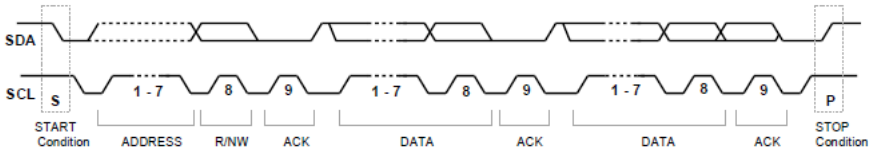


Figure 5.3 – General data transfer $I^2C$ protocol[22]

**Communication I2C between the sensor (IPS2200) and the nucleo board**

As explained earlier, the $I^2C$ communication is used in this project to set some parameters on the sensor. Indeed, each parameter is stocked in different register. With this communication, one can easily write in a register to set a new value and so change the parameter corresponding to the specific register. An example of how changing the gain of the sensor is developed below.
In order to program the IPS2200, a programming guide [22] is provided by Renesas. In this one, one can find how the $I2C$ communication can be implemented but also the register corresponding to a specific parameter which is also reported in the . Let start with the procedure to write data in a register.

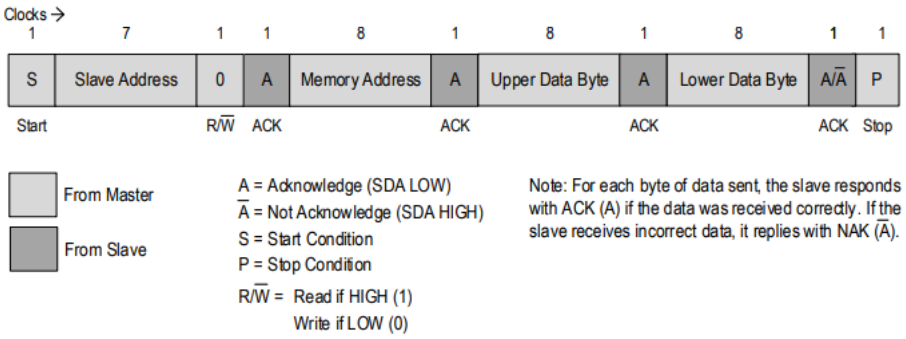


Figure 5.4 – General data transfer $I^2C$ protocol - Write operation [22]

In this paragraph, an instance on how one can change the gain of the sensor is developed. For sure, the process is exactly the same with other parameters, only the register value and data are changed. As can be seen in the Figure 5.4, the first step is to send the address of the device. In this case, it corresponds to the address of the IPS2200 which is found in [22] and is expressed by the seven following bits $0010000_{bin}$. As it is a writing operation, the following bit is $0_{bin}$.
Then, the other important data are the memory addresses. It corresponds to the one of the register in which we want to change the value. All the specific memory addresses of each register are reported in the Appendix B which comes

from [22]. Let us stay focused on the gain whose the address is expressed by $22_{hex}$. Note that the memory addresses are the ones expressed by the Serial Register Bank (SRB) addresses. The memory address is coded on 8 bits but the two first bits are reserved so it is mandatory to set them to 1 ([22]). So, by replacing these two reserved bits, the memory address for the gain is $E2_{hex}$. The final step is to send data coded on 16 bits and corresponding to the value of the new gain that need to be set. Using the Appendix C.1, one can see that, in this register, it is possible to set the gain but also the integration cycles.
In the datasheet of the IPS2200 [21], a relation between the data propagation delay and the integration factor such as the data propagation [µs] delay is given by :

$$\frac{2 \cdot (IF + 1)}{f_{LC}} + 1 \cdot \tau$$

with :

- $IF$, Integration factor (programmable from 5 to 31);
- $f_{LC}$, frequency of the oscillator equal to $3.326$ MHz as find in subsection 4.3.1;
- $\tau$, internal time constant defined to be equal to $2.2$ µs.

In order to have the smaller delay as possible, $IF$ is set to 5 and the final data propagation delay is equal to $5.81$ µs. Now, let us come back to the 2 bytes of data for the gain register. Regarding the Appendix C.1, by choosing $IF = 5$, one can already know the first dozen bits. The last four correspond to the gain. In order to have large amplitude signals to more precisely detect zero crossings (useful for the programming part), the gain is set at its maximum value. As defined in the Appendix C.1, the gain is defined by :

$$\text{Gain } = 2^{\frac{n}{2}} \text{ where } n = \text{dec (gain stage )}$$

. So, using $n = 13$ which is the maximum, one obtains a gain equal to $90.51$ and the last four bits to set this value are $13_{dec} = D_{hex} = 0111_{bin}$.

Finally, using this process, I can, now, set all registers without having to use the application module provided by Renesas but by using directly the nucleo board programmed in the development environment *Cube IDE*.

Furthermore, the read operation can also be implemented. Indeed, it could be useful to be able to read the value set in different registers in order to check if the sensor is well initialized. First, an illustration of the read operation is shown in the Figure 5.5:

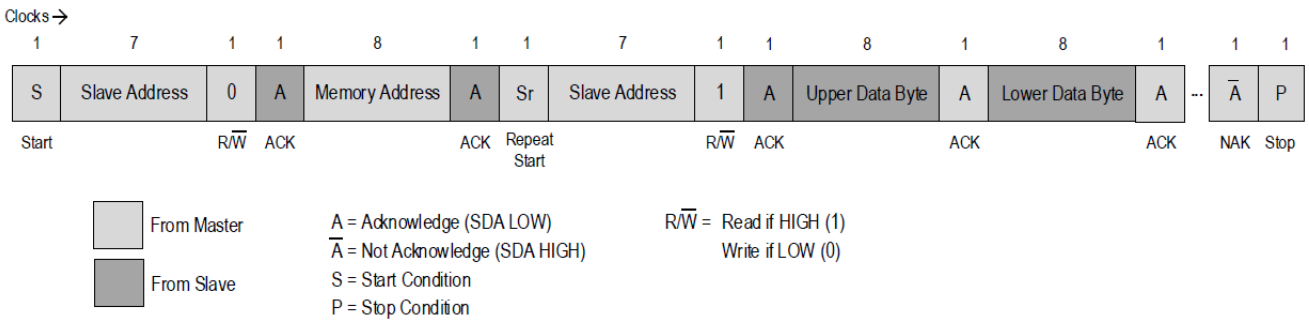


Figure 5.5 – General data transfer $I^2C$ protocol - Read operation [13]

The read operation is a little bit different from the write operation. First, it is easier because only 2 bytes are needed, the slave address one and the memory address one. Data bytes are not needed as it is what we want to know. So, slave and memory addresses are determined exactly in the same way than in the write operation. The particularity is that one need first to start a write operation and then restart a read operation. Without this process, the chip is unable to understand that a read operation is asked.

Using the development environment *Cube IDE*, the $I^2C$ bus communication can be easily implemented. Indeed, the functions write and read are already implemented. The difficulty in this part was to search and find exactly the correct addresses for the slave and the different registers. Once this step is done taking into account all the subtleties such as last bit set to 1 or 0, reserved bits, or other, the functions receive as input the different bytes and the communication is done. To conclude, $I^2C$ bus communication is important in this project because it allows to communicate with the chip and be able to set all parameters of the sensor directly from the micro controller simply by writing a C code source that follows the process of writing operation and read operation.

### 5.1.2 UART communication

UART is an abbreviation for designing Universal Asynchronous Receiver Transmitter. This communication is directly integrated in the micro controller. UART is very useful for serial communication over a computer. In fact the micro controller is connected to the computer by a serial port. Using this channel, the micro controller can set one by one a set of bits and the information can be displayed directly on the computer using an RS232 terminal, a serial port terminal, such as *Termite* [1]. This communication is mainly used for debugging but also to print some results corresponding to the value of some variables.

### 5.1.3 1-wire bus communication

The 1-wire bus communication is used for a project separated from the main project of development of the position sensor. In fact, it concerns the development of a digital thermometer (precisely the DS18B20). This small project allowed me to become more familiar with the management of a clock in a micro controller. Indeed, this digital thermometer has been developed using a micro controller that comes from the ST company as the micro controller used for the position sensor development. The difference is the serial F2 instead of G4. Actually, the micro controller STM32F2 is a version less efficient regarding the motor control but largely sufficient for this application. The basic using of the two micro controllers are the same and a little project such this one is useful to try his hand with ST components.

Moreover, implement this communication in order to develop a digital thermometer is very interesting for temperature measurement in different project. Actually, such a thermometer has an accuracy of 0.5°C, it is low cost and above all the digital communication leads to a small noise sensitivity.

The subsection 5.1.3 is dedicated to an explanation about the 1-wire bus protocol applied on the DS18B20 digital thermometer and the subsection 5.1.3 presents more particularly the digital thermometer DS18B20 and its final design.

### 1-wire bus protocol development for the digital thermometer DS18B20

The 1-wire bus communication is a communication in open drain. Like the $I^2C$ bus communication, in open drain, it is possible to communicate only in one direction. In other words, at each time, the device is only able to send or receive data but never the both. To ensure this one-way communication, a pull-up resistor is used. This component allows to the master to set the line high when it wants the send an information the the slave and so stops the possibility for the slave to also send an information at the same time. In this way, the master is always the winner to send an information and a bi-directional communication cannot occur.

To implement the communication between the micro controller stm32F2 and the digital thermometer, the datasheet of this one is needed [13].
The protocol is divided in three parts :

- Initialisation : the line is set to 1 when there is no action. The first step consists in a reset pulse sent by the master (the micro controller) to the slave (the thermometer) to ask it if it is present (functional). Then, the slave confirms its presence also by a reset pulse.
- ROM command : allow the master to refer the slave with which it wants to enter in communication.
- DS18B20 function command : the function that need to be executed is chosen at this step.

In this protocol, it is really important to respect the timings imposed by the datasheet for each operation. Indeed, if the timing is wrong, the sensor is unable to recognize the information and does not work. For that, the initialization command, the write operation and read operation for the bit 1 or 0 are implemented respecting the different timing defined in the datasheet, they can be found in the Appendix D.

Finally, using this protocol, a communication is possible between the micro controller and the sensor and that is developed in the next subsection.

### 1-wire digital thermometer (DS18B20) development

The 1-wire digital thermometer DS18B20 is a quite simple sensor composed by three wires. One for the communication, one for the power supply and one connected to the ground. The basic schematic of it is shown in the Figure 5.6.

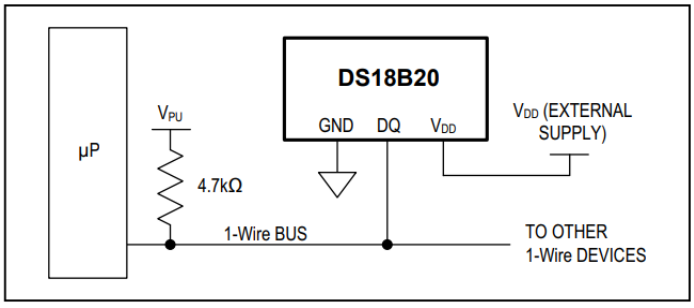


Figure 5.6 – Schematic of the connection of the DS18B20[13]

As explained previously, a pull-up resistor is used as it is a bi-directional communication in half-duplex and so the master cannot receive and send data in the same time.

Once the 1-wire bus is connected to a common pin of the micro controller, the implementation of the protocol can start.

The first step is the initialization. A function is directly implemented respecting the timing presented in the Appendix D.
Then, a ROM command need to be sent. As there is a lot of pin on the micro controller STM32F2 and that all the pins are dedicated only for this project, one can simply connected different thermometers on different pins and so for one pin there is only one slave address. In this case, the ROM command can be skip and this is translate by using the byte $CC_{hex}$. Note that all addresses are defined in the datasheet of the digital thermometer[13]. In practice, the master send the bits one-by-one respecting the timing of writing operation described in the Appendix D. The bits are sent from the LSB (Least Significant Bit) to the MSB (Most Significant Bit), this information will be useful when the signal will be analyzed with an oscilloscope (Figure 5.8).
Finally, the function command is sent on the bus by the master. As in this application one need only to read the temperature (alarm or other functionalities are not implemented), the corresponding function is expressed by the address $44_{hex}$.

Once the three steps are performed, the cycle need to restart. A new initialization is done, as before, the master skip the ROM command and, as the temperature has been converted, the master can now asks for the slave to read the value. This function corresponds to the address $BE_{hex}$. Then, the slave sends to the master 2 bytes of data that corresponds to the current temperature measured by the sensor. These 2 bytes of data are described as shown in the Figure 5.7.

| | BIT 7 | BIT 6 | BIT 5 | BIT 4 | BIT 3 | BIT 2 | BIT 1 | BIT 0 |
|---|---|---|---|---|---|---|---|---|
| LS BYTE | $2^3$ | $2^2$ | $2^1$ | $2^0$ | $2^{-1}$ | $2^{-2}$ | $2^{-3}$ | $2^{-4}$ |
| | **BIT 15** | **BIT 14** | **BIT 13** | **BIT 12** | **BIT 11** | **BIT 10** | **BIT 9** | **BIT 8** |
| MS BYTE | S | S | S | S | S | $2^6$ | $2^5$ | $2^4$ |

S = SIGN

Figure 5.7 – Temperature register format [13]

The final step is to stock these bytes in memory and transform them to correctly display, using the UART communication, the temperature in decimal numbers. The possible output range of the sensor is between -55°C and 125°C.

To conclude, an analyze of the 1-wire bus signal is presented in the Figure 5.8 and a picture of the final design is shown in the Figure 5.9. The Figure 5.8 has been obtained with a digital oscilloscope, the *PicoScope 6*. In the Figure 5.8, one can observe the different steps described previously.

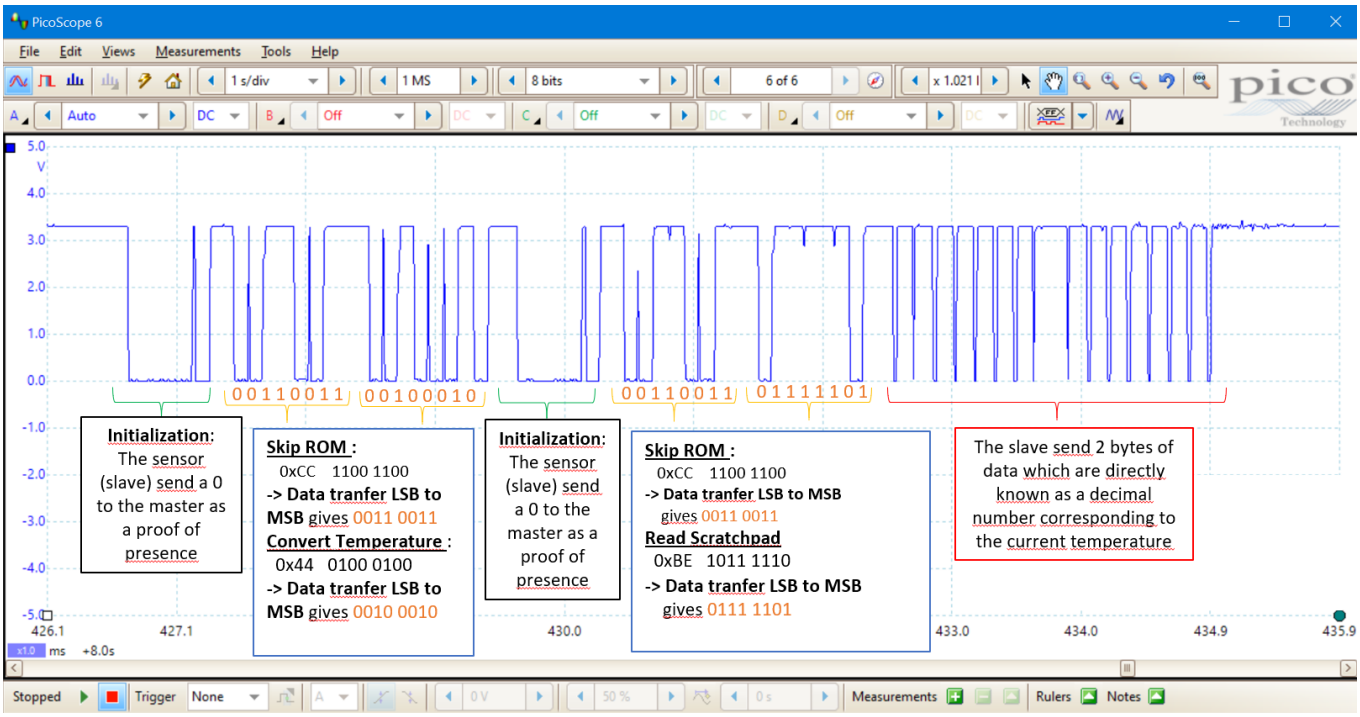


Figure 5.8 – 1-wire bus signal analyzing

Then, in the Figure 5.9, a handmade assembly has been made in order to have a clean board with all sensors connected.

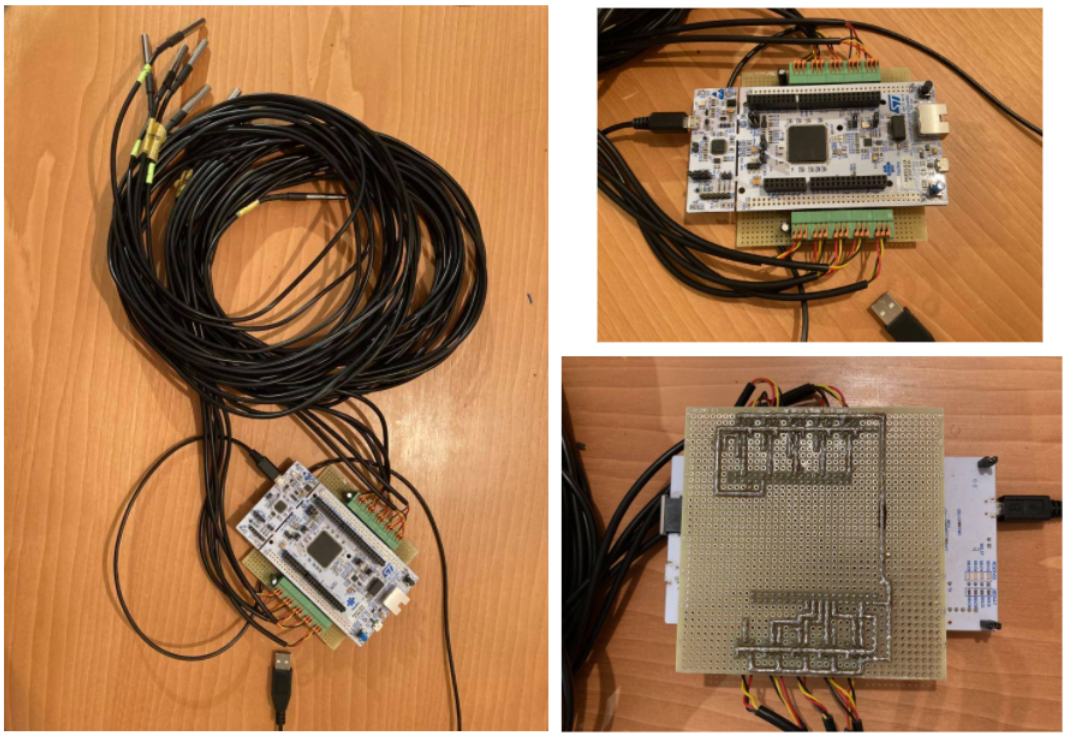

Figure 5.9 – Final design digital thermometer

In this final design, ten thermometers are connected to the micro controller. This one asks, one-by-one, to each sensor to receive the temperature that it measures, records each answer in a table and display on the computer, using the UART communication, the updated table every second. Using *Termite* [1] for this UART communication, the output of the sensor can be displayed and this is presented in the Figure 5.10, where the ten temperatures are shown and they are updated every second.

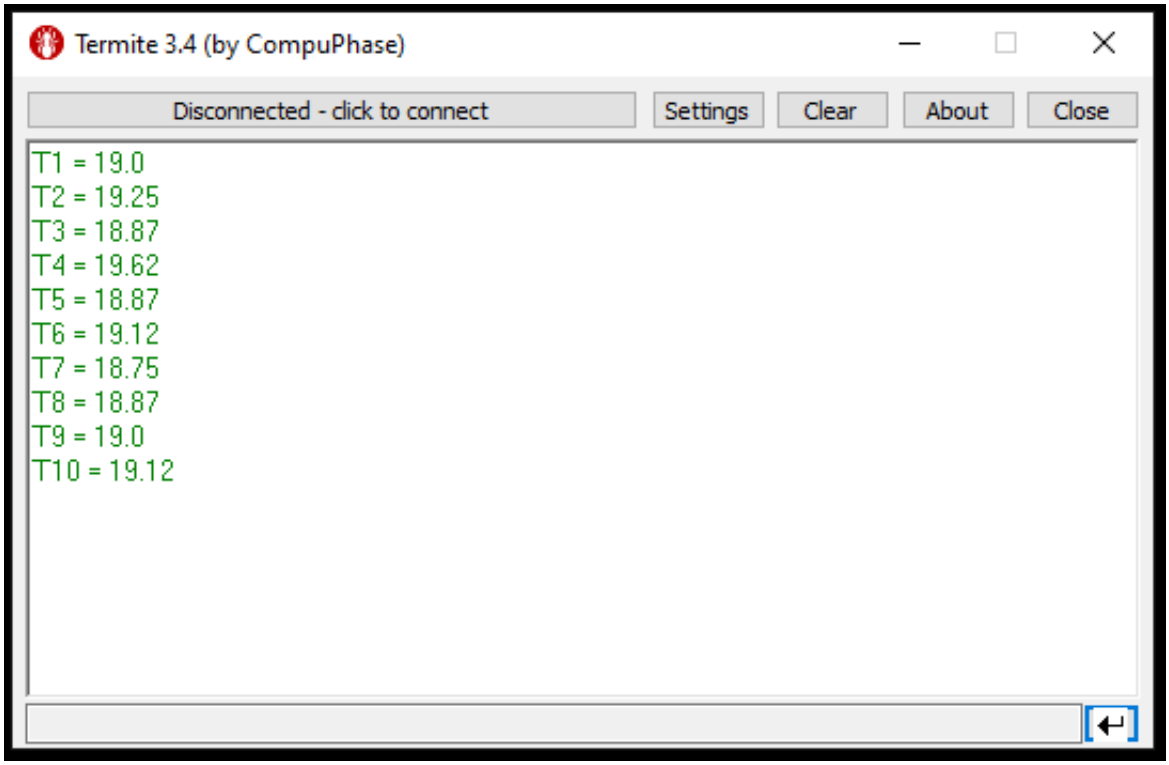


Figure 5.10 – Output of the digital thermometer DS18B20 displayed on *Termite*

## 5.2 Code implementation for using the position sensor

Once the position sensor hardware design is terminated, the next step is the acquisition of data. Indeed, the sensor returns, as output, a sine and a cosine signal but these ones reworked in software in order to receive the useful information for the future control, an angular position and a rotation speed.
For this purpose, I use the integrated development environment *CubeIDE*. This one allows to program the micro controller, the nucleo-G474RE. By the intermediary of a C source code, the cosine and sine signals are received and an algorithm with some mathematical operations is performed to obtain the angular position and rotation speed of the sensor.

As the rotation speed of the PMSM can reach 120 000 rpm, the rapidity of data acquisition is very important. In this section, I start to explain what was my first idea of implementation in the subsection 5.2.1. Then, after encountering issues of data acquisition, I decided to use some useful functions and components directly suggested by the micro controller in order to improve the time of execution of some operations and this is the subject of the section 5.2.2.

### 5.2.1 First idea of implementation

As explained in the chapter 4.2.2, the sensor returns a sine and a cosine signal that vary with the position of a metallic plate. The basic idea of the algorithm that I implemented is the following.
First, I start with two ADC conversions. ADC converters are available and directly implemented in hardware in the micro controller. So, simply by assigning the pins corresponding to the sine signal to one ADC converter and the cosine signal to another one, digital values of the two signals are available and can be assigned to a variable and stocked in memory.
The next step consists in removing the offset on the two signals. For that, the digital value corresponding to a sine equal to zero and a cosine equal to zero are determined and directly subtracted from themselves. In this way, digital values are centered which is important for the following step.
Then, the final step to get the angular position of the metallic plate is to use the trigonometric function $\arctan$ as below :

$$\theta = \arctan(\tan(\theta)) = \arctan \frac{\sin(\theta)}{\cos(\theta)}$$

with :

- $\theta$, the angular position of the metallic plate which corresponds to the angular position of the motor;
- $\sin(\theta)$, given by the digital value of the sine signal;
- $\cos(\theta)$, given by the digital value of the cosine signal.

So, in software, the function **atan2()** that comes from the library **math.h** is used to compute the $\arctan$ and the angular position is obtained.

After, the rotation speed has to be computed. Indeed, for a closed-loop control of a PMSM, the angular position and the rotation speed are necessary. For this output, the idea was to compare the actual angle at the time t and the angle computed at t-1. As the angular position is comprised between 0° and 359° increasing from 0° to 359° at each turn, if the angle t is lower than the angle t-1 that means that the metallic plate has done one complete turn.
Moreover, as the system is composed of only one pair of poles, one turn corresponds to one period. This correspondence is the reason of the choice of a semi-circle for the metallic plate in the section 4.2.1.

The idea is just to use a timer as a chronometer to get the time taken by the metallic plate to do one complete turn. In this way, the rotation speed is known using the following relation :

$$\text{Rotation speed [rpm]} = \frac{1}{\text{time for one complete turn}} \times 60.$$

The algorithm developed in this section is functional but only at low rotational speed. Indeed, using a screw-driver to test the software, it can be seen that above approximately 400 rpm, the value of rotational speed computed by the micro controller in software is totally wrong compare to the real speed. In fact, on second thought, I realized that the algorithm is correct but not enough efficient. The issue is mainly due to a too long time carrying out the operations.
Before to explain the solution, let start with a few explanations about the interruptions. An interruption is a part in the C source code which has to be executed with a priority more important than the rest of the code. In fact, an interruption is managed by its proper clock. The frequency of its clock corresponds to the frequency at which it will be triggered.

In this project, two interruptions are used, one for the chronometer and one for the angular position and rotation speed computation.
The chronometer is an interruption that is triggered every 20 µs and whose the operation is just to add one to a variable. In this way, when a turn is detected, the value of this variable is multiplied by 20 µs and the time taken by the plate for performing one turn is known. Then the variable is reset to zero and will increase until the next complete round.
The second interruption contains all the operations such as ADC conversion, trigonometric function, arithmetic operations and comparison. These ones need a long time of execution and so the total time of execution of the interruption is very long. This fact has as consequence that the clock frequency cannot be high. Indeed, in this case, the micro controller will spend its time only in this interruption and will not have the time for other interruptions or the rest of its operation.
To resume, a clock frequency too high with respect to the time of execution of its interruption brings the micro controller continuously blocked in the interruption and all the other operations are frozen. To avoid it, a lower clock frequency is assigned to the interruption but, for this project, it means that the angle will be updated with an longer interval of time.
This remark is exactly the cause of the issue explained previously. Indeed, the angle being updated with a long interval of time, when the rotation speed becomes to be too high, it occurs that a complete turn is not detected due to the too slow angle computation.

Several solutions had been found to counter this issue and it is the subject of the section 5.2.2.

### 5.2.2 Improvements

For solving problems encountered in the previous section, the idea is, on one part, reduce to the maximum the time of the angular position value acquisition and, on the other part, compute the rotational speed by using yet a chronometer but using now a comparator implemented in hardware in the micro controller instead of the algorithm that needs the angle value. In this way, the time of execution of the interruption will be smaller and the clock frequency going to be able to increase in order to have an angular position updated much more often than with the first idea of implementation. These solutions are developed in the following paragraphs and a part dedicated to the results is presented to close this section.

#### ADC with DMA

DMA means Direct Memory Access. It is a data transfer strategy that allows to skip the throught the CPU and directly stock the data in memory.

The micro controller can be divided in three main parts. The memory where the data are stocked, the CPU (Central Processing Unit) which is the brain of the micro controller and is responsible for managing the data transfer and execute all types of operations and finally the I/O (inputs and outputs) which are the read and write operations of data. These different parts are able to communicate with the intermediary of bus system.

In a micro controller, there are three different ways to stock a data in the memory.
First, the most basic one is the polling. In this configuration, the CPU asks continuously to the I/O part if some operations need to be managed and execute on its behalf. So, the data go in the CPU that manage it and then is stocked in the memory. This principle is illustrated in the Figure 5.11.

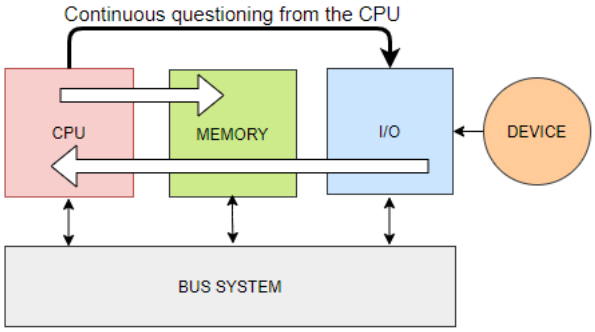


Figure 5.11 – Polling data transfer principle

Then, another way for transferring data is the interruption. As explained before, in this situation, the I/O device interrupts the CPU which stop immediately its operations and manage the data received from the I/O part. Once it is done, the data are stocked in memory. It is more efficient than the polling but the data still needs to pass thought the CPU before to be stocked. The interruption process is illustrated in the Figure 5.12.

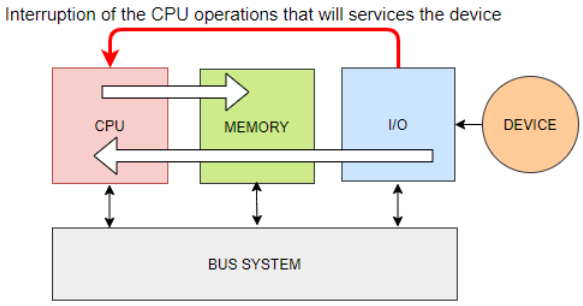


Figure 5.12 – Interruption data transfer principle

Finally, the last way is the DMA. It consists in directly goes in the memory without pass through the CPU. This data transfer can be very useful when the data received from the device do not need to be subject to some operations. Indeed, the advantage is a large time saving as the data is directly stocked. An illustration is shown in the Figure 5.13.

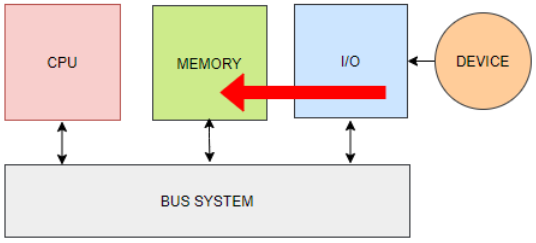


Figure 5.13 – DMA data transfer principle

So, coming back to the issue developed in the previous section. For the purpose of reducing the time of acquisition of the angular position, the ADC converter will be link to a DMA transfer. In this way, the converter sends directly its data to the memory without pass thought the CPU and the digital data acquisition is really faster than with the interruption mode.

### CORDIC

Cordic, that means COordinate Rotation DIgital Computer, is an algorithm used for the computation of trigonometric or hyperbolic function. This algorithm is already implemented in the micro controller. It is enough to use the predefined function available in the **HAL Library**.

The **HAL library** is a software sub-system provided directly by the company ST [24] that suggests a lot of different function already implemented in the background of the principal C source code. In fact, they allow to configure the micro controller faster and therefore be more efficient when developing the software. All the functions are not necessary available, it depends on the micro controller used. Here, the *NUCLEO-G474RE* is well adapted for the motor control because it contains a lot of useful functions for this application such as CORDIC.

With the CORDIC algorithm, the execution of the operation of $\arctan$ is more faster than **atan2()** which is a basic a function implemented in the library **math.h** and whose the efficiency is more lower than CORDIC.

To resume, CORDIC is used instead of a basic function to compute the $\arctan$ and thanks to it the time of execution is once again sharply reduced.

### Comparator

For the rotation speed acquisition, another strategy is developed. This one consists in using a comparator. This analog feature is an operational amplifier that allows to compare two analog signals. When one signal is greater than the other, the output signal is set to 1. In the other case, it stay to 0. The basic schematic of the comparator already implemented in hardware in the micro controller and the principle of operating is shown in the Figure 5.14

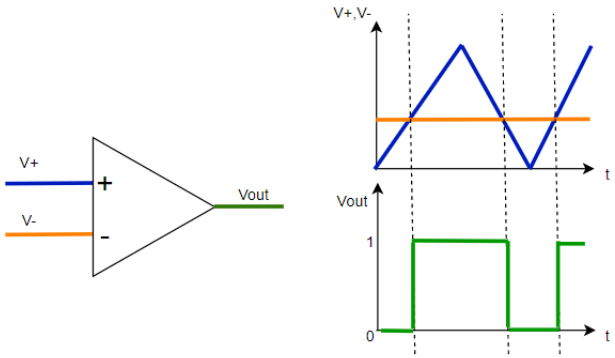


Figure 5.14 – Comparator basic principle

So, in order to compute the rotation speed, the strategy will be to connect the positive input to the cosine signal (the sine one gives could give the same result) and the negative input to a constant signal whose the amplitude corresponds exactly to the offset of the cosine signal. In other words, the cosine signal will be compared to its horizontal axis of symmetry.

As the comparator is only able to take in inputs analog signals and in order to have a constant signal corresponding to the offset at the negative input, a DAC converter is used. This one is a converter that takes a digital value in

input, converts it, and has a corresponding analog signal in output. So, setting the input equal to the value sent by the ADC converter when the metallic plate of the sensor is oriented such as the cosine signal is zero (90° or 270°), the DAC converts correctly an analog signal that corresponds to the horizontal axis of the cosine signal. Then, the output of the DAC is connected to the negative input of the comparator.
In this way, $V_{out}$ will have a rising edge at each time that the cosine signal starts a new period which corresponds to a complete turn. The algorithm to compute the rotation speed is now resume to start the chronometer at each time that there is a rising edge in the output of the comparator. This implementation is more efficient than the first one. Indeed, in this case, the rotation speed does not depend on the angle computation, and the comparator is always operating whatever the frequency of the signal.

To conclude, in the Figure 5.15, the observation of the output signal of the comparator with respect to the cosine signal is shown. In this Figure, it can be seen that the rising edge of $V_{out}$ (in green) is well corresponding to the starting of one period of the cosine signal. In this way, as explained in the section 5.2.1, the time elapsed between two rising edges corresponds to one period and so one complete turn of the metallic plate on the sensor and the rotation speed in rpm is finally obtained by the following expression

$$\frac{1}{\text{time elapsed between 2 rising edges}} \times 60.$$

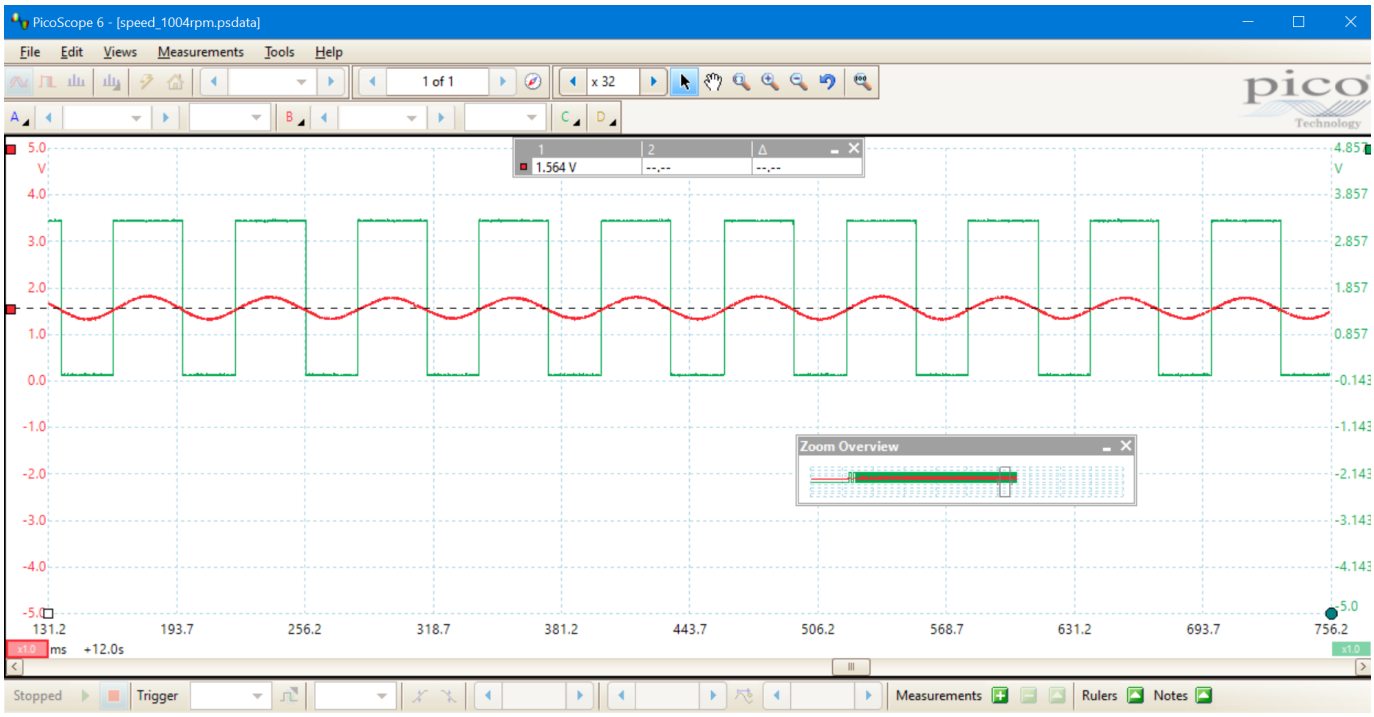


Figure 5.15 – Analyse of the output signal of the comparator (green) with respect to the cosine signal (red) with the digital oscilloscope *PicoScope*

**Results**

This final part demonstrates the usefulness of all these improvement techniques.

Let start with a screen of the oscilloscope (Figure 5.16) showing the execution time of the interruption that calculated the angular position and the rotation speed using the first idea of implementation.

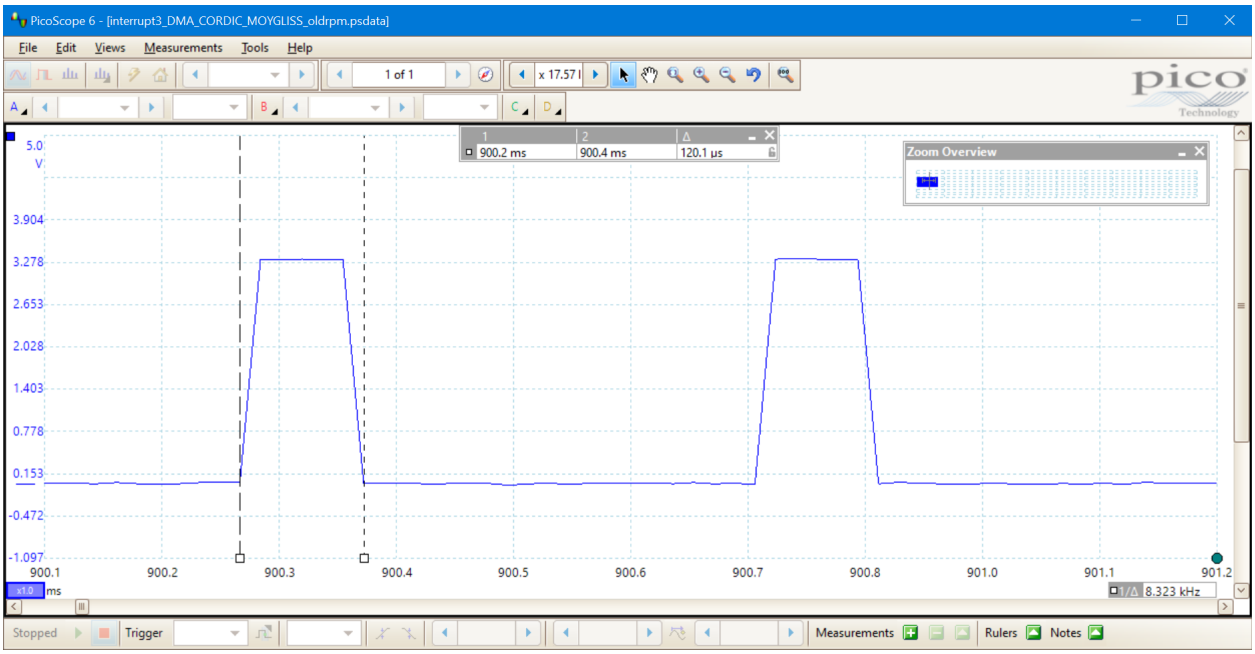


Figure 5.16 – Execution time of the interruption responsible for computing the angular position and the rotation speed with the digital oscilloscope *PicoScope*

In the Figure 5.16, it can be seen that the execution time of the interruption is equal to 120.1 µs. Here, the interruption is executed only each 500 µs. By reducing the execution time of the interruption, one will be able to considerably reduce this period in order to have an angular position updated more often. It is really important to reduce at maximum this period in order to have a new angle as much as possible during one turn. Indeed, in the closed-loop control, the feedback on the angle will be important and if there is not enough information, the control will be not efficient.

As expected, once all the improvement techniques are implemented, the execution time of the interruption is strongly reduced. This one is now only responsible for the angular position computation, the rotation speed being computed using the comparator linked to the chronometer. With all the improvements techniques, the execution time of the interruption is equal to 11.44 µs. Compared to the 120.1 µs obtained previously, it is a real enhancement. As the time of execution is much lower, one can largely improve the frequency in order to have an updated angle more often.So, the frequency of execution is 35 kHz which corresponds to a period of 28.57 µs that is a really better than the first idea of implementation. Indeed, with this frequency, when the motor will be at its maximum rotation speed, 120 000 rpm, which corresponds to kHz.

To resume, with this improvement, it will be possible to calculate a new angle minimum 17 times in one turn, as at maximum rotation speed there is the rapport $\frac{35\text{ kHz}}{2\text{ kHz}}$. The result of improvement is shown in the Figure 5.17.

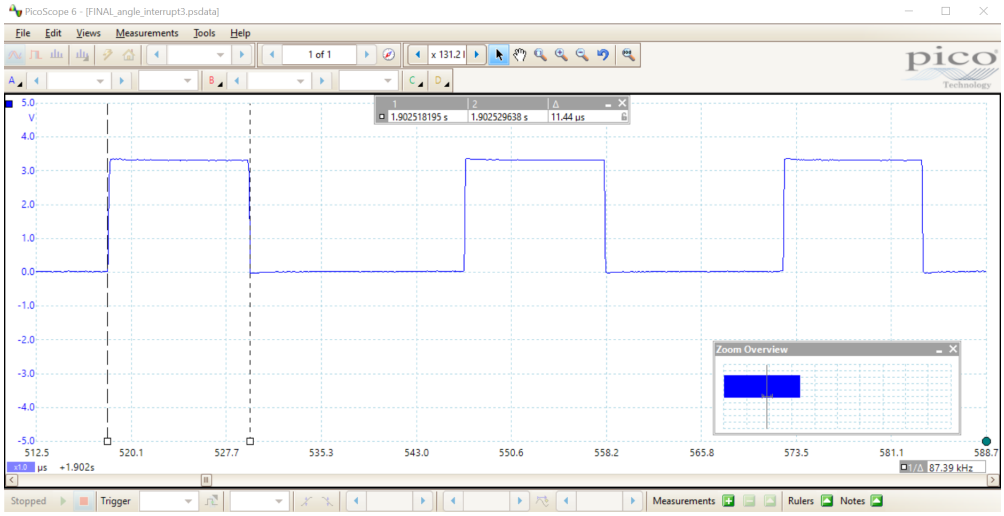


Figure 5.17 – Improvement of the execution time of the interruption for computing the angular position with the digital oscilloscope *PicoScope*

Finally, in the Figure 5.18, one can see a final test test performed with a balancing machine. Indeed it was impossible for the mechanical team to assemble the motor for a final test due to some other issues that does not concern this project. An alternative has been found in order to test the sensor at high rotation speed, the balancing machine is used in mechanic to balance some pieces and can reach 5000 rpm. So, the idea is to attach the metallic plate of the sensor to the rotating part and fix, in front of the metallic plate, the sensor with the electronic part. The cosine signal is then observed on the digital oscilloscope and the frequency is well corresponding to the one expected. Indeed, it is approximately 82.1 Hz which is equal to 4926 rpm. Moreover, the variable containing the rpm value in software indicated a correct value.

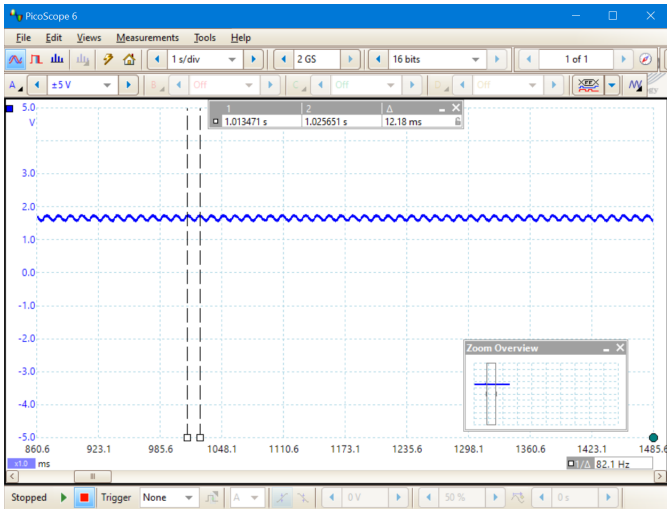


Figure 5.18 – Final test at high rotation speed (approximately 5000 rpm) with the digital oscilloscope *PicoScope*

As the hardware design and the software development of the Eddy current sensor is finished, it is the time to switch to the PMSM control part. In the next part, two ways to implement a closed-loop control will be developed and simulations on *Simulink* to test the ideas of implementation are presented.

# Chapter 6

# Closed-loop control using an Eddy current sensor

The purpose of this thesis is to develop an angular position sensor in order to be able to implement a closed-loop control.
A control is very important in this project because we need to impose a desired speed at different given time. Indeed, in the micro turbine domain, there is rotation speed of the shaft that need to be reached to be operational. In this case, the range of power produced is 10kWe. This range demands a rotational speed of 120 000 rpm. It is important to increase the rotation speed progressively to be more efficient and it is why a control is needed.
With a closed-loop control, as explained in the chapter 1, some issues such as current peaks, dropout, failed start that occur in the open-loop control can be avoided. Indeed, with the feedback information, some corrections can be imposed to the system in order to keep a stability and a proper functioning.

For the control part, I decided to test two kinds of control, a speed control and a speed and torque control combined. The first one is the simplest one and the second one is more complex but very promising. The idea is to implement and test the different controls on *Simulink* to have a good understanding of the different controls and analyzed which one could be the more interesting for a future real implementation on a micro controller.

## 6.1 Speed control

Let start with a speed control. In this closed-loop control, there are two feedback information. One for the rotation speed and one for the current angle. The rotation speed is compared to a reference speed and the error is corrected by a PI (proportional-integrator) controller. The expression of a discrete PI controller is defined as following :

$$K_P + K_I \cdot T_s \frac{1}{z-1}$$

with :

- $K_P$, the proportional constant;
- $K_I$, the integrator constant;
- $T_s$, the sampling time;
- $z$, the discrete variable.

With the current angle, it is possible to correct, at each time, the phase of the sine signals in the three phases. In this way, the rotating magnetic field generated at the stator is always corresponding to the one of the rotor which is very useful at the start-up of the machine. Indeed, if the two magnetic fields have the same orientation, failed start issues no longer occurs.
So the principle consists in using the current angle to generate the sine signals and so the PWM ones. Moreover, comparing the reference speed and the current one and by the intermediary of a PI controller, an angle is obtained. This one corresponds to a request of acceleration or deceleration. Indeed, when the rotation magnetic field is in advance with respect to the magnetic field of the rotor, it corresponds to an acceleration and so a positive angle at the output of the PI. In opposite, a negative angle corresponds to a deceleration. In other words, a phase shift is in reality a power flux.
Furthermore, to avoid the dropout issue a limiter is used to limit the phase shift between the rotating magnetic field of the stator and the magnetic field of the rotor. Indeed, if a phase shift upper than 90° occurs it leads to a dropout and the synchronous speed is lost. In other words, the rotor cannot continue to follow the rotating magnetic field and the machine is stopped.

To resume, thanks to this control, dropout and failed start issues are resolved. In the subsection 6.1.1, a block diagram is illustrated. Then, in the subsection 6.1.2, the implementation on *Simulink* is presented and finally, the subsection 6.1.3 shows the simulations performed on *Simulink* and some comments about the results.

### 6.1.1 Block diagram

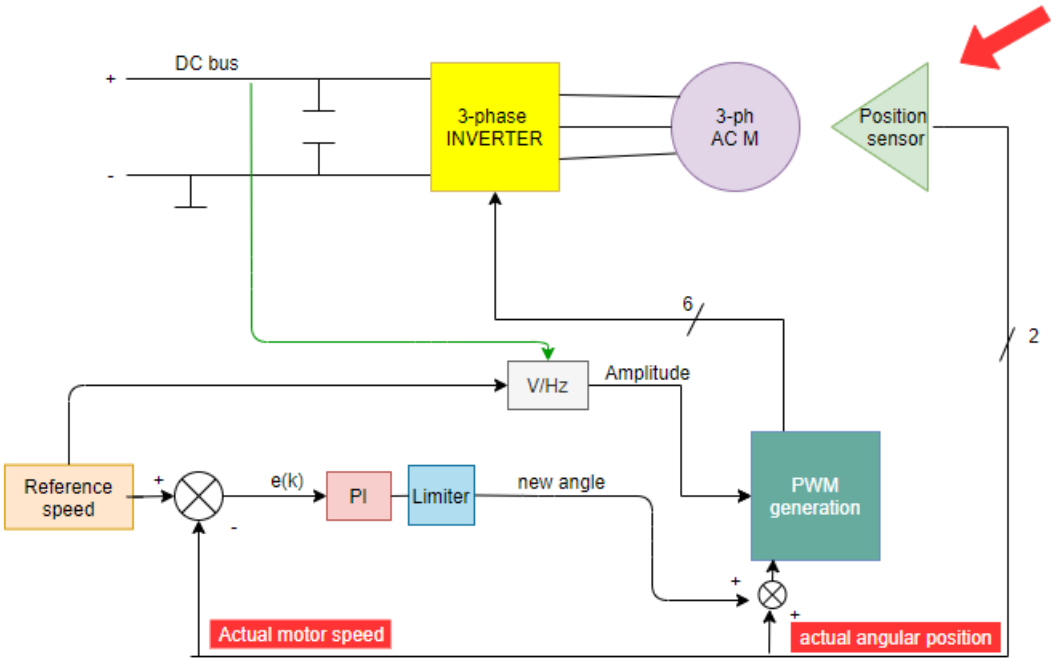


Figure 6.1 – Speed control - Block diagram

In the Figure 6.1, the part explained previously can be seen. The actual angle is used to be in phased with the rotor and avoid failed start. Then, the actual motor speed is used to obtain an angle that leads to a phase shift between the tho magnetic fields for the acceleration or deceleration.
In addition, a part over the amplitude is shown. Indeed, a sine signal is characterized by its phase but also by its amplitude. In PMSM, it exists a linear relation between the amplitude and the frequency of the motor (the frequency is the speed expressed in Hz which is the following :

$$A = \frac{f}{f\,\max} A\,\max \frac{Vdcmax}{Vdc}$$

where $f\,\max$, $A\,\max$ and $Vdcmax$ are known and depends on the characteristics of the motor, $Vdc$ comes from a measure on the bus and $f$ is the reference speed in Hz.
Note that an offset need to be set in order to counter the frictional force at the start-up of the system.

Finally, with the amplitude and the angle, a sine signal is obtained for the three phases (phase shift of 120° with respect to each one). These ones are compared to a carrier function and the PWM for each switching element are generated, as explained in the section 2.3. The implementation of this algorithm is presented in the next subsection.

### 6.1.2 Implemention on simulink

This subsection is dedicated to the implementation of the speed control in *Simulink*. The Figure 6.2 illustrates the block diagram used in *Simulink*.

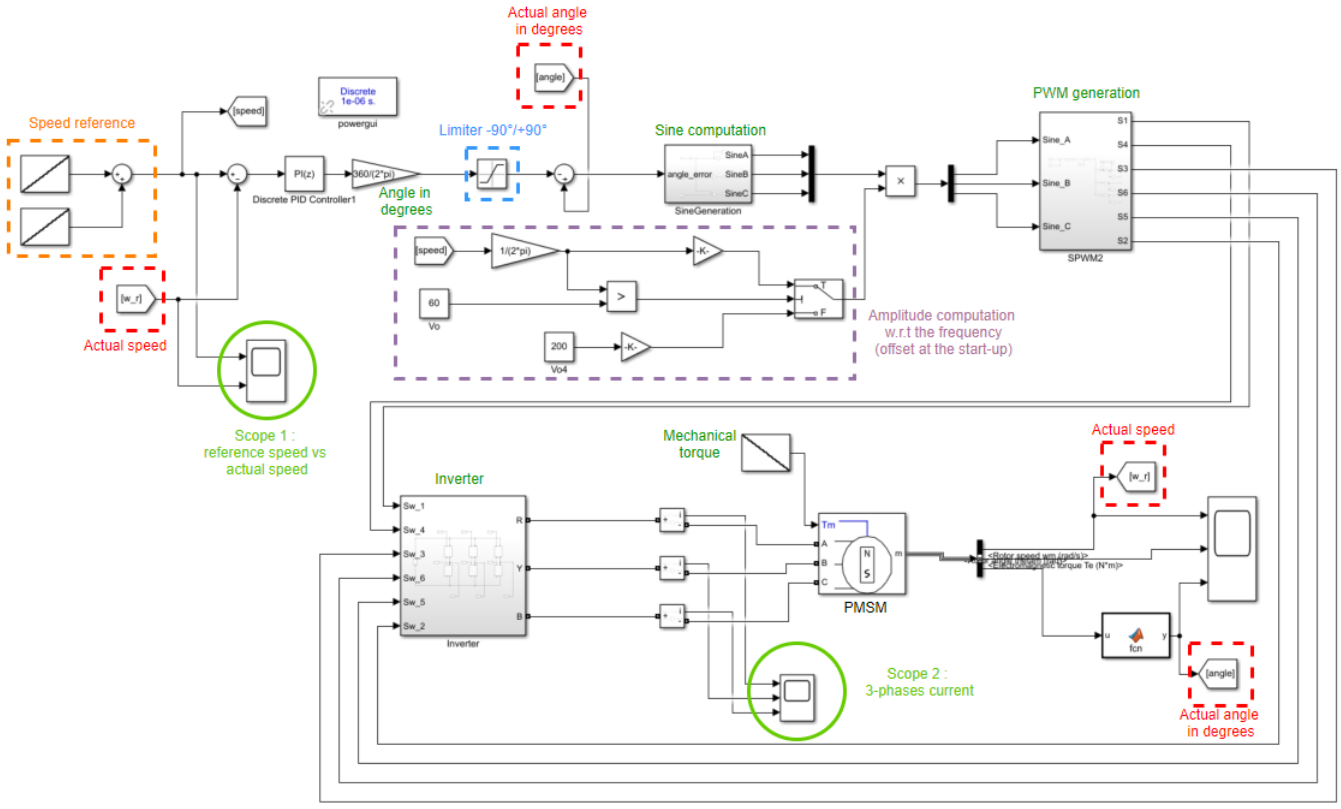


Figure 6.2 – *Simulink* - Block diagram of speed control

It is important to remark that this implementation is done in the purpose of well understanding the algorithm and observe the advantages and disadvantages for each kind of control. Here, the motor used is a system already implemented in *Simulink*. The main characteristics such as pair of poles or number of phases are corresponding to the real one but some precise physical characteristics such as the viscous damping, or the static friction are not known. So, it is evident that some adaptions will be performed when the closed-loop system will be really implemented on the real system.

The difficulty in the control is to design the PI. Here, the constant $K_P$ and $K_I$ are set by empirical method. The most important is to understand what is the output of the PI. A good practises method is to observe the behaviour of the system by setting a constant at the output of the PI which corresponds to an open-loop system. In this way, one can easily determine the correct sign for each variable in order to have an acceleration corresponding to a PI output positive. Then, analyzing the acceleration obtained with the chosen constant, $K_P$ can be approximately known and finally $K_I$ is set to remove the static error. Here , $K_P$ is set to 43 and $K_I$ to 7. The results achieved with this closed-loop system are presented in the next subsection.

### 6.1.3 Simulations and results

In the Figure 6.3 and Figure 6.4 it can be seen that the current speed is following correctly the reference one.It is a real good point for this control which is simple to be implemented. Here, the start-up is simulated with an objective of 18 000 rpm (equal to 1884.95 $\mathrm{rad\,s^{-1}}$) in 3 $\mathrm{s}$. This objective is necessary to allows to the foil-bearings to be in levitation as explain in the chapter 1. Then, the final rotation speed needed, 120 000 rpm (equal to 12 566.37 $\mathrm{rad\,s^{-1}}$) is progressively reached so the range of speed is largely accepted.

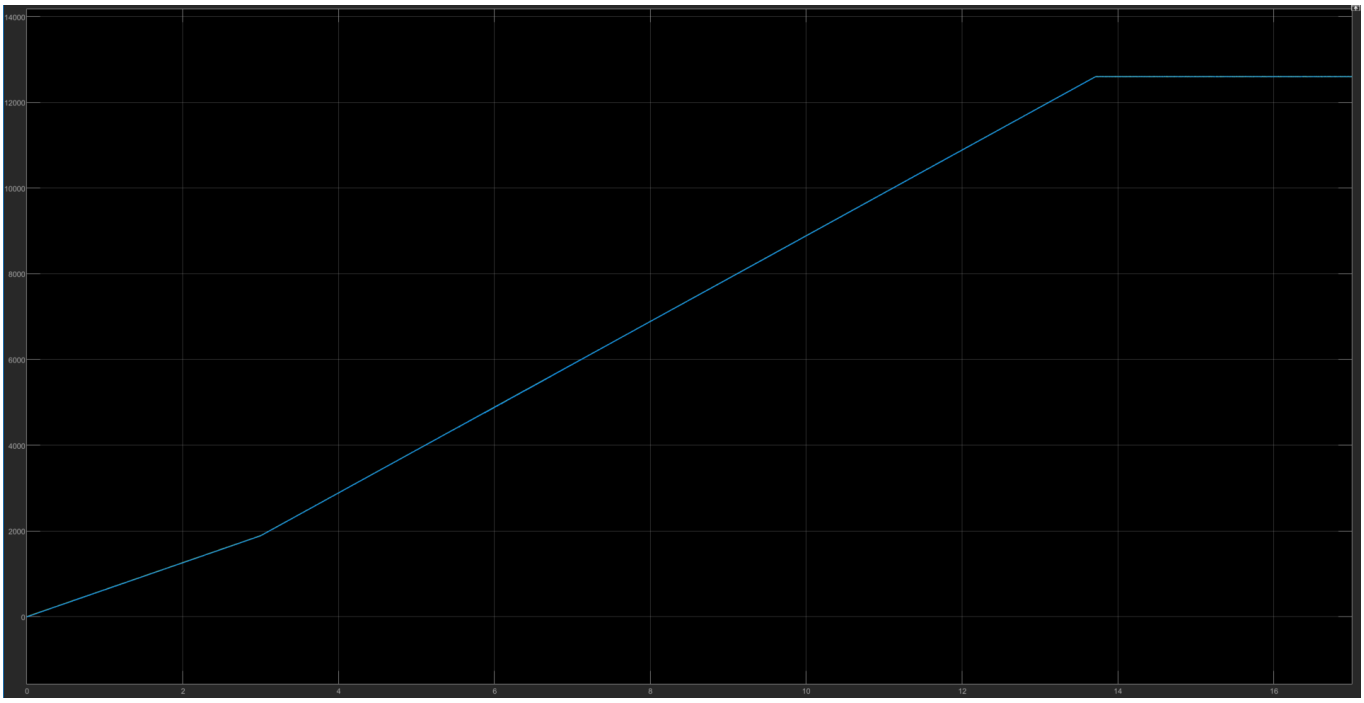


Figure 6.3 – Reference speed (yellow) vs actual speed $\mathrm{rad\,s^{-1}}$ (blue)

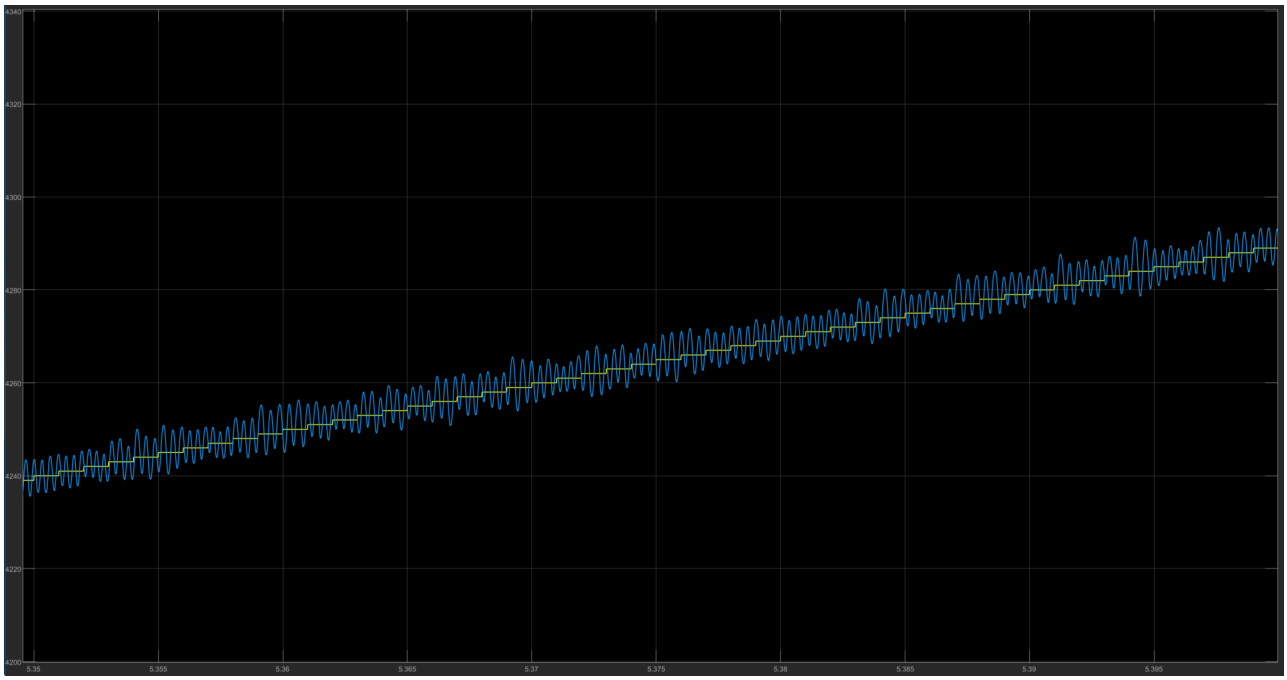

Figure 6.4 – Reference speed (yellow) vs actual speed $\mathrm{rad\,s^{-1}}$ (blue) - ZOOM over 0.05s

At first, this control seems perfect for the project but a problem is not resolved. Indeed, the large peaks current issue are still presents. In the Figure 6.5, the current in the three phases are shown. It can be seen that they can reach 250 A and that the mean value of the current is approximately 100 A

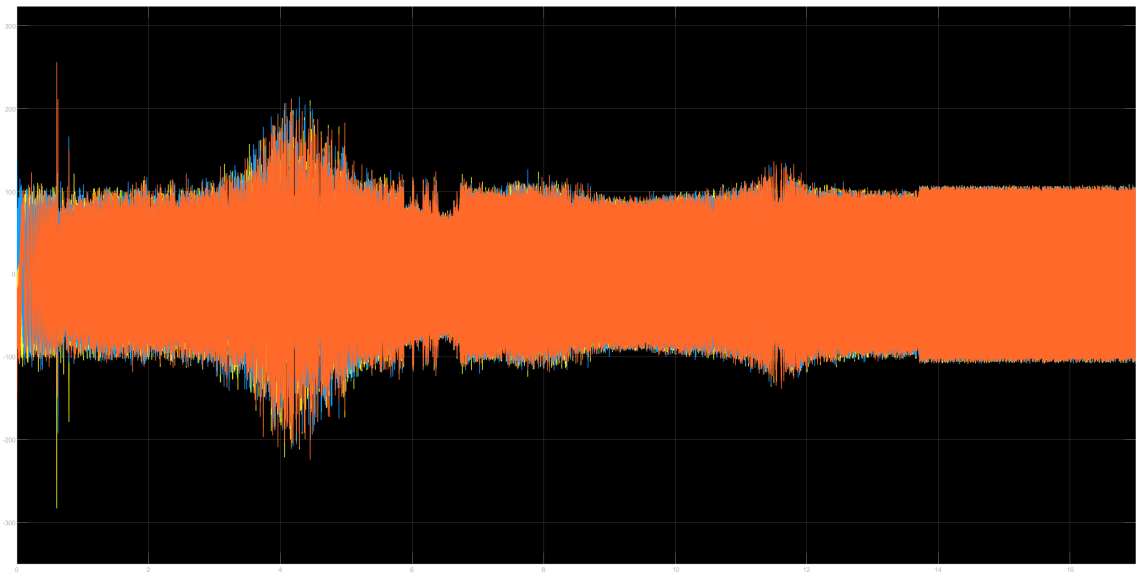

Figure 6.5 – 3-phase current

To conclude, with a speed control the problems of dropout and failed start are resolved but the one over large current and so large consumption and bad efficiency is still happening. The idea is to implement a more complex control that allows to control the current too and it is the subject of the section 6.2.

## 6.2 Torque and speed control

For this control, three PI controllers are used. One for the speed correction, one for the direct current and one for the quadrature current. In fact, the direct current and the quadrature one are used in other to simulate a DC machine. In this way, the 3-phase currents that need to be controlled are no longer sinusoidal but continuous and the control becomes really simple. It is a vector control.
Let start with a little development about the direct and quadrature currents.

First, the Clarke transform is used. This one is necessary for the vector control. It allows to change the reference frame. In fact the three phase system is transformed in a two phase system. This is illustrated in the Figure 6.6.

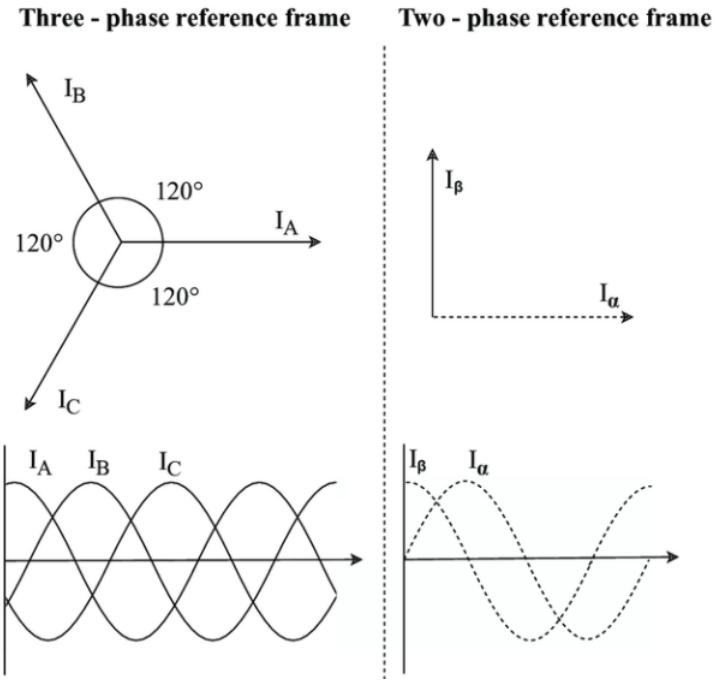


Figure 6.6 – Clarke transformation [15]

For this transformation, the following mathematical relation is used :

$$\begin{bmatrix} i_\alpha \\ i_\beta \end{bmatrix} = \begin{bmatrix} 1 & -\frac{1}{2} & -\frac{1}{2} \\ 0 & \frac{\sqrt{3}}{2} & -\frac{\sqrt{3}}{2} \end{bmatrix} \begin{bmatrix} i_a \\ i_b \\ i_c \end{bmatrix}$$

Not that the Clarke frame is still fixed to the stator and so the current is still alternative.

The next step is to transform the Clarke frame in a reference frame that is moving with the rotor. It is the Park frame obtained by the Park transform. With this moving frame, the currents of the machine are continuous. Indeed, as the frame is moving with the rotor, the rotating magnetic field is seen like a constant. The Park transform is illustrated in the Figure 6.7.

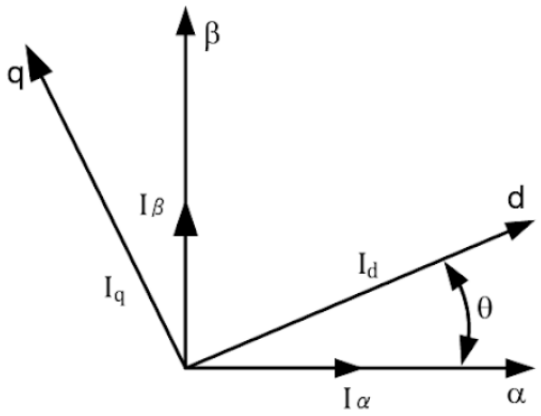


Figure 6.7 – Park transformation [8]

In fact, the Park frame is the Clarke frame that is subject to a rotation. This rotation depends on the angular position of the rotor. The mathematical expression that link the two frames is the following :

$$\begin{bmatrix} I_d \\ I_q \end{bmatrix} = \begin{bmatrix} \cos\theta & \sin\theta \\ -\sin\theta & \cos\theta \end{bmatrix} \begin{bmatrix} i_\alpha \\ i_\beta \end{bmatrix}$$

To resume, the clarke transformation is used to switch from a three-phase reference frame to a two-phase one and the Park transformation allows to obtain a moving reference frame and so continuous current for the machine. This is resume with an illustration in the Figure 6.8.

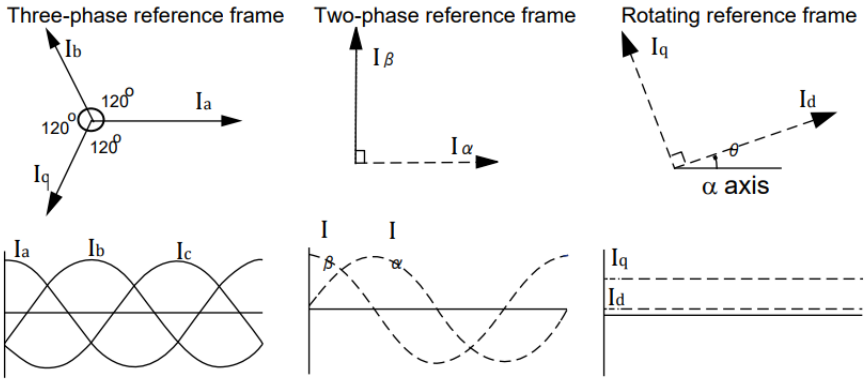


Figure 6.8 – Clarke and Park transformation [14]

The quadrature current corresponds to the one used for the acceleration, it controls the torque and the direct current is theoretically equal to zero as the rotor is a permanent magnet. In practise, there is a small current $I_d$, in fact, it is a reactive current due to different physical phenomenon. As, in the Park frame, they are continuous two PIs can be used to correct them. The concept of torque and speed control is explained in the subsection 6.2.1 where the block diagram of the control is presented.

### 6.2.1 Block diagram

Let start with the illustration of the block diagram in the Figure 6.9.

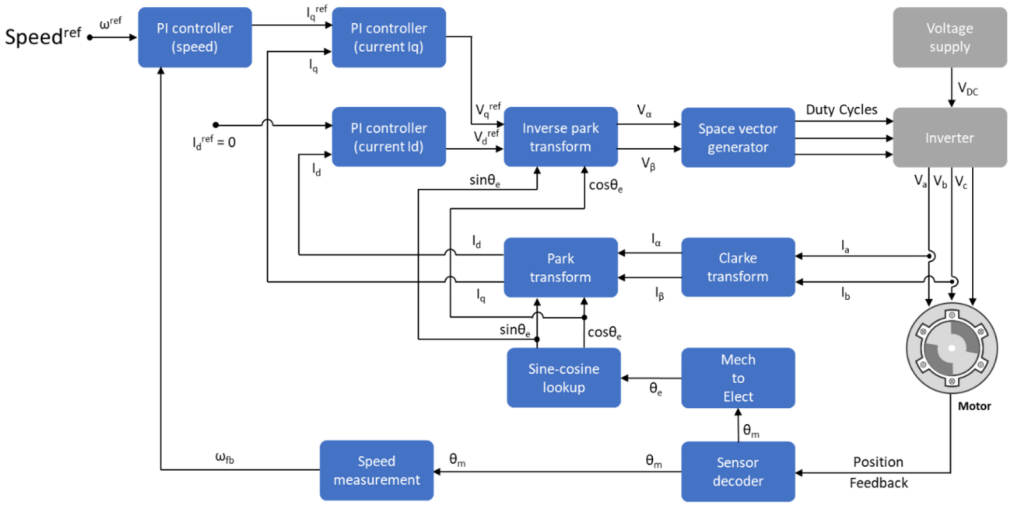


Figure 6.9 – Speed and torque control - Block diagram [14]

This kind of control is well known as FOC (Field Oriented Control). As explained previously, the reference reference frame of the 3-phase current is transformed by Clarke and Park and the continuous currents obtained after these transformations are controlled. $I_d$ is theoretically equal to zero so the reference is zero. $I_q$ is responsible for the torque of the machine directly link with the rotation speed Indeed, to accelerate, $I_q$ need to increase. With this logic, three loops are implemented to form a closed-loop control with a good control capability over the full torque and speed ranges. There are 2 loops for $I_q$ and $I_d$ respectively and one loop for the speed control. This loop influences the torque control loop in order to force an acceleration (or deceleration) in the system.

The space vector generator is a specific block for the vector control. It allows to generate PWM in function of the orientation of the vector in the Clarke frame. Note that before the space vector generator block, an inverse park transform is performed in order to return in the Clarke frame. The space vector generator is a block already implemented in *Simulink*, it can be directly used. An illustration to explain its algorithm is shown in the Figure 6.10.

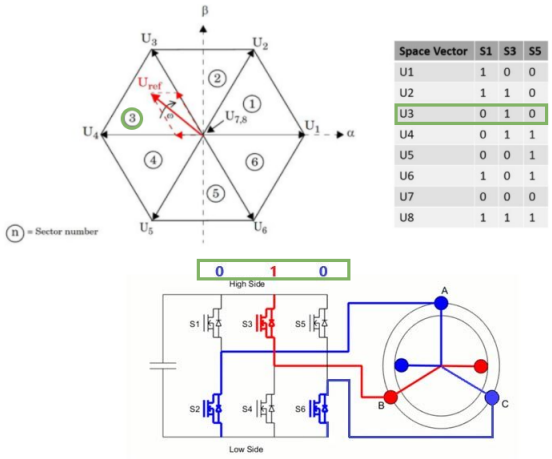


Figure 6.10 – Space vector generator - Upper left : hexagon plan for the different sector - Upper right : Switches combination w.r.t. the sector number - Bottom : Inverter with the switches connected to the stator[12]

In the Figure 6.10, it can be seen that in function of the position of the vector $U_{ref}$ which is expressed in the Clarke frame ($\alpha$ and $\beta$), the combination of the switches that has to conduct is defined. For instance, the sector number 3 corresponds to the low side (0) switch on the branch 1, the high side (1) switch on the branch 2 and the low side (0) 1 for the last branch. In order to analyze the advantages and disadvantages of this control, this block diagram is implemented in *Simulink*.

### 6.2.2 Implemention on simulink

In *Simulink*, the main blocks such as Clarke and Park transform, inverse Park transform and space vector generator are already implemented. The difficulty is the three PIs that needs to be designed in order to have a stable closed-loop control. The *Simulink* block diagram is shown in the Figure 3.2.

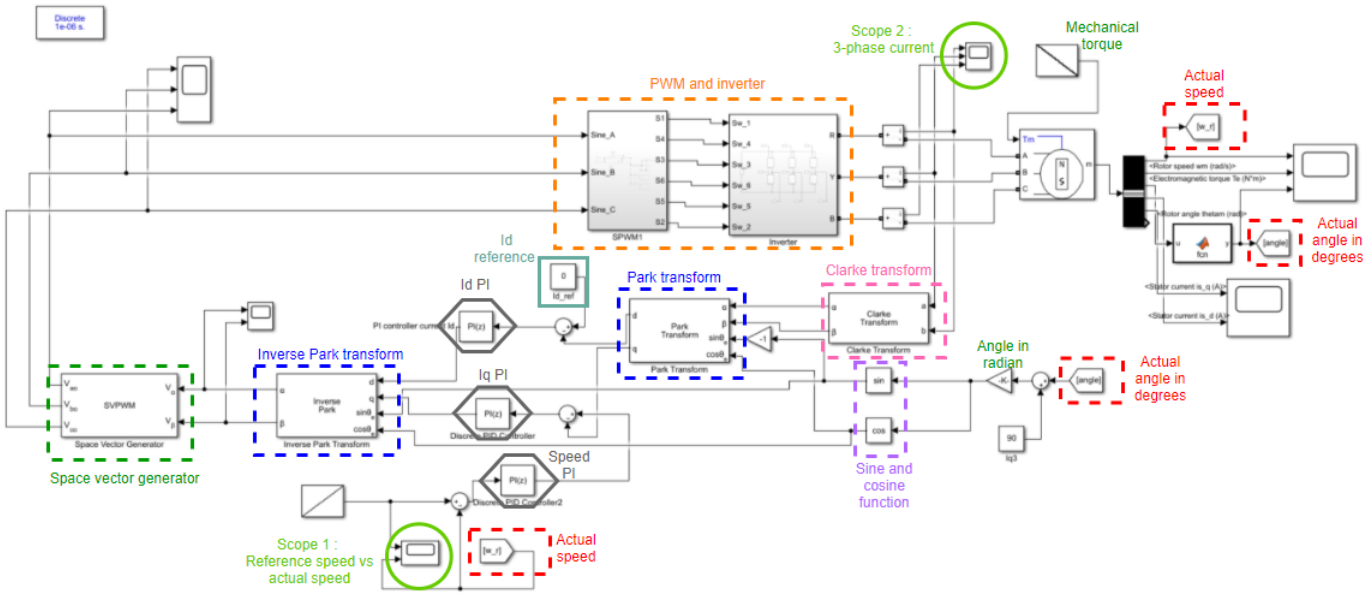


Figure 6.11 – *Simulink* - Block diagram of torque and speed control

The method to design the three PIs is the following. First, the speed control loop is not used. $I_q$ and $I_d$ are set as two constants two simulate an open-loop system and the speed, $I_q$ and $I_d$ are analyzed. In this way, the PI for $I_d$ can be designed by using the relation between the constant chosen for $I_d$ and the corresponding output. Indeed, $K_p$ is the multiplier corrector and it is set to 0.5. Then $K_I$ is chosen in order to remove the static error and equal to 0.001. Each value is set empirically but observe the difference between a constant imposed in open-loop and its output is a good way to choose approximately a good constant $K_P$.
Once the PI for $I_d$ is operational, the one for $I_q$ can be designed. The constants are chosen in the same way and they are set to $K_p$ equal to 0.05 and $K_I$ equal to 0.00005.
Finally, the speed control loop is added to the system. The PI is designed by empirical method in order to have a stable system. The best value found for $K_P$ and $K_I$ are respectively 60 and 0.001.

Finally, simulations can be performed and the results are presented in the next subsection.

### 6.2.3 Simulations and results

This subsection is dedicated to the simulations of the rotation speed and the 3-phase current in order to compare the results with the speed control implemented in the section 6.1.

First, in the Figure 6.12 and the Figure 6.13, it can be seen that, as expected, the current rotation speed is correctly following the reference one.

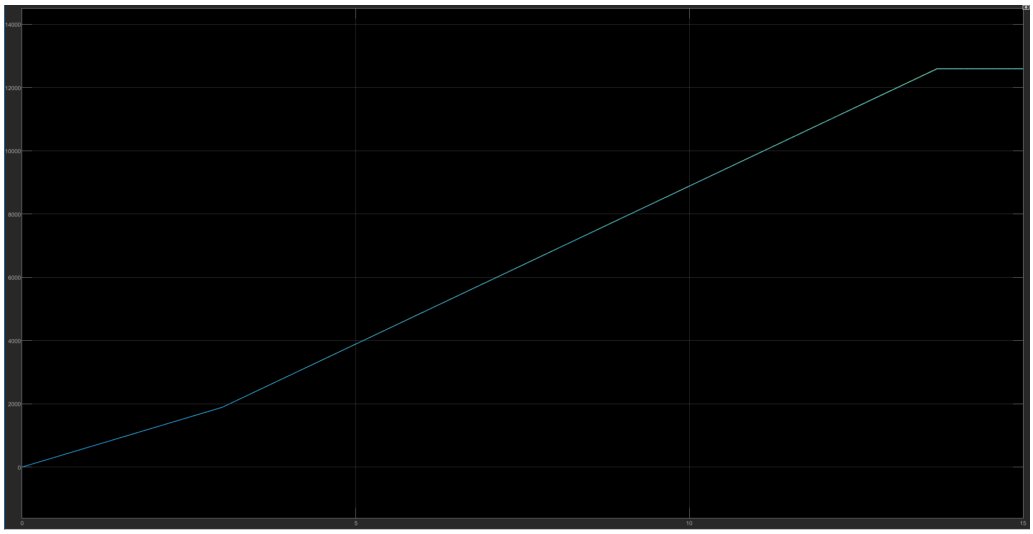

Figure 6.12 – Reference rotation speed (yellow) compared to the current rotation speed $\mathrm{rad\,s^{-1}}$ (blue)

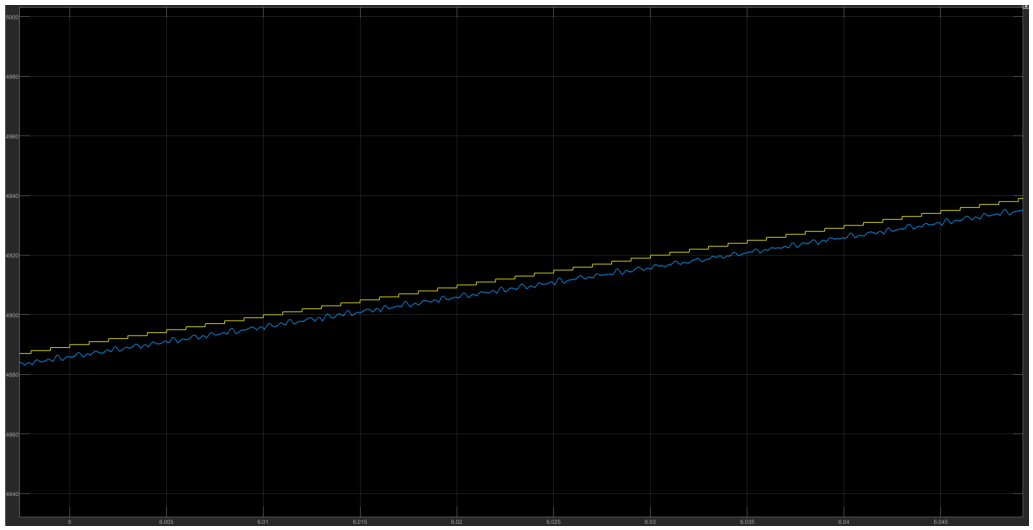

Figure 6.13 – Reference rotation speed (yellow) compared to the current rotation speed $\mathrm{rad\,s^{-1}}$ (blue) - Zoom over 0.05 $\mathrm{s}$

Compared to the closed-loop system implemented in the section 6.1, the important advantage for this one is the control on the 3-phase current. Indeed, this control promise to remove the large current peaks and that can be observed in the Figure 6.14.

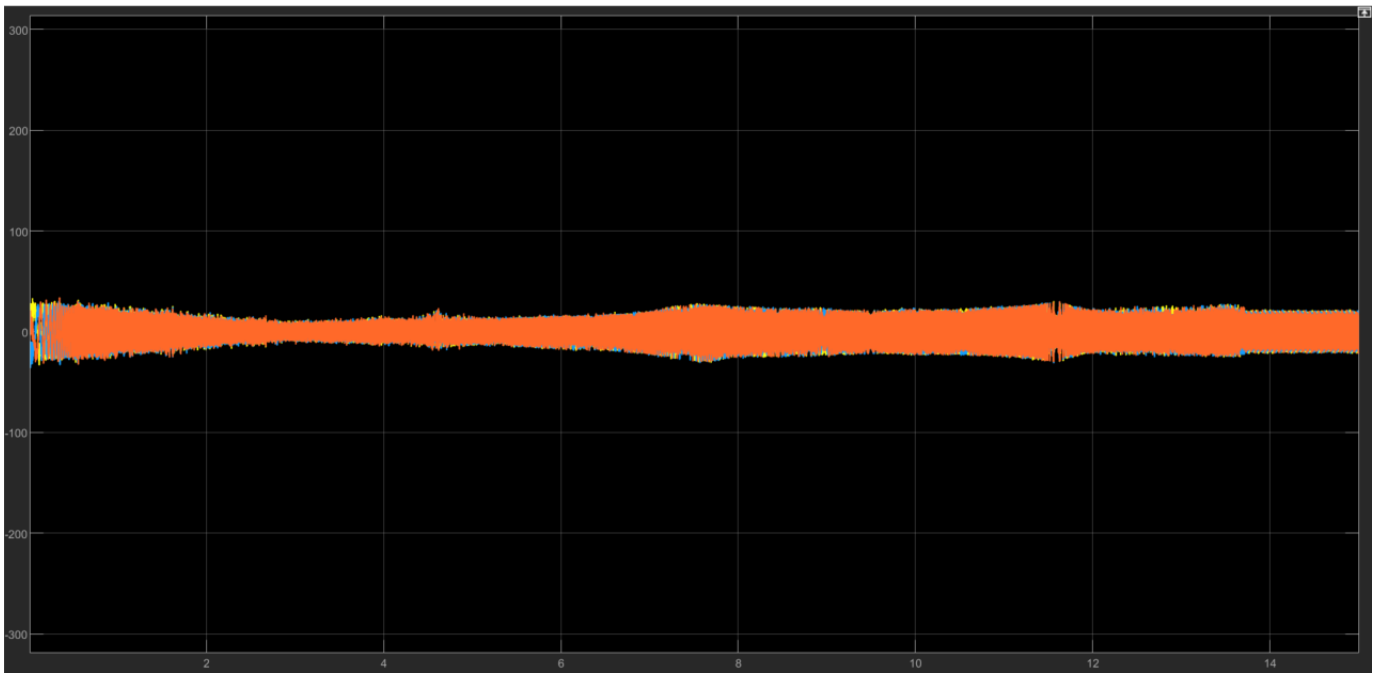


Figure 6.14 – 3-phase current [A] with a speed and torque control (FOC)

Here, a real improvement in the 3-phase current can be observed. Indeed there is no longer large peak of current and the average amplitude of the current is about 30 A which is really decreasing in consumption and improve the efficiency of the system.

To conclude, with the speed and torque control, more commonly called FOC, it is possible to control the speed while maintaining low current in the 3-phase. This result is very promising compared to the open-loop system already implemented and where different issues such as dropout, failed start and large current are observed.

# Chapter 7

# Conclusions and perspectives

This master thesis is dedicated to the development of an angular position sensor in the purpose of implementing a closed-loop control. This control is important to improve the stability and efficiency of a PMSM (Permanent Magnet Synchronous Motor).

The PMSM is included in a micro turbine system and the final objective of the motor is to reach rapidly 120 000 rpm to have a rotation speed of the shaft that corresponds to the sufficient one to drive the complex compressor-turbine. Indeed, compressor, turbine and motor are located on the same shaft and a rotation speed of 120 000 rpm is needed when the range of power production is 10 kWe. This speed need to be controlled to increase progressively and reach a final speed smoothly with a good efficiency.

With an open-loop control, different issues. First, the dropout of the magnetic field of the rotor with respect to the rotating magnetic field of the stator. It is the case where the synchronous speed is lost. Then a failed start is often occurring. Finally, large peak of currents are present in the stator windings. To counter these problems, a closed-loop system need to be implemented to improve the stability and efficiency by the intermediary of a feedback information, the angular position of the rotor.

In this thesis, the main part the development of the angular position sensor. Indeed, the position sensor need to be efficient in a large range of rotation speed, precisely from 0 to 120 000 rpm. A comparison of different angular position sensor has been realized and the choice for the most appropriate one was an Eddy current sensor. Indeed, this technology is really recent and very promising. It is particularly its quality of low maintenance, accuracy, and the lack of need to be close to the magnet compared to a hall effect sensor commonly used for the motor control that motivate this choice.

For start, a kit of development provided by Renesas is used with an Eddy current sensor and a chip that allows a communication between the sensor and the computer. Then, the design of the Eddy current sensor need to be adapted to this project. This is performed in Altium, a program used for PCB design and still by using different tools provided by Renesas such as the basic schematic and the footprint of the coil used in the design and adapted to the dimensions of the project. The design part is very complex with some mechanical and manufacturing constraints that have to be strictly respected.
Once the design is terminated, a communication between the new sensor and can be done still by the intermediary of the chip provided by Renesas. The following step is the software development in order to use our proper micro-

controller instead of this chip. This one is the STM32G474RE perfectly adapted to the motor control and provided by the company ST. The challenge was the time of execution and so some techniques of improvement had been used.

Once the micro controller is able to measure an angular position and a rotation speed at each time, the idea of closed-loop control can be considered. The first idea is a speed control which is sufficient but does not allow to avoid large peaks of current in the stator. The other solution is to implement a speed and torque control, known as FOC, which , in addition of the advantages of the speed control, allows to remove these large peaks of current and keep maintaining them lower. Simulations are performed in *Simulink* and the expected results are demonstrated.

For the global project, there are different perspectives that can be envisaged.
First, the sensor need to be tested on a real machine to be sure that the software part is able to follow a rotation speed such as 120 000 rpm.
After that, the main next step is to implement the closed-loop control in a micro controller in order to really try to control a motor by experiment. Indeed, a perfect design of the different PIs used will be accomplished only when the control implementation will be faced to the real system.

Finally this project has been really interesting and is promising for the future development of the micro-turbine system. Indeed, this idea of control can also be implemented for controlling the turbine. That is known as VOC (Voltage Oriented Control) and the contribution to efficiency and power productivity could be a real improvement for the MITIS company.

# Bibliography


[1] Termite - RS232 terminal. https://infocenter.nordicsemi.com/index.jsp?topic=%2Fug_gsg_ses%2FUG%2Fgsg%2Fconnect_uart.html.

[2] C. automation. Antennas and resonant circuits (tank circuits). https://control.com/textbook/ac-electricity/antennas/.

[3] B. Boigelot. Uliège course : INFO0064 - embedded systems. 2021.

[4] P.-X. X. H.-C. H. G.-T. B. Da-Chen Pang, Zhen-Jia Shi. Investigation of an inset micro permanent magnet synchronous motor using soft magnetic composite material. https://www.mdpi.com/1996-1073/13/17/4445, 2020.

[5] Eurocircuits. *PCB Design Guidelines*.

[6] Eurocircuits. *PCB Prototypes  Small Series, Manufactured and Assembled in Europe, Fast  Easy*.

[7] C. Geuzaine. Uliège course : ELEN0074-1 - electromagnetic energy conversion. 2019.

[8] O. Keysan. Ee-464 static power conversion-ii other pwm techniques. http://keysan.me/presentations/ee464_svpwm.html#1.

[9] Lesics-français. Youtube - moteur à réaction, comment ça marche ? https://www.youtube.com/watch?v=QZUNHHfZm5k&t=185s.

[10] lumen. Magnetic fields produced by currents: Ampere's law. https://courses.lumenlearning.com/physics/chapter/22-9-magnetic-fields-produced-by-currents-amperes-law/.

[11] V. D. T. H. Mathias Schubert, Philipp Kühne. Optical hall effect—model description: tutorial. *OSA publishing*, 2016.

[12] MathWorks. Space vector modulation (svm) for motor control. https://nl.mathworks.com/solutions/power-electronics-control/space-vector-modulation.html.

[13] Maxim-Integrated. *DS18B20 Datasheet*.

[14] Microsemi. Park, inverse park and clarke, inverse clarke transformations mss software implementation. https://www.microsemi.com/document-portal/doc_view/132799-park-inverse-park-and-clarke-inverse-clarke-transformations-mss-software-

[15] J. B. J. B. R. K.-R. J. L. D. J. R. H. W. Radek Martinek, Petr Bilik. Design of a measuring system for electricity quality monitoring within the smart street lighting test polygon: Pilot study on adaptive current control strategy for three-phase shunt active power filters. https://www.researchgate.net/figure/Clarke-transformation-coordinates_fig2_340042886.

[16] RealPars. Youtube - what is the difference between absolute and incremental encoders ? https://www.youtube.com/watch?v=-Qk--Sjgq78.

[17] Recurdyn. PMSM (Permanent Magnet Synchronous Machine). https://functionbay.com/documentation/onlinehelp/default.htm#!Documents/pmsmpermanentmagnetsynchronousmachine.htm.

[18] Renesas. *Inductive Position Sensor for High-Speed Motor Commutation*.

[19] Renesas. *IPS2200STKIT - IPS2200 Evaluation kit user manual and software*.

[20] Renesas. *IPS2200 - Family overview*, 2020.

[21] Renesas. *IPS2200 - Inductive Position Sensor IC : Datasheet*, 2021.

[22] Renesas. *IPS2200 Programming Guide*, 2021.

[23] ST. STM32 Nucleo-64 development board with STM32G474RE mcu, supports arduino and st morpho connectivity. https://www.st.com/en/evaluation-tools/nucleo-g474re.html#overview&secondary=st_all-features_sec-nav-tab.

[24] STMicroelectronics. https://www.st.com/content/st_com/en.html.

[25] E. tutorial. Passive low pass filter. https://www.electronics-tutorials.ws/filter/filter_2.html.

[26] P. Vanderbemden. Uliège course : ELEC0431-2 - sensors, microsensors and instrumentation. 2020.

[27] WatElectronics.com. Wireless power transfer. https://www.watelectronics.com/wireless-power-transfer/.

[28] S. B. L. D.-M. L.-D. F. D. R. F. B. Yonghyun Park, Chanseung Yang. On-line detection and classification of rotor and load defects in pmsms based on hall sensor measurements.

# Appendix A

# Schematic of the IPS2200

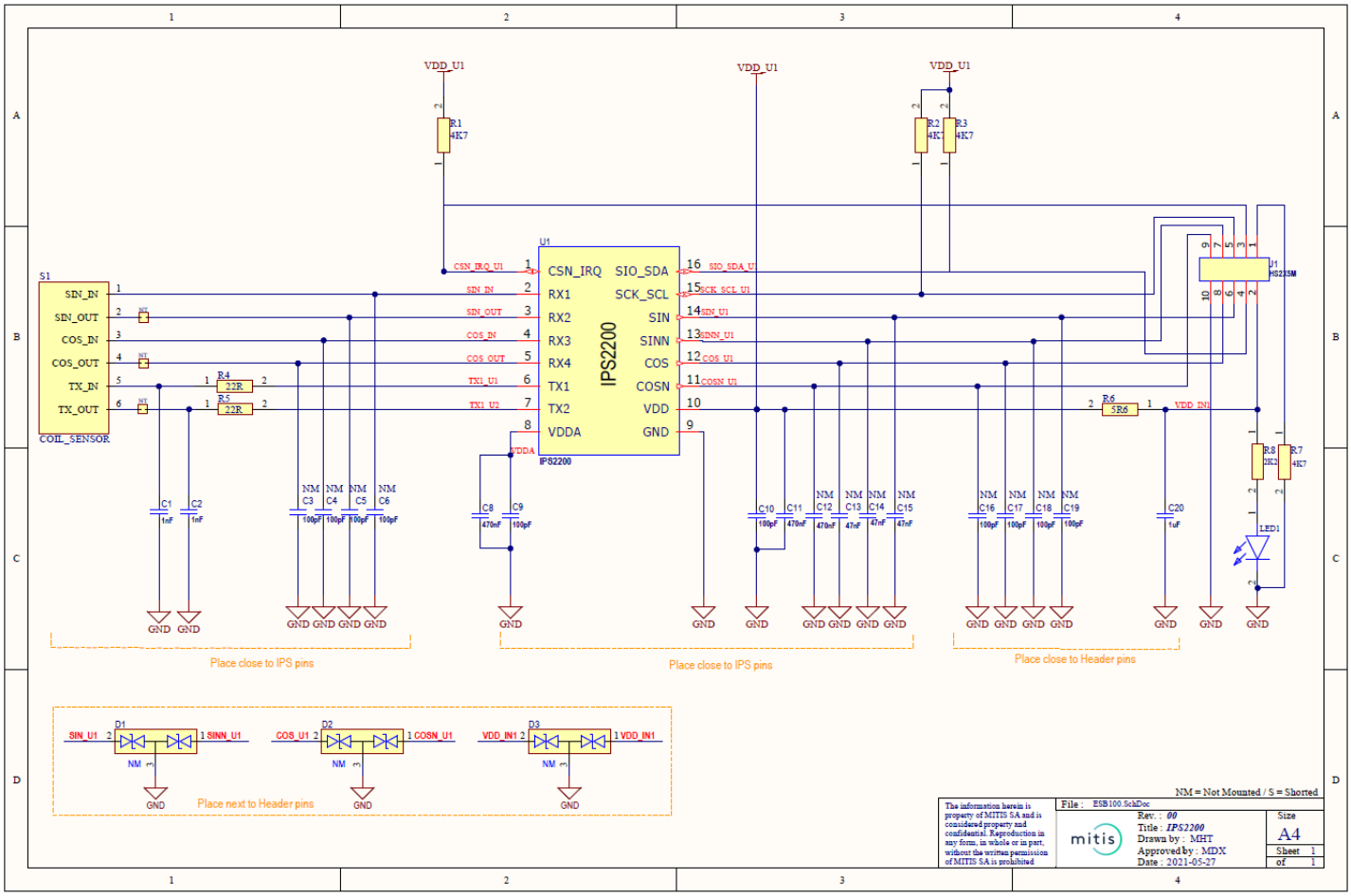


Figure A.1 – IPS2200 schematic

# Appendix B

# NVM to SRB address mapping

| NVM Address | SRB Address | Description | Bit Position | | |
|---|---|---|---|---|---|
| | | | Bits 15 to 12 | Bit 11 | Bits 10 to 0 |
| $00_{HEX}$ | $20_{HEX}$ | System configuration 1 | ECC | $P_{DED}$ | Data 10 to Data 0 |
| $01_{HEX}$ | $21_{HEX}$ | System configuration 2 | ECC | $P_{DED}$ | Data 10 to Data 0 |
| $02_{HEX}$ | $22_{HEX}$ | R1/R2 gain | ECC | $P_{DED}$ | Data 10 to Data 0 |
| $03_{HEX}$ | $23_{HEX}$ | System configuration 3 | ECC | $P_{DED}$ | Data 10 to Data 0 |
| $04_{HEX}$ | $24_{HEX}$ | R2 coil offset | ECC | $P_{DED}$ | Data 10 to Data 0 |
| $05_{HEX}$ | $25_{HEX}$ | internal use | ECC | $P_{DED}$ | Data 10 to Data 0 |
| $06_{HEX}$ | $26_{HEX}$ | R1 coil offset | ECC | $P_{DED}$ | Data 10 to Data 0 |
| $07_{HEX}$ | $27_{HEX}$ | Transmitter calibration | ECC | $P_{DED}$ | Data 10 to Data 0 |
| $08_{HEX}$ | $28_{HEX}$ | Transmitter frequency timebase | ECC | $P_{DED}$ | Data 10 to Data 0 |
| $09_{HEX}$ | $29_{HEX}$ | Transmitter frequency lower limit | ECC | $P_{DED}$ | Data 10 to Data 0 |
| $0A_{HEX}$ | $2A_{HEX}$ | Transmitter frequency upper limit | ECC | $P_{DED}$ | Data 10 to Data 0 |
| $0B_{HEX}$ | $2B_{HEX}$ | Iren 1 | ECC | $P_{DED}$ | Data 10 to Data 0 |
| $0C_{HEX}$ | $2C_{HEX}$ | Iren 2 | ECC | $P_{DED}$ | Data 10 to Data 0 |
| $0D_{HEX}$ | $2D_{HEX}$ | IRQN watchdog 1 | ECC | $P_{DED}$ | Data 10 to Data 0 |
| $0E_{HEX}$ | $2E_{HEX}$ | IRQN watchdog 2 | ECC | $P_{DED}$ | Data 10 to Data 0 |
| $0F_{HEX}$ | $2F_{HEX}$ | IDT internal configuration registers | ECC | $P_{DED}$ | Data 10 to Data 0 |
| $10_{HEX}$ | $30_{HEX}$ | IDT internal configuration registers | ECC | $P_{DED}$ | Data 10 to Data 0 |
| $11_{HEX}$ | $31_{HEX}$ | IDT internal configuration registers | ECC | $P_{DED}$ | Data 10 to Data 0 |
| $12_{HEX}$ | $32_{HEX}$ | R1 fine gain | ECC | $P_{DED}$ | Data 10 to Data 0 |
| $13_{HEX}$ | $33_{HEX}$ | R2 fine gain | ECC | $P_{DED}$ | Data 10 to Data 0 |
| $14_{HEX}$ | | Not used | Read as 'x | | |
| $15_{HEX}$ | | Not used | Read as 'x | | |
| $16_{HEX}$ | | Not used | Read as 'x | | |
| $17_{HEX}$ | | Not used | Read as 'x | | |
| $18_{HEX}$ | | Not used | Read as 'x | | |
| $19_{HEX}$ | n.a. | Product identifier | IDT internal | | |
| $1A_{HEX}$ | n.a. | Product identifier | IDT internal | | |
| $1B_{HEX}$ | n.a. | Product identifier | IDT internal | | |
| $1C_{HEX}$ | n.a. | Product identifier | IDT internal | | |
| $1D_{HEX}$ | n.a. | Product identifier | IDT internal | | |
| $1E_{HEX}$ | n.a. | Product identifier | IDT internal | | |
| $1F_{HEX}$ | n.a. | Product identifier | IDT internal | | |

Figure B.1 – NVM to SRB address mapping

# Appendix C

# Receiver 1/2 gain

| Bit | Symbol | Default | Type | Description |
|---|---|---|---|---|
| r12_gain.15<br>r12_gain.14<br>r12_gain.13<br>r12_gain.12 | ECC | $0000_{BIN}$ | | Parity word for error correction. For the internal use of the IC. |
| r12_gain.11 | $P_{DED}$ | $0_{BIN}$ | | Parity bit for double bit error detection. |
| r12_gain.10<br>r12_gain.9 | IDT internal configuration | $00_{BIN}$ | R/W | IDT internal feature. Do not change the default setting. |
| r12_gain.8<br>r12_gain.7<br>r12_gain.6<br>r12_gain.5<br>r12_gain.4 | Integration cycles | $00101_{BIN}$ | R/W | The integration cycles parameter defines the integration time of the integrator in excitation clock units.<br>The minimum setting is 5 cycles.<br>**Setting** / **Integration Time**<br>$00000_{BIN}$ to $00101_{BIN}$ — 5 period of LC oscillator<br>$00110_{BIN}$ — 6 period of LC oscillator<br>$00111_{BIN}$ — 7 period of LC oscillator<br>.... — ....<br>$11111_{BIN}$ — 31 period of LC oscillator |
| r12_gain.3<br>r12_gain.2<br>r12_gain.1<br>r12_gain.0 | gain stage | $0110_{BIN}$ | R/W | The gain stage parameter defines the input resistor of the integrator by this formula:<br>$Gain = 2^{\frac{n}{2}}$ $where$ $n = dec$ (gain stage )<br>A total 14 stages in multiplication steps of sqrt(2) are implemented.<br>$E_{HEX}$ and $F_{HEX}$ are unused.<br>For example:<br>• $0_{HEX}$, n = 0 , Gain = 1<br>• $1_{HEX}$, n = 1, Gain = $2^{\frac{1}{2}}$<br>• $2_{HEX}$, n= 2, Gain = $2^{\frac{2}{2}}$<br>until<br>$D_{HEX}$ , n=13, Gain = $2^{\frac{13}{2}} = 64 \times 2^{\frac{1}{2}}$ |

Figure C.1 – Receiver 1/2 gain [22]

# Appendix D

# DS18B20 - Timing for initialization, read and write operation

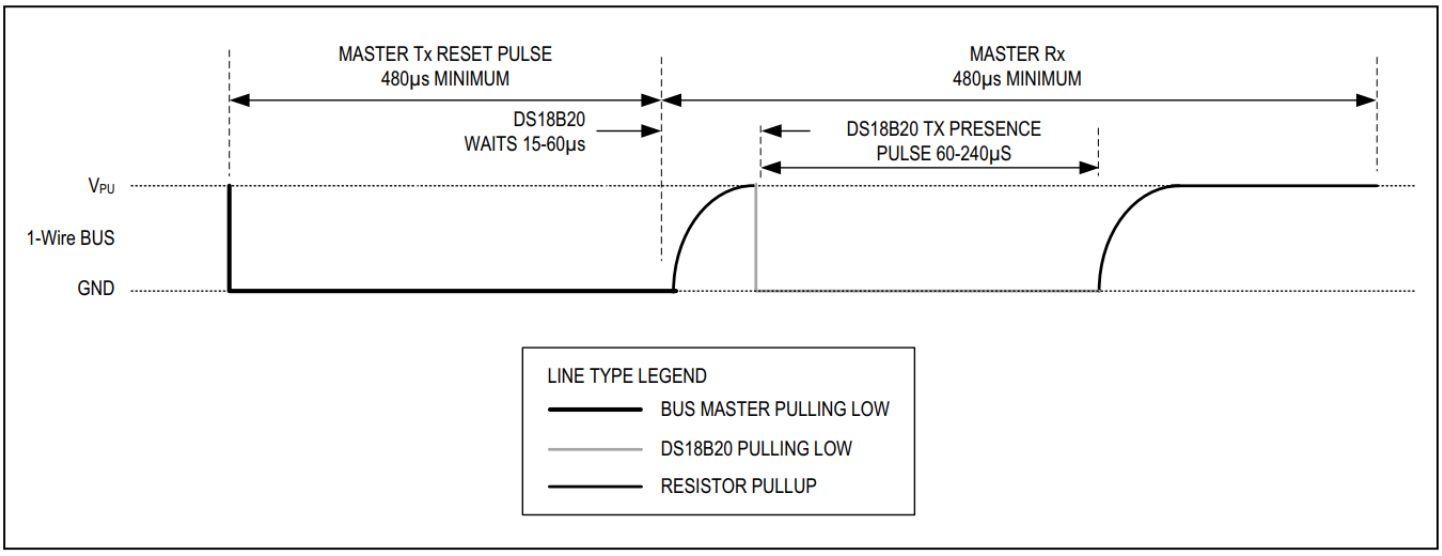


Figure D.1 – Initialization timing [13]

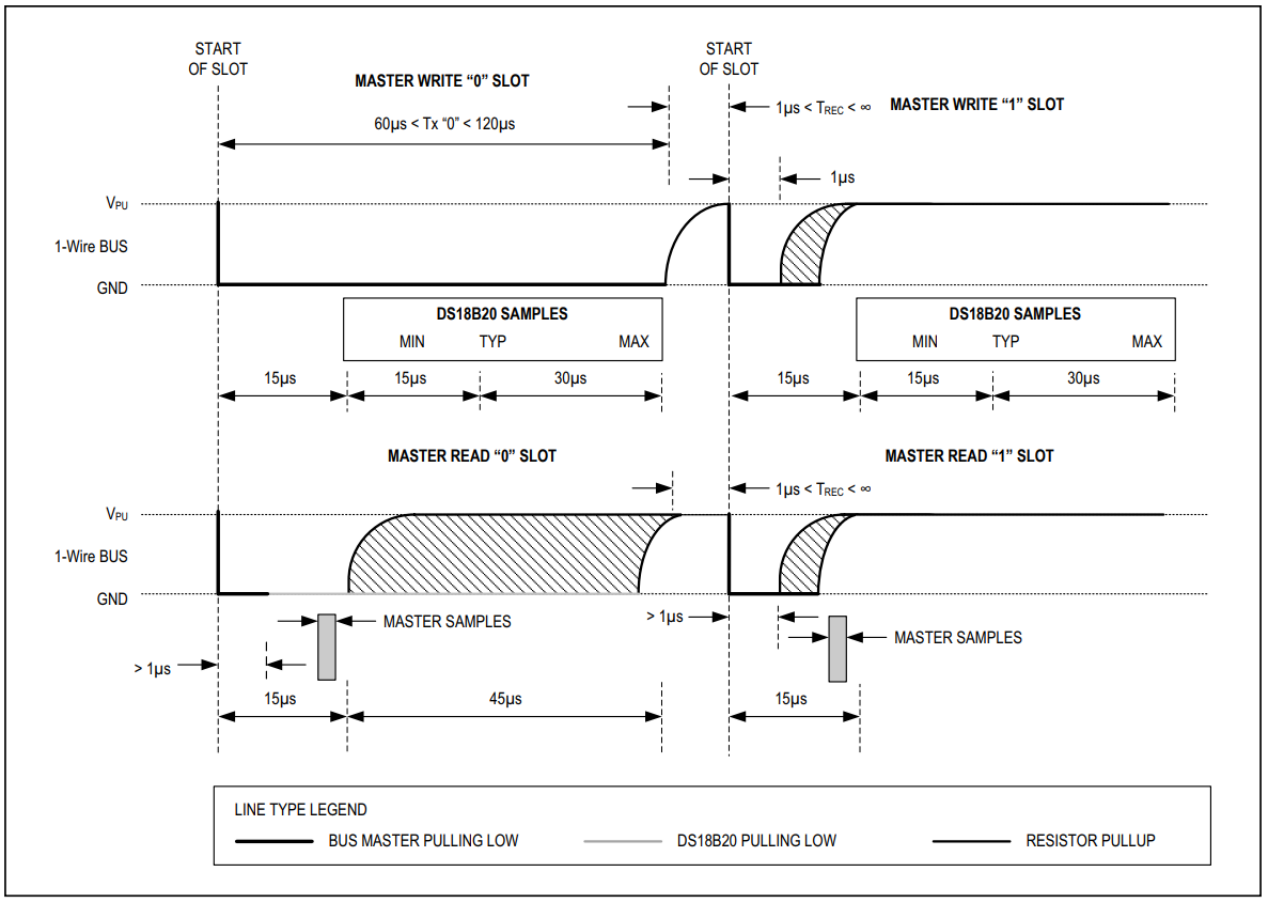


Figure D.2 – Write and read timing for each bit [13]